Università Politecnica delle Marche
Scuola di Dottorato di Ricerca in Scienze dell'Ingegneria
Curriculum in Biomedical Engineering

Digital health technologies to improve diabetes prevention and optimize therapy: from model-based approaches to feature-based machine learning

Advisor:
Dott.ssa Micaela Morettini

Co-advisors:
Prof.ssa Laura Burattini

Dott. Andrea Tura

Curriculum supervisor:
Prof.ssa Laura Burattini

Ph.D. Dissertation of:
Agnese Piersanti

XXXVI edition - 22° new series

Acknowledgements

I would like to express my sincere gratitude to my family and friends, all the colleagues and all the mentors that played a role during my PhD journey.
To my supervisor, Dr Micaela Morettini, who guided me, supported me and taught me with tireless enthusiasm and patience.
To Dr Andrea Tura for his invaluable spervision.
To Prof. Laura Burattini for her insightful suggestions and encouragement.
To Dr Giovanni Pacini and Prof. David Z D'Argenio for their supervision during my visit to LA and after.
I am grateful for all the opportunities, knowledge, connections, and friendships.

Abstract

Diabetes in its main categories, namely type 1, type 2 and gestational is determined by different factors and characterized by several metabolic perturbations which makes it a complex disease and whose burden is continuously increasing. Recently, innovation has been given by the introduction of devices for continuous glucose monitoring (CGM), which record glycemia every 1-5 minutes. In addition, the management of the disease includes pharmacological therapy which, in cases of poor endogenous insulin secretion, involves exogenous administration that to date occurs via multiple daily injections or infusion pump. Over the years, however, attempts have been made to find alternative and less invasive routes of administration, and an example is inhaled insulin. Still, the gap between the potential of innovative digital health solutions and their actual development is still large and has not yet crossed all open issues in the diabetes field.

In this context, the objective of the research carried out was to combine model-based and feature-based data-driven approaches to develop innovative digital health technologies aimed at improving the disease prevention and at optimizing its diagnosis and therapy. This research question is expressed in the different developed approaches that have been applied starting from two different sources of metabolic data, that are standard clinical data and CGM data.

After briefly introducing diabetes pathology and its management and treatment, Chapter 2 is dedicated to the description of pure physiological system modeling methodologies that have therefore been developed to extract significant parameters from standard clinical data (intravenous and oral glucose tolerance tests), also exploring regularization techniques to deal with identifiability problems. It will be shown that model-based parameters allow per se to gain knowledge on the pathophysiology of diabetes and to quantitatively assess physiological processes (i.e., insulin clearance, α-cell insulin sensitivity) involved in disease development and progression.

Chapter 3 investigates the possibility of considering the above-mentioned clinical data and combining modeling and data-driven methodologies to develop a digital prevention framework in the field of gestational diabetes to identify women at greater risk of type 2 diabetes progression. Starting from a dataset containing model-based features it will be shown what are the relevant features that could play a role in the progression.

In the case of CGM data, characterization in terms of features requires the extraction of the so-called "metrics". Given the lack of guidelines on this topic, Chapter 4 aims at standardizing the calculation of the multiplicity of metrics available by the different software solutions (13 in total) to be used in the subsequent steps of the research.

Then, in Chapter 5 the potential of such metrics is explored through the formulation of feature-based machine learning approaches laying the foundation for an integrated diabetes prevention/management multipurpose tool for: i) innovative diagnosis and early identification of complications (i.e., diabetic retinopathy) ii) management of open problems related to replacement therapy (i.e., hypoglycemia from hemodialysis) and to insulin therapy (i.e., hypoglycemia from physical exercise), leading to the formulation of a dedicated metric called HIKE.

Chapter 6 relies again on the use of mathematical models and is framed in the field of pharmacological therapy, particularly focusing the attention on the open problem of quantifying the exogenous insulin that reaches the circulation (bioavailability). An in-silico approach based on dynamic modeling is here developed using meal tolerance test data following inhaled insulin administration and finally, Chapter 7 summarizes the main findings, together with providing a hint about future developments.

Contents

Abbreviations

ACPR Acute C-peptide response

ADA American diabetes association

ADRR Average daily risk range

AGP Ambulatory glucose profile

AI Artificial intelligence

AIR Acute insulin response

AUC Area under the curve

BIE Basal insulin effect

BMI Body mass index

BSR Basal secretion rate

CA Classification accuracy

CDSS Clinical decision support system

CEACAM1 Carcinoembryonic antigen-related cell adhesion molecule 1

CGM Continuous glucose monitoring

CI Confidence interval

CII Continuous insulin infusion

CNT Control

COGI Continuous glucose monitoring index

CONGA Continuous overall net glycemic action

CV Coefficient of variation

DI Disposition index

DR Diabetic retinopathy

DYS Do-it-by-yourself

eA1c Estimated glycated hemoglobin

EF Excursion frequency

FD Fractal dimension

FDA Food and drug administration

FN False negatives

FP False positives

GD Gestational diabetes

GEZI Glucose effectiveness at zero insulin

GIP Glucose-dependent insulinotropic polypeptide

GLM Generalized linear model

GLP-1 Glucagon-like peptide-1

GMI Glucose management indicator

GRADE Glycemic risk assessment in diabetes equation

GRI Glycemia risk index

GVP Glycemic variability percentage

GUI Graphical user interface

HBGI High blood glucose index

IGC Index of glycemic control

IM-IVGTT Insulin-modified intravenous glucose tolerance test

IQR Interquartile range

IVGTT Intravenous glucose tolerance test

LBGI Low blood glucose index

LI Lability Index

MAD Mean absolute deviation

MAG Mean absolute glucose

MAGE Mean amplitude of glycemic excursions

MDI Multiple daily injections

MGE Mean of glucose outside range

MGN Mean of glucose inside range

ML Machine learning

MMTT Mixed meal tolerance test

MODD Mean of daily differences in glucose

MSE Multiscale sample entropy

NPV Negative predictive value

OGTT Oral glucose tolerance test

PG Plasma glucose

PGS Personal glycemic state

PK Pharmacokinetic

PD Pharmacodynamic

PIR Percent inside range

POR Percent outside range

PPV Positive predictive value

PR Precision

ROC Receiver operating characteristics

SAP Sensor augmented pump

SE Sensitivity

SD Standard deviation

SMBG Self-monitoring of blood glucose

SP Specificity

T1D Type 1 diabetes

T2D Type 2 diabetes

TAR Time above range

TBR Time below range

TIR Time in range

TN True negatives

TP True positives

List of Figures

List of Tables

1 Introduction

Diabetes is a chronic metabolic disease characterized by a condition of high blood glucose that occurs when the pancreatic beta cells essentially fail to secrete insulin or lose the ability to adapt to the degree of the sensitivity to insulin of the body tissues. Nowadays, it affects more than 463 million people and its prevalence is expected to rise up to 700 million people in 2045. Moreover, fluctuations in blood glucose level characterizing diabetic patients are strongly associated with the onset of further complications, thus increasing its socioeconomic burden (10% of global health expenditure is spent on diabetes for a total of around USD760 billion) [1]. For this reason, an early detection of the disease and its complications together with an optimized management is desirable. In recent years, cutting-edge technologies like new devices, drug delivery systems, and software have been introduced in the field and started improving diabetes management. However, the gap between the potential of innovative digital health solutions and the actual development of the latter is still very large and has not yet crossed the numerous open issues in the diabetes field. This chapter aims to briefly describe diabetes pathology and its management and treatment, giving an overview of newly developed diabetes technologies and providing the reader with the context in which the thesis is intended to encompass.

1.1 Diabetes development and progression

Diabetes is a group of metabolic diseases characterized by the presence of high levels of glucose in the blood, a condition known as *hyperglycemia*. Chronic hyperglycemia is associated with the development of long-term complications due to dysfunction and failure of different organs. In healthy individuals, insulin is an hormone devoted to the regulation of blood glucose homeostasis, being responsible in promoting glucose transport from the blood to the main glucose dependent tissues. The pathogenic processes at the basis of diabetes development are several, spanning from a deficiency in insulin secretion by the β-cells of the pancreas to the tissue resistance to the action

of insulin (i.e., insulin resistance) and the altered insulin removal from the blood (i.e. insulin clearance) [2]. The impairment of one or more of these processes finally lead to hyperglycemia.

The standard criteria for the clinical diagnosis of diabetes are based on the evaluation of the levels of plasma glucose (PG), either in fasting conditions (FPG) or 2-hours after the administration of a 75 grams dose of glucose (2h-PG) during an Oral Glucose Tolerance Test (OGTT) or based on assays of glycated hemoglobin (HbA1c), an established biomarker of glucose control. The American Diabetes Association (ADA) set the diagnosis of diabetes in case of one of these criteria is met for two times [3]:

1. FPG ≥ 126 mg/dL (≥ 7.0 mmol/L), with 8 or more hours of no caloric intake;
2. 2h-PG ≥ 200 mg/dL (≥ 11.1 mmol/L) during an OGTT;
3. HbA1c ≥ 6.5% (≥ 48 mmol/mol);
4. random PG ≥ 200 mg/dL (≥ 11.1 mmol/L) in presence of classic symptoms of hyperglycemia or hyperglycemic crisis.

Classification of diabetes in its subtypes may be complex, however, a brief description of the most common types and of the main complications that can arise as a result of this condition is relevant for the purpose of the thesis and thus is provided in the following paragraphs.

1.1.1 Type 1 diabetes

Type 1 diabetes (T1D) accounts for the 5-10% of all diabetes cases and is mainly due to an autoimmune reaction of the body which results in the destruction of the β-cells of the pancreas. Although this type of diabetes was associated to youth, it is now commonly known that its onset can occur at all ages. The inability of the β-cells to secrete insulin translates into the impossibility to maintain blood glucose homeostasis, resulting in hyperglycemia. Exogenous insulin administration is the primary therapy to maintain glucose levels as close as possible to physiological ranges and counteract hyperglycemia. However, insulin dosing exposes to a higher risk of glucose drop under critical levels (PG <70 mg/dL), a condition known as *hypoglycemia*. This condition is

associated with a higher risk of morbidity and mortality and it is characterized by short term symptoms i.e., confusion, loss of consciousness, blurred vision and seizures, which can also be unperceived, thus causing anxiety to the patients.

1.1.2 Type 2 diabetes

Type 2 diabetes (T2D) is the most common form of diabetes, accounting for 90-95% of all diabetes cases and affecting about 10.5% of the world adult population [4]. Although it is more common in adults, also in this case it can have its onset at all ages. The first stages of the disease are characterized by insulin resistance which in turn leads to the progressive loss of adequate β-cell insulin secretion with subsequent hyperglycemia. Other physiological processes that may be involved in T2D pathophysiology are for example abnormalities in insulin clearance [3]. T2D is usually preceded by a condition called *prediabetes*, characterized by hyperglycemia in the form of impaired fasting glucose, defined as PG from 100 to 125 mg/dL (from 5.6 to 6.9 mmol/L) and/or impaired glucose tolerance, defined as 2h-PG during an OGTT from 140 to 199 mg/dL (from 7.8 to 11.0 mmol/L) and/or HbA1c from 5.7 to 6.4% (from 39 to 47 mmol/mol), thus still not recognizable as diabetes but with an increased the risk for its development [2].

1.1.3 Gestational diabetes

According to the most recent definition, gestational diabetes (GD) is a diabetes diagnosed in the second or third trimester of pregnancy that was not clearly overt diabetes prior to gestation. This condition usually resolves at the end of the pregnancy but exposes women to a higher risk to experience it again in other pregnancies and to develop T2D later in their life [3]. It is straightforward that the determination of factors influencing development of T2D after GD may also shed light on factors determining this condition and potentially accelerate opportunities for its prevention and treatment [5].

1.1.4 Maturity-onset diabetes of the young

It is important to have in mind that identification of diabetes type is not always straightforward. An example could be that of individuals with maturity-onset diabetes

of the young (MODY) who are commonly misdiagnosed as having type 1 diabetes. MODY is a form of diabetes which accounts for the 1-2% of all diabetes cases and is characterized by impaired insulin secretion but for most cases no or minimal impairment in insulin action, being it due to inherited abnormalities at specific genetic loci, that cause β-cell disfunction and subsequent hyperglycemia onset usually at an early age. The main reported forms are hepatocyte nuclear factor (HNF)-1α (MODY 3), HNF-4α (MODY 1), HNF-1β and Glucokinase (GSK)-MODY (MODY 2) [3]. Among all, MODY 2 is likely to be misdiagnosed as GD since its mild hyperglycemia is often detected during pregnancy. Especially in this latter case the diagnosis, achieved through genetic screening, is crucial since it has been shown that by avoiding glucose-lowering therapy patients are free from developing complications.

1.1.5 Complications of diabetes

The main acute complications of diabetes include the previously defined conditions of high and low blood glucose, i.e., hyperglycemia and hypoglycemia, respectively, together with other conditions that represent life threatening events, such as diabetic ketoacidosis (DKA) and hyperosmolar hyperglycemic state (HHS). DKA occurs in conditions of very high blood glucose when the buildup of acidic ketone molecules as fat stores are burned to provide energy. If progressive, DKA can cause metabolic problems and lead to coma or death. HHS is a medical emergency which occurs only to patients with T2D and is primarily characterized by very high glucose level (above 600 mg/dL) and severe dehydration.

On the other hand, hyperglycemia condition is associated with the development of long-term or chronic complications due to dysfunction and failure of different organs. Long-term complications of diabetes are usually divided into macrovascular and microvascular. Macrovascular complications include stroke, coronary heart disease and heart failure, atherosclerosis, and peripheral arterial and cerebrovascular disease. Microvascular complications include retinopathy with potential vision loss; nephropathy leading to renal failure; peripheral neuropathy with risk of foot ulcers, amputations, and Charcot joints; and autonomic neuropathy causing gastrointestinal, genitourinary, and cardiovascular symptoms and sexual dysfunction. Moreover,

emerging disorders have been recently identified, including associations with cancer, infections, functional and cognitive disability, liver disease and affective disorders [6].

Among all the possible complications, as this work does not focus only on this aspect, the ones that will mainly be addressed will be the problem of hypoglycemia and diabetic retinopathy; however, an overview has been provided for completeness.

1.2 Diabetes management and therapy

Diabetes management generally includes recommendations for a healthy lifestyle together with the prescription of physical exercise; then, the primary and lifesaving treatment for T1D, consists in insulin administration, sometimes used also in T2D and GD when oral medications fail to achieve targeted outcomes. Insulin is usually administered via insulin pens or infusion pumps. Over the years, however, many attempts have been made to find alternative and less invasive routes of administration, and an example is that of inhaled insulin, currently approved for use only in the USA and produced by the company MannKind. Moreover, regular blood glucose monitoring is of major importance since external administration of insulin expose to the risk of experiencing hypoglycemia. Self-monitoring of blood glucose is done through finger pricks or, thanks to the development of new technologies, is increasingly performed via Continuous Glucose Monitoring (CGM) devices normally placed in the belly or in the arm and which continuously sample interstitial glucose every 5 minutes. Detailed description of such diabetes management technologies is provided in the following paragraphs.

1.2.1 Continuous Glucose Monitoring (CGM)

Over the past two decades, the advancement of technology in the field of blood glucose monitoring has led to the extensive use of continuous glucose monitoring (CGM) devices, which are wearable devices equipped with a minimally invasive sensor, i.e., transcutaneous needle type or implantable, a transmitter and a receiver or smart device that allow data storage and display [7]. Before the development and spread of CGM devices, the most used method for checking that blood glucose levels were inside safe ranges was the self-monitoring of blood glucose (SMBG), consisting of a single

measurement point of capillary blood glucose that was performed 5-6 times per day. SMBG is done through finger pricks that after pricking the fingertip require the user to place a small blood drop on top of a test-stripe and to insert it into a glucometer in order to see the punctual blood glucose concentration [8]. This method is known to cause discomfort and subsequent poor patient compliance; its major limitation, however, is the impossibility to ensure a continuous glucose tracking over time. On the contrary, CGM systems are capable to provide measures of interstitial glucose throughout the day, e.g., every 5 minutes. The electrochemical sensor inserted in the subcutaneous tissue transduces the glucose concentration in the interstitial fluid into current, the transmitter to which it is attached, sometimes part of the same hardware and sometimes separable from the disposable sensor, sends the information to an external receiver that converts the signal into blood glucose concentration and allows frequent storing of data through the dedicated apps. An example of CGM system is shown in Figure 1.

Figure 1: Example of integrated CGM sensor and transmitter, the Freestyle Libre 3, on the left, with two different kinds of receivers. In the middle the Freestyle Libre 3 reader and on the right a smartphone. https://www.freestyle.abbott/

These devices faced progressive refinement in terms of accuracy (reaching a mean absolute relative difference lower than 8%), comfort (smaller dimensions reached less than 2 cm), wearing time (from 7–14 days to up to 180 days for implantable ones) and ease of use. Thanks to that, this technology is nowadays used not only in addition but also in replacement to the standard SMBG [9], [10], [11]. Indeed, it have been not only

used among adults and adolescents with T1D but also people with T2D and diabetes in pregnancy[12], [13], [14], [15], [16], [17].

Main advantages of CGM technology rely on the possibility to get real time alarms of impending risk conditions, and on the potential use of this technology in conjunction with others, e.g., in the case of artificial pancreas that will be furtherly presented in the next subchapter among innovative digital health technologies for diabetes. Use of CGM technology has been also associated to a significant reduction of pain and discomfort in a cohort of young patients with type 1 diabetes [18] and with controlled glucose variability and patient's lifestyle improvement [19].

1.2.2 Insulin therapy

Insulin is the main hormone devoted to glucose control, i.e., glycemia maintenance inside optimal ranges and it secreted by the pancreatic β-cells when blood glucose concentration rises. When there is an impairment in its secretion, exogenous insulin administration is used to counteract hyperglycemia and to maintain blood glucose levels within a narrow range; in particular, it represents the primary and lifesaving treatment for T1D [20] and is used in T2D and GD when oral antidiabetic medications fail to achieve adequate glucose control [21], [22]. Insulin regimens usually aim to mimic physiology as much as possible and involve several components: basal insulin, usually the same day to day, provides background insulin levels; mealtime (or prandial) insulin, used to cover the intake of carbohydrate and other macronutrients and whose amount is usually manually computed in order to match the food that is going to be consumed; and correction insulin, to treat hyperglycemia and bring blood glucose back to normal ranges. In case of injection-based therapy, multiple daily injections (MDI) of subcutaneous long-acting insulin are required for basal insulin, while rapid-acting or ultra-rapid-acting insulin can be administered for mealtime and correction insulin boluses. In case of continuous insulin infusion (CII) therapy via pumps, continuous subcutaneous infusion combined with manual mealtime boluses of rapid-acting insulin are administered. Currently, the most diffused insulins worldwide are recombinant human insulin or human insulin analogues.

MDI therapy can be administered through vials and syringes, or with insulin pens. The latter has now its new version, namely smart pen, which consists in a

technology that can take track of previous insulin injections. Smart pens can also communicate via Bluetooth with other devices where information is stored and where it is also possible to perform computation of the right amount of insulin required after a certain meal intake or where remind alerts can be delivered to the user. For what concerns CII therapy, different insulin pumps exist, mainly categorized in those with a fine external tube that connects the pump to the cannula and the patch or mini pumps, where the tube is not present or very short and the pod is attached to the skin. Similarly to smart pens, current insulin pumps also include calculators that allow obtaining personalized insulin to carbohydrate correction factors to determine the proper insulin bolus [20].

As a further step toward technology, sensor augmented pump (SAP) therapy can be obtained by combining pumps with CGM in a way that insulin infusion is suspended when the CGM detects low blood glucose or predicts that glucose will decrease within the next 30 minutes. Moreover, by combining CGM and insulin pumps with closed-loop algorithms fed with CGM, meal and insulin information, a step forward have been made in the automation of insulin delivery, giving birth to the technology also known as “artificial pancreas”. At present, hybrid closed-loop systems are available, that automatically deliver basal and correction insulin but still require manual mealtime insulin boluses. In parallel with hybrid closed-loop systems, do-it-by-yourself (DIY) systems have been developed without approval from regulatory bodies, where the control algorithm is usually freely available on the internet and can be autonomously used. However, fully automated closed-loop systems are still under development and will expectedly be available in the next few years.

1.2.3 New insulin delivery routes

Although insulin is typically delivered by subcutaneous injection, alternate routes of administration are also used including peritoneal delivery via intraperitoneal catheter, currently available in some European countries [23], and pulmonary delivery via inhalation, approved in the United States. Other attempts have been made with transdermal, oral and rectal delivery routes, but without reaching clinical use [24], [25], [26]. The first inhaled insulin was Exubera (Pfizer), FDA approved in 2006 and discontinued in 2007 due to the low sales. Then, Afrezza (Mannkind) inhalation

powder, a rapid-acting insulin based on human insulin formulation, was FDA approved for mealtime use in 2014 and it is nowadays the only inhaled insulin on the market, in the form of Technosphere® Inhaled Insulin (TI).

With respect to subcutaneous insulin delivery, pulmonary inhalation has the advantage of being noninvasive. Moreover, in addition to less burden to the patient, inhaled insulin has demonstrated advantages compared with subcutaneous insulin in treating patients with T1D and T2D [27], [28]. These include a faster onset of action and a more rapid return to baseline, possible thanks to the large alveolar surface area that allow a rapid absorption in the systemic circulation, a reduction in the incidence of hypoglycemia and improvement of glycemic control [29], [30], [31]. The unique pharmacokinetic (PK)/pharmacodynamic (PD) properties of TI has made this product a valid alternative capable to mimic the physiological metabolic effect that insulin should have in response to a meal. Of note, its use is not recommended in case of respiratory problems or for people who smoke.

1.3 Innovative digital health technologies and clinical decision support systems (CDSS) in diabetes

The big amount of diabetes data generated from the diffusion of CGM, insulin pumps, artificial pancreas, and other wearable technologies raised the need and the opportunity to develop different digital health technologies in the field of diabetes, encompassing both digital care and digital therapeutics solutions. The use of connected devices has given the possibility to clinicians to remotely monitor patients thus increasing telehealth monitoring seeking to reverse metabolic impairments. Clinical trials data are no longer the sole source of data to inform decisions since they are now supplemented by real-world data and artificial intelligence (AI) represents a candidate tool for the development of clinical applications to diabetes. AI started to be deployed in the prediction of short-term glycemic changes to automate part of the therapeutic decision typically performed by a human, such as in the case of closed-loop insulin delivery systems [32].

Besides artificial pancreas, the use of AI also started to be used to suggest lifestyle and behavioral decision support, to predict the risk of developing diabetes,

optimize treatments for people with diabetes, and diagnose diabetic complications in their early, treatable stages, obtaining several positive outcomes. Indeed, a number of software solutions using CGM data in order to monitor risk biomarkers have been developed and achieved important results (i.e., improvement in glycemic control). Digital therapeutic strategies are also increasingly being deployed as they provide clinical decision support to tailor the dose and type of care to individuals with diverse needs and health statuses [33], [34]. All these technologies can be viewed as clinical decision support systems (CDSS), that usually comprise a software aimed to aid clinical-decision making, in which individual patient data are retrieved and evaluated against evidence based rules, and in this case the system is known as knowledge-based CDSS, or, on the other hand, against AI, machine learning (ML), or statistical pattern recognition, and in this case the system is known as non-knowledge-based CDSS. The final output usually provides patient-specific assessments or recommendations that are finally presented to the clinician [35].

However, the gap between the potential of innovative digital health solutions and the actual development of the latter is still very large and has not yet crossed all open issues in the diabetes field. In particular, the next paragraphs will give a definition of what is intended in this thesis for “model-based” and “feature-based data-driven” CDSSs, starting from two different sources of data.

1.3.1 Different sources of data: challenge tests and CGM

Among all the different sources of data that can be retrieved to be used in the formulation of solutions for diabetes there are standard clinical data obtained from experiments involving challenge tests, and the data collected from CGM devices. These data are used both in clinical settings (e.g., in the case of OGTT for the diagnosis of diabetes or CGM used to monitor glucose in the management of diabetes) and in research contexts.

In addition to OGTT experiments, challenge tests also comprise the intravenous glucose tolerance test (IVGTT) and the mixed meal tolerance test (MMTT). They consist in the administration of a standard glucose dose intravenously or orally (for IVGTT and OGTT respectively), and of a standardized mixed meal consumption (for MMTT), all followed by the collection of blood samples for some

hours after the stimulus (varying from 2 to 5 hours in relation to the test and the protocol), for the measure of glucose and, in some cases, insulin and other hormones/peptides [36], [37], [38]. Even when frequently sampled, challenge test data do not usually reach a number of measurement data points higher than some tens in the single individual, differently from CGM recordings, that are sampled every 15 or 5 minutes, providing almost 288 samples per day. Challenge test, on the other hand, are collected in very controlled conditions and after standardized specific stimuli, while CGM are generally acquired in free living conditions, even if with the possibility of involving standardized protocols, e.g., in research context.

In view of providing support to the clinical decision, different approaches may be used to extract information from individual data, that can be subdivided into two macro categories [39]:

- physiological system modeling, which attempts to represent with a certain level of approximation the underlying physiological system by exploiting a priori knowledge;
- data-driven modeling, which mathematically describes the data without explicit correspondence with the underlying physiology.

The two approaches can also be integrated and combined to fit the data analysis to the specific purpose of the single application [40]. Thus, one could envisage a framework exclusively based on system modeling and intended to gain knowledge on the pathophysiology of a certain condition in one side, or another that combines the two approaches using in series system modeling to extract relevant parameters that then are used to feed data-driven approaches to obtain the inference engine of the final CDSS, until arriving at the other end of the spectrum to full data-driven approaches. In relation to the two sources of data on which the focus has been made, physiological system modeling certainly may apply to challenge test data, as they have been already extensively coupled with mathematical modeling methodologies for the assessment of important metabolic parameters which cannot be directly measured noninvasively [41]. Application of system modeling to CGM data have been also explored in the literature, mainly focusing on blood glucose forecasting and simulation [42]. Although full data-driven approaches may apply on CGM data due to the large number of data

points of raw CGM timeseries [43], the extraction of information in the form of metrics from the CGM data is an interesting opportunity to transform and reduce data dimensions. The next paragraphs will detail how were articulated the building blocks of the approaches that will be presented along the thesis.

1.3.2 Definition of model-based CDSS

As previously pointed out, physiological system modeling may allow, by itself, to gain insights into metabolic processes, thus providing knowledge that can be exploited in multiple ways, i.e., to better understand the pathophysiological mechanism that are related with diabetes, to quantify metabolites that are not directly measurable, to examine experimental design. Such information could be relevant for enlarging the knowledge base of CDSS, however, it may also enable an hybrid approach, different from the first one. Indeed, it is possible to exploit the information extracted through physiological system modeling by feeding ML models, thus combining the first approach with a data-driven one. In this case, the so known feature extraction process coincides/overlaps with the application of system modeling techniques. The two above mentioned approaches will be pigeonholed with the keyword "*model-based CDSS*", to reference applications that involve the use of mathematical modeling of the system under study.

1.3.3 Definition of feature-based data-driven CDSS

Full data-driven approaches are also known as black-box approaches since they describe input-output relationships without specifying the underlying mechanisms. While deep-learning methodologies usually take raw data as input data and are capable to autonomously learn some representative features through the training process, the traditional ML-based approaches usually rely on handcrafted feature extraction processes to transform input data before embarking on analysis. Even when not relying on physiological system modeling, some prior knowledge and expertise are still needed. In the case of CGM data, for example, features from different domains, namely CGM metrics, can be extracted. This first step then allows, when moving on to the analysis of the data that will feed the inferential machine of the CDSS, to obtain interpretable results and at the same time reduce computational costs. Thus the use of

a handcrafted feature-extraction step combined with a data-driven analysis through ML will give rise to the second keyword that will characterize some of the approaches developed, that is "*feature-based data driven CDSS*".

In an effort to let the reader figuring out the path that have been followed to develop the approaches that will be presented in the following chapters, a pictorial representation of the adopted framework is summarized in Figure 2.

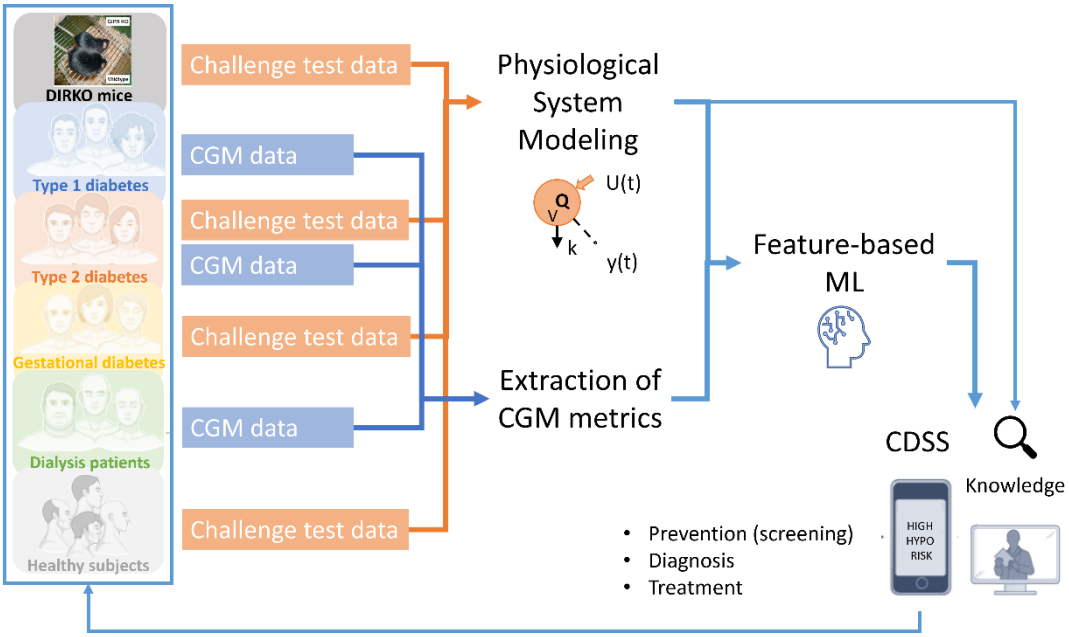

Figure 2: Summary framework of the carried out approaches.

1.4 Aim and outline of the thesis

As detailed in the above sections of this first chapter, diabetes in its main categories, namely: type 1 diabetes, type 2 diabetes and gestational diabetes is determined by different factors and characterized by several metabolic perturbations which makes it a complex disease and whose burden is continuously increasing. In recent years, a strong impetus to innovation has been given by the introduction of devices for continuous glucose monitoring (CGM), which record glycemic values every 1-5 minutes. In addition to blood sugar monitoring, the management of the disease includes pharmacological therapy which, in cases of poor endogenous insulin secretion, involves exogenous administration that to date occurs via multiple daily injections or via infusion pump. Over the years, however, many attempts have been

made to find alternative and less invasive routes of administration, and an example is that of inhaled insulin, currently approved for use only in the USA and produced by the company MannKind. However, despite the introduction of new diabetes technologies, it is a fact that individuals with diabetes still achieve suboptimal outcomes, and for this reason there is an increasing focus in translating evidence-based diabetes prevention and therapy into validated digital health technologies.

In this context, the objective of the research carried out was to develop a combined model-based and feature-based data-driven approach in the field of innovative digital health technologies for diabetes and aimed at improving the disease prevention and at optimizing its diagnosis and therapy. This research question is expressed in the different developed approaches that have been applied starting from two different sources of metabolic data, that are challenge data and continuous glucose monitoring data.

To this end, *Chapter 2* is dedicated to the description of pure physiological system modeling methodologies that have therefore been developed to extract significant parameters from standard clinical data (Intravenous Glucose Tolerance Test, Oral Glucose Tolerance Test), also exploring regularization techniques to deal with identifiability problems. It will be shown that mathematical modeling has the power of extracting in a non-invasive manner parameter of utmost physiological importance that allow per se to gain knowledge on the pathophysiology of diabetes and to quantitatively assess physiological processes (i.e., insulin clearance, alpha cell insulin sensitivity) involved in the disease development and progression. In detail, the modeling approaches will be applied to different sets of data for each case, with the following objectives:

- to quantitatively assess insulin clearance specific contributions (i.e., hepatic and extrahepatic) in women with a history of gestational diabetes, also considering a simplified experimental setup;
- to quantitatively assess the above mentioned contributions of insulin clearance by exploiting an animal model which allow to investigate potential differences in the presence or absence of the effect known as incretin effect;

- to quantitatively assess alpha-cell sensitivity to both glucose and insulin in a healthy sample with respect to one with type 2 diabetes.

Focus on those physiological processes that have been usually less investigated is driven by the idea to provide tools that may allow an overall characterization of diabetes pathophysiology, leading to the fine phenotyping of diabetes-related data. Indeed, the parameters estimated with the proposed modeling methodologies can be regarded as a contribution to CDSS knowledge base enlargement on one hand, and may have potential application if deployed upstream of machine learning models.

According to this last concept, *Chapter 3* investigates the possibility of considering the above mentioned challenge data and combining modeling and data driven methodologies to develop a digital prevention framework in the field of gestational diabetes to identify women at greater risk to develop type 2 diabetes. Starting from a dataset obtained from women who experienced a history of gestational diabetes analyzed early postpartum, the main objectives will be:

- to apply a feature-based machine learning approach for the identification of women who progress against those who did not progress to type 2 diabetes;
- to unveil what are the relevant features that could play a role in the progression from gestational to type 2 diabetes.

This will be achieved by including in the initial dataset both anthropometric characteristics and model-based features accounting for metabolic processes such as insulin sensitivity, β-cell function and insulin clearance.

In the case of CGM data, the characterization of the CGM signal in terms of features requires the extraction of the so-called "metrics". Given the lack of guidelines on this topic, Chapter *4* aims at standardizing the calculation of the multiplicity of metrics available to be used in the subsequent steps of the research. The main differences of the software available for the analysis of CGM data (13 in total) will be elucidated, with particular attention to coherence in the calculation of the metrics. Thus, the main objectives of this chapter will be:

- to report which are the data display options and preprocessing features offered by each software package;
- to investigate the correct implementation of metrics computations also testing it across all the different packages.

The study will be carried out also taking into account CGM metrics already included in consensus guidelines authored by clinical experts in the field.

In light of the considerations made in the previous chapter, in *Chapter 5* the potential of metrics is explored through the formulation of feature-based machine learning approaches laying the foundation for an integrated diabetes prevention/management multipurpose tool covering the following aspects:

- innovative diabetes/prediabetes diagnosis and early identification of complications (i.e., diabetic retinopathy);
- prediction of hypoglycemic events induced by different causes such as hemodialysis or physical exercise.

The latter case (i.e., physical exercise-induced hypoglycemia risk) will lead to the formulation of a dedicated metric called HIKE.

Chapter 6 relies again on the use of mathematical models and is framed in the field of pharmacological therapy, particularly focusing the attention on the open problem of quantifying the exogenous insulin that reaches the circulation (bioavailability). Investigation of such an aspect will involve:

- the development of an in-silico approach based on dynamic modeling
- the application of the approach to meal tolerance test data following inhaled insulin administration.

The proposed approach will then allow to assess the effect of inhaled insulin on endogenous secretion.

Finally, *Chapter 7* summarizes the main findings of the research carried out, discuss limitations and draws some overall conclusions, together with providing a series of future developments that could follow the present thesis.

2 Physiological system modeling

[1] Physiological system modeling has been largely employed in the study of the glucose-insulin regulatory system, and depending on which is the purpose for its use, it can present highest or lowest level of complexity. If the model is intended for simulation purposes, it usually requires a high level of complexity and consist of a high number of differential equations and parameters, in order to have a detailed description of the system; highly complex models are usually referred as "maximal" models. If the main purpose is to quantify specific metabolic relationships, the formulation of the model may involve a lower number of equations and parameters, thus it will be referred as "minimal" model. Minimal models, among which stands the Bergman et al. model, were very successful in the estimation of parameters of physiological interest such as insulin sensitivity, which is an index quantifying the hormone control on glucose production and utilization, and β-cell function, an index related to insulin secretion [44], [45], [46], [47]. Compartmental models represent a subcategory of mathematical models, which is based on the principle of conservation of mass of entities that are considered homogeneously distributed in the state space (i.e., the compartment); partitioning of the system under study is done even if with some incompatibilities with the anatomy in order to obtain a finite number of manageable compartments.

In this chapter, a series of compartmental model-based approaches involving the assessment of parameters having specific physiological meaning, in some cases also exploiting regularization techniques, are presented. First, investigation of the two different components of insulin clearance, namely, hepatic and extrahepatic components, is carried out through a previously proposed mathematical approach and applied to a short insulin-modified IVGTT in women with a history of gestational diabetes (Section 2.1). Similarly, a novel methodology to assess the two insulin clearance components is described and applied to IVGTT data from mice characterized by knockout of incretins receptors (Section 2.2). Then, a model of glucagon (the

[1] This chapter contains material published in [103], [281], [282] and in press in [68].

hormone antagonist of insulin in the regulation of glucose homeostasis) is presented, which allows the assessment of a dual glucagon suppression mechanism (Section 2.3). All these approaches decline in various ways, which will be detailed within each section, the same research question, i.e. the possibility to increase the knowledge base on aspects related to diabetes.

2.1 Hepatic and extrahepatic insulin clearance in women with a history of gestational diabetes

Insulin clearance, i.e., the removal of insulin from blood, is a process that together with its secretion determines plasma insulin concentration [48]. This process is highly variable and occurs in different sites, the main one being the liver, which accounts for around 80% of total insulin clearance (i.e., hepatic insulin clearance); the remaining occurs in several other organs, mainly kidneys and skeletal muscles (i.e., extrahepatic insulin clearance) [49]. It has been shown that this process has a role in T2D pathophysiology since it was found altered among T2D population [50]. As previously mentioned, women who had GD during pregnancy are classified as individuals at high risk of developing T2D, thus insulin clearance was also investigated in this population. Morettini et al., found that it was not altered compared to healthy women when observed immediately after pregnancy, [51], [52] while in Tura et al., it was found altered in women who were observed after pregnancy and who developed T2D later in life [53]. Considering that hepatic and extrahepatic insulin clearance are differentially regulated [54], [55], literature findings suggest the importance of insulin clearance assessment tools capable to separate hepatic and extrahepatic contributions.

2.1.1 Model-based assessment of hepatic and extrahepatic insulin clearance

A review study outlined different mathematical models for the assessment of insulin clearance and highlighted that those assessing separately the hepatic and extrahepatic components are rare [56]. Polidori et al. recently proposed an approach to estimate the two contributions from an insulin-modified intravenous glucose tolerance test (IM-IVGTT) [54]. IM-IVGTT is a modified version of the standard IVGTT, in which the

experiment involves the infusion of an insulin dose 20 minutes after administration of the glucose dose and usually lasting few minutes.

Model formulation

According to the mathematical modelling approach proposed by Polidori et al., hepatic clearance may assume a linear or a saturable dynamics depending on the subject. For conciseness, it is shown the case of assuming a linear dynamics. The approach is summarized in Figure 3 and the differential equation that describe changes in plasma insulin concentration I(t) (pmol·L^{-1}) is as follows:

$$V_P \frac{dI(t)}{dt} = IR(t) + (1\text{-}FE_L)\cdot ISR(t) - (HPF\cdot FE_L + CL_P)\cdot I(t) \qquad (1)$$

where V_P (L) is the extrahepatic distribution volume, IR(t) (pmol·min^{-1}) is insulin infusion rate during the test, FE_L (%) is the hepatic fractional extraction, ISR(t) (pmol·min^{-1}) is the prehepatic insulin secretion rate, CL_P (L·min^{-1}) is the extrahepatic insulin clearance, and HPF (L·min^{-1}) is the hepatic plasma flow rate. In relation to (1), the hepatic insulin disappearance rate (HR(t), pmol·min^{-1}) and the extrahepatic insulin disappearance rate (ER(t), pmol·min^{-1}) are:

$$HR = FE_L\cdot(ISR(t) + HPF\cdot I(t)) \qquad (2)$$

$$ER = CL_P\cdot I(t) \qquad (3)$$

ISR(t) and IR(t) represent the endogenous and exogenous insulin and are the inputs to the model. ISR(t) can be computed according to the extensively used procedure by Van Cauter et al. [57] which exploits computation of individualized (depending on subject' anthropometric characteristics) C-peptide kinetic parameters and performing deconvolution from plasma C-peptide concentration. Indeed, C-peptide is a marker of endogenous insulin secretion since it is secreted with insulin in equimolar amount but it is not extracted by the liver to a significant extent as it happens for insulin. Another assumption needed to run this model is to assume a constant hepatic plasma flow, HPF, set at 0.576 L/min/m^2, while it is known that during a glucose test this flow is variable [58].

Parameter estimation

The vector of model parameters that has to be estimated is $p = [CL_P, FE_L, V_P]$. By performing a best-fit procedure on plasma insulin concentration data, individual estimates of key parameters related to the two components of insulin clearance can be obtained. To get the model discrete time response the *ltitr* MATLAB built-in function was adopted. Best-fit procedure was carried out using the *lsqnonlin* function, by solving the following nonlinear least-square curve fitting problem:

$$\min_p \|f(p)\|_2^2 = \min_p \left\| R + w_1 \cdot \frac{1}{FE_L} + w_2 \cdot \frac{1}{CL_P} \right\|_2^2 \qquad (4)$$

where R represents the residuals, i.e., the differences between model insulin response and measured insulin data; the second and the third terms are regularization terms added as constraints to the minimization problem in order to facilitate a posteriori identifiability. This terms take into consideration that FE_L and CL_P should not assume values close to zero. Trust-region-reflective algorithm was preferred and lower and upper bounds for the parameters were set at $(0; +\infty)$. Function and step-size tolerances were set to 10^{-15}.

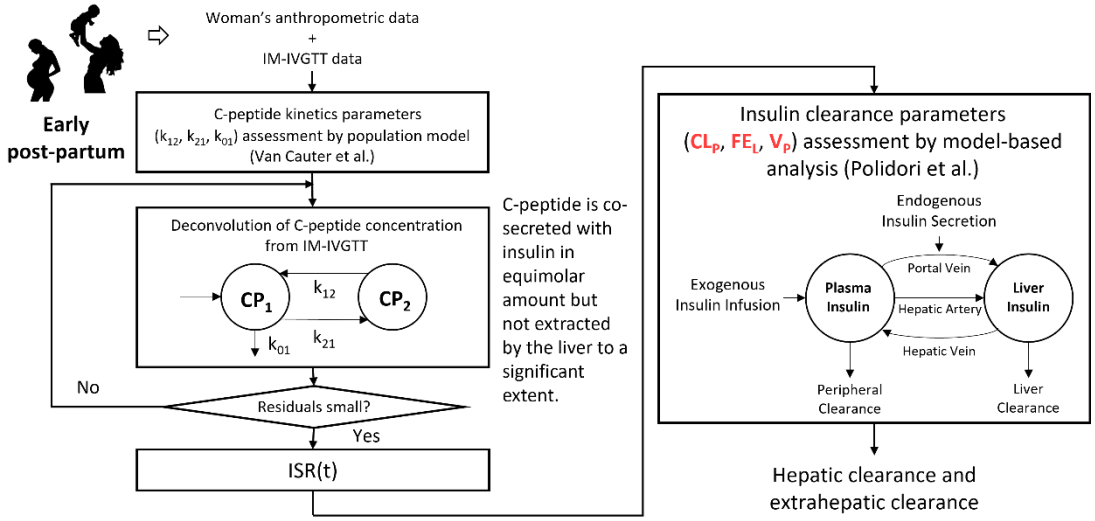

Figure 3. Model-based assessment of insulin clearance from IM-IVGTT data collected early postpartum. ISR(t) is insulin secretion rate; CL_P is the peripheral insulin clearance; FE_L is the hepatic fractional extraction; V_P is the extrahepatic distribution volume.

2.1.2 Declination of the research question

Insulin clearance evaluation in women who experienced GD during pregnancy was limited to the sole assessment of the overall process without distinguishing between hepatic and extrahepatic contributions. Weather differences in insulin clearance may be due to one or both of these two components may be investigated through the proposed approach based on Polidori et al. However, it has to be noted that the standard time frame of IM-IVGTT is 3 hours, which is a very long time for routinely application. Thus, assessing the reliability of a shorter IM-IVGTT (e.g., 1 hour long) may enhance applicability of such model-based method.

To answer this double question, application of the presented method for the assessment of hepatic and extrahepatic insulin is performed and it is done considering firstly the overall 3-hour data (3-hour IM-IVGTT experiment) and then limiting the data to 1 hour (1-hour IM-IVGTT experiment).

2.1.3 Study population and experiment

Data considered were existing data [59] that included 156 women analyzed early postpartum (4–6 months after delivery), subdivided in 115 who experienced GD and 41 who had a healthy pregnancy, thus considered the control group.

All the subjects underwent a 3-hour IM-IVGTT with glucose injection at time 0–0.5 min (0.3 g/kg) and insulin (0.03 U/kg, Humulin R; Eli Lilly, Indianapolis, IN) intravenous infusion at time 20 for 5 min [10]. For the original 3-hour IM-IVGTT experiment, blood sampling for the measurement of glucose ($mmol \cdot L^{-1}$), insulin ($pmol \cdot L^{-1}$) and C-peptide ($pmol \cdot L^{-1}$) concentrations was done with the following sampling scheme: [0, 3, 4, 5, 6, 8, 10, 14, 19, 22, 27, 30, 35, 40, 50, 70, 100, 140, 180] min. For the 1-hour IM-IVGTT experiment, the previous measurements were considered, but excluding samples taken after 60 min. For each subject, mean glucose, insulin and C-peptide concentrations were evaluated as the ratio between the related area under the curve and the test duration. Demographic characteristics of the considered population is reported in Table I.

Table I Demographic characteristics for the study population.

Demographic information	Control group	GD
Age (years)	31.6 ± 0.8	33.4 ± 0.4
BW (kg)	67.5 ± 11.9	75.5 ± 16.7 *
H (m)	1.66 ± 0.05	1.65 ± 0.08
BSA (m^2)	1.76 ± 0.15	1.85 ± 0.22 *
G_b ($mmol \cdot L^{-1}$)	4.56 [0.39]	4.94 [0.78] *
I_b ($pmol \cdot L^{-1}$)	46 [28]	47 [30]
CP_b ($pmol \cdot L^{-1}$)	150 [50]	166 [93]
G_{mean} ($mmol \cdot L^{-1}$)	4.63 [0.68]	5.39 [1.01] *
I_{mean} ($pmol \cdot L^{-1}$)	197 [113]	218 [116]
CP_{mean} ($pmol \cdot L^{-1}$)	178 [91]	218 [156] *

BW: Body Weight; H: Height; BSA: Body Surface Area; G_b, I_b, CP_b: Basal glucose, insulin, and C-peptide concentration; G_{mean}, I_{mean}, CP_{mean}: Mean glucose, insulin, and C-peptide concentration during the test. Values are expressed as mean ± standard deviation or as median [interquartile range]; * $p<0.05$.

2.1.4 Results

Results showed that the model was able to capture the dynamic plasma insulin profile in both IM-IVGTT experiments, as depicted in Figure 4. Values for model parameters (CL_P, FE_L and V_P) obtained considering the 3-hour IM-IVGTT and limiting the IM-IVGTT data to 1 hour are reported in Table II. Unpaired Student's t-test was used to test differences in mean values of variables between groups; paired Student's t-test was used to test differences in mean values of variables between the 3-hour and 1-hour IM-IVGTT. No significant difference was found in mean values between 3-hour and 1-hour IM-IVGTT. According to the two one-sided test for equivalence, i.e., TOST, performed to test the minimum equivalence margin (epsilon parameter), all the parameters estimated from the 1-hour IM-IVGTT data were shown to be equivalent to those estimated from the 3-hour IM-IVGTT data, with small equivalence margins: epsilon was in fact not higher than 0.1 standard deviation of the estimated parameter value from the 3-hour IM-IVGTT. No significant difference was also detected in model parameters (CL_P, FE_L and V_P) between control and GD groups, neither with 3-hour IM-IVGTT nor with 1-hour IM-IVGTT (Table II). Log-transformed values were used in case of skewed distributed variables.

Table II Model parameters and insulin clearance values for 3-hour and 1-hour IM-IVGTT for Control and GD groups.

		3-hour IM-IVGTT	1-hour IM-IVGTT	p-value
CL_P	**Control**	0.27 [0.43]	0.27 [0.43]	0.83
($L \cdot min^{-1}$)	**GD**	0.23 [0.30]	0.23 [0.29]	0.17
	p-value	0.63	0.64	
FE_L	**Control**	50.9 [11.6]	50.9 [11.7]	0.23
(%)	**GD**	49.7 [14.3]	50.2 [15.1]	0.57
	p-value	0.62	0.63	
V_P	**Control**	2.70 [4.00]	2.70 [4.00]	0.18
(L)	**GD**	2.01 [2.99]	2.01 [2.99]	0.19
	p-value	0.91	0.92	

CL_P: peripheral insulin clearance; FE_L: hepatic fractional extraction; V_P: extrahepatic distribution volume. Values are expressed as median [interquartile range].

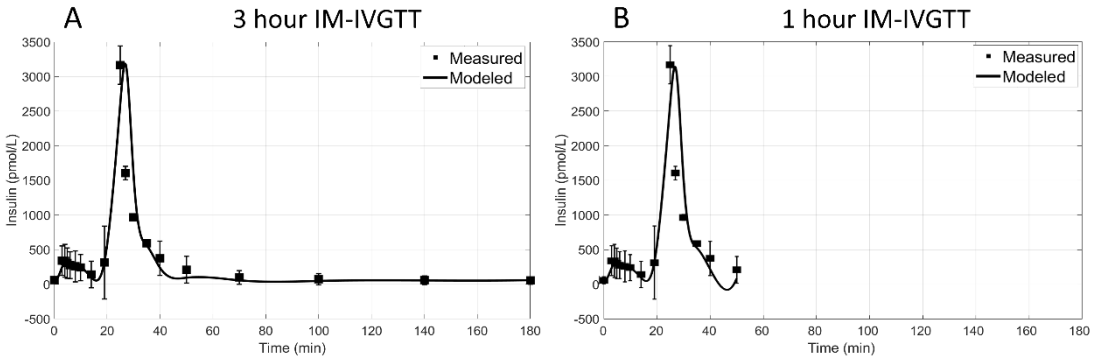

Figure 4 Comparison between mean measured plasma insulin concentrations and model outputs during the 3-hour (panel A) and the 1-hour (panel B) IM-IVGTT. Data are reported as mean ± standard deviation.

2.1.5 Discussion

The main findings that are worth being highlighted were:

- the reliability of short (1 hour) IM-IVGTT to assess hepatic and extrahepatic insulin clearance in women with a history of GD;
- the outcome, saying that at 4-6 months after delivery neither the hepatic clearance nor the extrahepatic clearance were different between the GD women and the control group with healthy pregnancy.

Indeed, with a simplified procedure the adherence to screening may improve and facilitate the early detection of possible metabolic impairments and reduce the risk of developing T2D [60]. Moreover, assessment of both components of insulin clearance improves characterization of the metabolic status, that can be added to other

parameters assessed from short and regular IVGTTs [61], [62], [63] . However, even if short IM-IVGTT is convenient with respect to the regular one, it is still more invasive than the OGTT, thus depending on the purpose it would be preferred to use modeling methodologies based on the OGTT instead of the IVGTT (in its different versions) [64], [65], [66].

With respect to the original modeling approach by Polidori et al., in the implementation that have been presented here, some improvements were introduced: numerically speaking, adding regularization terms to the minimization problem was done to enhance a posteriori identifiability; then, avoiding the configuration based on a saturable hepatic clearance dynamics did not prevent obtaining good results, thus arguing that, at least for this population, the linear dynamics sufficiently reflects the underlying physiology.

2.1.6 Optimization of experiments

At this point, is worth mentioning the contribution that physiological system modeling may provide not only when used for the assessment of parameters of interest, but also in applications were the methodological aspect concerning modeling of the system help obtaining advantages in experimental setups. For instance, the above presented approach revealed that the number of samples that should be withdrawn from the subject during an IM-IVGTT can be reduced without significant loss of information, in relation to the proposed application. Regularization techniques are also valuable in this sense.

A recent model of the glucose-insulin regulatory system developed by Contreras et al. exploited regularization in order to address identifiability problems in the case of a short OGTT (5-samples OGTT) and was able to demonstrate that with a lower number of collected samples it was possible to reliably estimate all the13 model parameters [67]. It was then demonstrated, in a study by our research team, that by leveraging a simplified regularization procedure is still possible to obtain satisfying results through such glucose-insulin system model and also to adapt its use to the case of a 4-samples OGTT [68]. In this latter case, however, 4 out the 13 parameters were fixed and optimal values for such parameters have been proposed.

2.2 Hepatic and extrahepatic insulin clearance in mice with incretin receptor knockout

Insulin clearance may depend on genetic other than metabolic variables [69] but also depend on many factors [70]. The incretin effect, a physiological process responsible for the potentiation of insulin secretion after food ingestion, may be one of those. Such potentiation is mainly accomplished thanks to the presence of incretin receptors on the pancreatic β-cells, and plays a role in the regulation of plasma insulin concentration. The main incretin hormones are the glucagon-like peptide-1 (GLP-1) and the glucose-dependent insulinotropic polypeptide (GIP) [71], [72]. Some studies started to investigate the possible effect of incretins on total insulin clearance [73], [74], [75] or on its hepatic component [76], [77], showing controversial results. Moreover, studies have been recently carried out in mice and showed that physiological levels of incretin hormones may reduce insulin clearance [78], but without determining if this reduction is attributable to its hepatic or extrahepatic component. Similarly to the previous, this section addresses the theme of hepatic and extrahepatic insulin clearance, but proposes a novel fine approach for its assessment.

2.2.1 A novel model-based method for the assessment of hepatic and extrahepatic insulin clearance

A novel methodology inspired by the previously proposed mathematical approach by Polidori et al. [54] was developed to assess hepatic and extrahepatic insulin clearance. The proposed methodology is detailed in the following.

Description of the model-based approach

According to the approach proposed and presented in the previous section, the hepatic disappearance rate, HR(t), was assumed linear with respect to insulin delivery to the liver, as previously reported in equation (1), and the extrahepatic disappearance rate, CR, was assumed proportional to the plasma insulin concentration, as previously reported in equation (2). Thus, equation (3), describing changes in the plasma insulin compartment (characterized by the distribution volume V) can be rewritten as follows:

$$V \cdot \frac{dI(t)}{dt} = ISR(t) - FE_L \cdot \big(ISR(t) + HPF \cdot I(t)\big) - CL_P \cdot I(t) \quad (5)$$

Then, total insulin disappearance rate can be described as the sum of HR and CR:

$$FE_L \cdot \big(ISR(t) + HPF \cdot I(t)\big) + CL_P \cdot I(t) = CL_T \cdot I(t) \quad (6)$$

where CL_T is the total insulin clearance ($L \cdot min^{-1}$), I(t) is the plasma insulin concentration measured during the test and ISR(t) was computed according to Van Cauter et al. [57] by deconvolution from plasma C-peptide concentration starting from computed individualized C-peptide kinetic parameters.

From equations (5) and (6) it is possible to consider their temporal integral calculated between initial and final time points of the test, indicated as t_i and t_f, thus obtaining:

$$\int_{t_i}^{t_f} V \cdot \frac{dI(t)}{dt} dt = \int_{t_i}^{t_f} ISR(t) - FE_L \cdot \big(ISR(t) + HPF \cdot I(t)\big) - CL_P \cdot I(t)\ dt \quad (7)$$

$$\int_{t_i}^{t_f} FE_L \cdot \big(ISR(t) + HPF \cdot I(t)\big) + CL_P \cdot I(t)\ dt = \int_{t_i}^{t_f} CL_T \cdot I(t)\ dt \quad (8)$$

Integration provides the following two algebraic equations:

$$[I(t_f) - I(t_i)] = AUC_{SECR} - FE_L \cdot (AUC_{SECR} + HPF \cdot AUC_I) \quad (9)$$

$$FE_L \cdot (AUC_{SECR} + HPF \cdot AUC_I) + CL_P \cdot AUC_I = CL_T \cdot AUC_I \quad (10)$$

where $I(t_i)$, $I(t_f)$, AUC_{SECR} and AUC_I are quantities that can be computed from the measured data, representing plasma insulin concentration at the initial and final time points, and the area under the curve of ISR(t) and I(t), respectively; HPF has been assumed equal to 2 L/h/kg of body weight [79]; CL_T and V were estimated by exploiting the mathematical modeling approach proposed by Tura et al. [78] ,which assumes a mono-compartmental description for insulin kinetics. In the latter approach ISR(t) is the model input and I(t) represents the model output. In addition to equations (9) and (10), a third equation taken from [17] and describing hepatic fractional extraction, FE_L, was considered:

$$FE_L = \frac{(AUC_{CP} \cdot CL_{CP} - AUC_I \cdot CL_T)}{(AUC_{CP} \cdot CL_{CP})} \quad (11)$$

where CL_{CP} is the C-peptide clearance; AUC_{CP} is the area under the curve of C-peptide and AUC_I that of insulin.

Parameter estimation

The three algebraic equations (9), (10), and (11), considered as a homogeneous system, were subsequently used as elements of a cost function that was minimized to reach an estimation of FE_L and CL_P parameters. The summary of the procedure is depicted in Figure 5. Minimum of cost function was obtained using the *lsqnonlin* function in MATLAB.

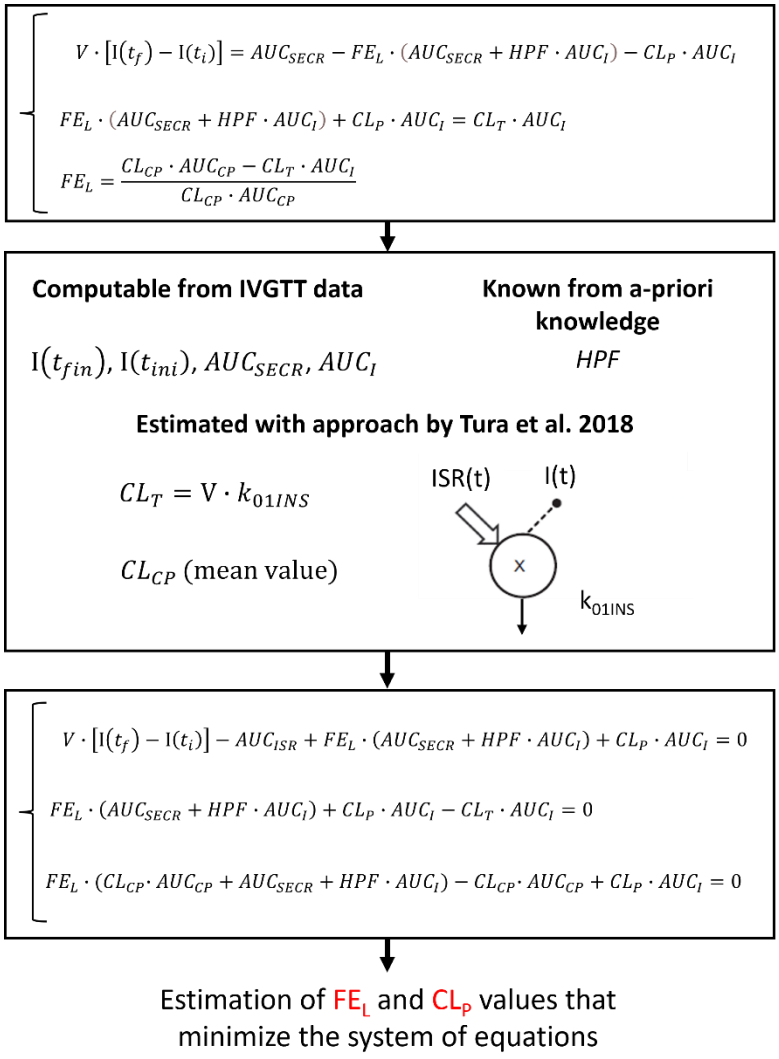

Figure 5. Summary of the methodology to assess hepatic and extrahepatic insulin clearance. V: distribution volume; ISR(t): insulin secretion rate; FE_L: hepatic insulin clearance; HPF(t): hepatic plasma flow rate; I(t): plasma insulin concentration; CL_P: extrahepatic insulin clearance; CL_T: total insulin clearance; CL_{CP}: C-peptide clearance; AUC_{CP}: area under the curve of C-peptide; AUC_I: area under the curve of insulin; AUC_{SECR}: area under the curve of ISR(t); t_i, t_f: initial and final time of test.

2.2.2 Declination of the research question

Double incretin receptor knockout (DIRKO) is a mouse model characterized by knockout of both the GLP-1 and GIP receptors and for this reason it does not have incretin effect and represent a model of interest for the study of this process when compared to wild-type (WT) mice, which instead does not present any receptor knockout. Moreover, differently from single incretin receptor knockout mice, knockout of both incretin receptors prevents the possibility that one hormone compensates for the lack of biological action of the other.

Whether incretins at physiological, non-stimulated levels affect hepatic and/or extrahepatic insulin clearance was still an open question. To this purpose, application of a mathematical modeling approach able to segregate hepatic and extrahepatic components is a valuable option to investigate the issue.

Animal dataset

Hepatic and extrahepatic insulin clearance was studied in 31 DIRKO and 45 WT female mice, previously analyzed in another study [78]. During experimental days, animals were fasted from 7.30 AM and after 5 h of fasting, mice were firstly anesthetized and after 30 min, an IVGTT was performed; Glucose was injected in a tail vein at a dose of 0.35 g/kg and blood samples were collected before and at [0, 1, 5, 10, 20, and 50] min after glucose administration.

Assessment of parameters of interest

In response to a glucose input like the one administered during an IVGTT, insulin is commonly known to be secreted in a biphasic pattern consisting of two phases: a first phase lasting around 5 min, and a second phase where insulin is released in a sustained manner with usually distinct pulses lasting few minutes each. The method summarized in Figure 5 was used to estimate two pairs of values ($FE_{L\text{-}P1}$, $CL_{P\text{-}P1}$, and $FE_{L\text{-}P2}$, $CL_{P\text{-}P2}$) accounting for the first and second phase hepatic and extrahepatic clearances. The first phase parameters were estimated assuming $t_i = 0$ min and $t_f = 5$ min, while for the second phase parameters, the initial and final time points were $t_i = 5$ min and $t_f = 50$ min. Insulin and C-peptide plasma concentrations were used for the estimations. To be

consistent, the total clearance was also estimated for first and second phase, denoted as $CL_{T\text{-}P1}$ and $CL_{T\text{-}P2}$.

In order to better characterize the problem, a detailed metabolic description can be achieved by assessing other IVGTT-based indexes accounting for different physiological processes as for: glucose tolerance, computed as the K_G index [80]; acute insulin response to glucose (AIR_G), computed as average suprabasal insulin between 1 and 5 min after glucose administration; insulin sensitivity during the IVGTT (SI), as an empirical parameter predicting insulin sensitivity from the minimal model approach [18,19]; insulin sensitivity at fasting state, as QUICKI index [81]; glucose effectiveness (S_G) [80], [82]; disposition index (DI), as product between SI and AIR_G, similarly to what has been done in human subjects[83]; β-cell function, as ratio of area under the curve of C-peptide to that of glucose, extending an approach used in human subjects [84]; area under the curve of the insulin secretion rate AUC_{SECR} calculated as previously indicated according to Van Cauter et al. [57].

2.2.3 Results

Values for hepatic, extrahepatic and total insulin clearance in the first and second phase of the IVGTT are reported in Table III for both DIRKO and WT mice. A significant difference between DIRKO and WT was found in $CL_{T\text{-}P1}$, which was reflected in the peripheral (i.e., extrahepatic) component, $CL_{P\text{-}P1}$, but not in the hepatic component, $FE_{L\text{-}P1}$. No difference was detected in $CL_{T\text{-}P2}$ in any of its components, that is, neither in $CL_{P\text{-}P2}$ nor in $FE_{L\text{-}P2}$. In addition, the ratio between the two insulin clearance components was statistically different between the two groups for the first phase ($p=0.03$) but not for the second phase ($p=0.30$).

A detailed IVGTT-based metabolic assessment for DIRKO and WT mice is reported in Table IV. Statistically significant differences were found in K_G, S_G, DI, SI, and AUC_{SECR}, accounting for the glucose tolerance index, the glucose effectiveness, the disposition index, the insulin sensitivity during the IVGTT and the area under the curve of the insulin secretion rate calculated from C-peptide. β-cell sensitivity (computed as ratio of AUC of C-peptide to AUC of glucose) showed borderline p-value. Insulin sensitivity at fasting, QUICKI, showed no difference.

Table III Values for hepatic, extrahepatic and total insulin clearance in the first and second phase of the IVGTT for DIRKO and WT mice.

		WT	DIRKO	p-value
First phase	FE_{L-P1} (%)	28.9 [25.7-32.0]	29.7 [26.7-34.9]	0.18
	CL_{P-P1} (10^{-3} l·min^{-1})	0.15 [0.11-0.22]	0.18 [0.13-0.27]*	0.04
	CL_{T-P1} (10^{-3} l·min^{-1})	0.51 [0.46-0.65]	0.61 [0.48-0.82]*	0.02
Second phase	FE_{L-P2} (%)	39.8 [35.8-44.2]	37.8 [35.1-43.1]	0.46
	CL_{P-P2} (10^{-3} l·min^{-1})	0.79 [0.69-0.87]	0.72 [0.64-0.81]	0.27
	CL_{T-P2} (10^{-3} l·min^{-1})	1.69 [1.48-1.87]	1.38 [1.13-1.75]	0.10

Data reported as median [interquartile range]; FE_{L-P1}, CL_{P-P1}, CLT-P1: hepatic, extrahepatic and total insulin clearance in the IVGTT first phase, respectively; FE_{L-P2}, CL_{P-P2}, CL_{T-P2} hepatic, extrahepatic and total insulin clearance in the IVGTT second phase, respectively; * $p<0.05$ DIRKO vs. WT.

Table IV. Metabolic assessment for DIRKO and WT mice.

	WT	DIRKO	p-value
K_G (%/min)	2.49 [1.85-3.14]	1.98 [0.96-2.41]*	<0.01
S_I (10^{-4} min^{-1}/pmol/l)	1.37 [0.97-1.78]	0.85 [0.77-1.39]*	<0.01
QUICKI (non- dim.)	0.123 [0.119-0.126]	0.120 [0.116-0.123]	0.07
S_G (min^{-1})	0.052 [0.037-0.063]	0.037 [0.028-0.055]*	0.02
AIR_G (pmol/l)	445 [288-635]	426 [195-634]	0.16
DI (10^{-3} min^{-1})	1.17 [0.70-1.64]	0.72 [0.34-1.03]*	0.02
AUC_{SECR} (pmol)	13.0 [12.0-16.8]	17.0 [14.3-21.0]*	<0.01
β-cell sensitivity (mmolCP/mmolGlu)	0.022 [0.018-0.027]	0.025 [0.021-0.030]	0.05

Data reported as median [interquartile range]; K_G: intravenous glucose tolerance index; SI: insulin sensitivity during the IVGTT; QUICKI: insulin sensitivity at fasting; S_G: glucose effectiveness; AIR_G: acute insulin response to glucose; DI: disposition index; AUC_{SECR}: area under the curve of insulin secretion rate; β-cell sensitivity: ratio of area under the curve of C-peptide to area under the curve of glucose; * $p<0.05$ DIRKO vs. WT.

Univariable linear regression analysis was used to assess associations between insulin clearance and the other metabolic parameters. Tests were applied to the log-transformed values. The two-sided significance level was set at 5% ($p < 0.05$).

Results of linear regression analysis to evaluate associations between insulin clearance and the other metabolic parameters are not shown for conciseness, but the most significant associations are reported in Figure 6.

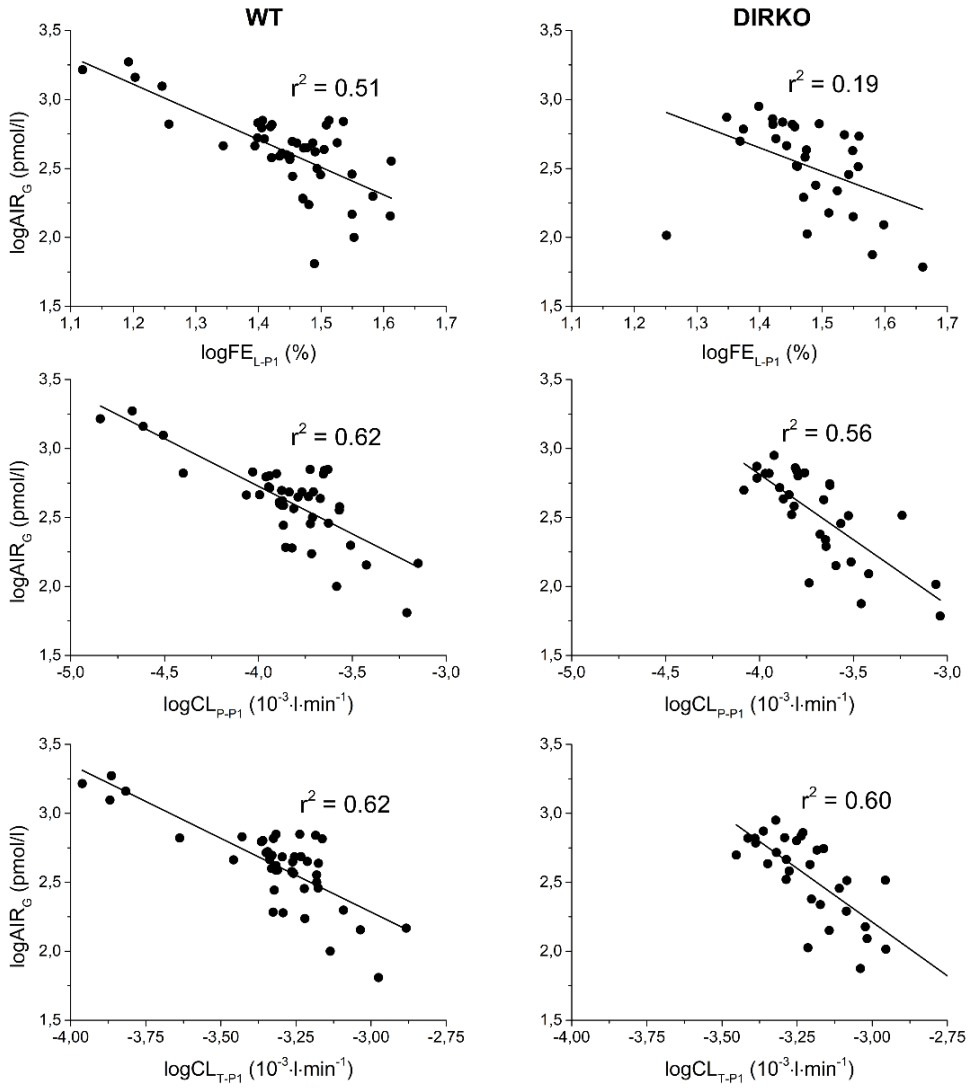

Figure 6. Most significant associations (r2) of hepatic, extrahepatic and total insulin clearance with metabolic parameters in DIRKO and WT mice. FEL-P1, CLP-P1, CLT-P1: hepatic, extrahepatic and total clearance during the first phase of the test, respectively; AIRG: acute insulin response to glucose.

2.2.4 Discussion

It was investigated whether the reduction in insulin clearance reduction previously observed in DIRKO compared to WT mice (under non-stimulated levels of incretin hormones) is explained by a reduction in its hepatic or extrahepatic component, or both. It emerged that:

- the hepatic component of insulin clearance (quantified by FEL), did not show differences in DIRKO compared to WT mice for any of the two IVGTT phases; this may be explained with reference to the role of carcinoembryonic antigen-related cell adhesion molecule 1 (CEACAM1) through which insulin stimulates its own clearance in hepatocytes [85], [86], [87]; indeed, FEL during the first phase is significantly correlated with first-phase insulin secretion (i.e., AIRG), but no difference has been detected between DIRKO and WT mice in AIRG, thus suggesting that expression of CEACAM1 in the liver was unaltered among the two.
- as the most interesting finding, during the first phase of the IVGTT, the higher total insulin clearance in DIRKO than in WT may be due to the higher extrahepatic component; indeed, kidneys are the primary site of extrahepatic insulin clearance [88], [89] with the major enzyme responsible for degradation (IDE) being regulated by a protein belonging to the SNXs family [90], that themselves affect GLP-1 receptor [91]; thus, since WT mice express GLP-1 receptors and DIRKO does not, we can hypothesize that the difference observed in the extrahepatic insulin clearance can be linked to that mechanism; on the other hand little is known about GIP role on insulin clearance regulation, and the few published studies support the idea that GIP does not affect insulin clearance [73].

To conclude, these findings may help to shed light in the mechanisms involving insulin clearance and in their possible role in the pathogenesis of type 2 diabetes. In fact, T2D therapy based on incretins is increasing its interest and the knowledge of the relative importance the two components of insulin clearance and how they are related to the

incretin system may be of help in addressing possible defects in the balance between these mechanisms.

2.3 Mathematical model accounting for a dual regulation of glucagon inhibition

Glucagon is a hormone secreted by the α-cells of the pancreas and it has the effect of elevating blood glucose level when it drops under normal values. Thus, it has an opposite action with respect to insulin in maintaining glucose homeostasis. However, beyond simple counter regulation of insulin, glucagon also show a role in pathophysiology of T2D, but this is still controversial [92]. Indeed, people with T2D have secretory defects of glucagon, resulting in inappropriate high levels in both fasting and postprandial states; opposite to this, also beneficial effects have been observed [93].

The regulation of glucagon secretion is mainly due to the α-cell paracrine control by insulin (i.e., the control exerted by neighboring β-cells secreting insulin according to the so-called "intra-islet interaction"), but other factors may contribute to control glucagon secretion or inhibition and glucose may play a not-negligible role. Indeed, studies performed considering different macronutrients ingestion in healthy and in T2D subjects demonstrated that heterogeneous glucagon time patterns and their relationship with glucose and insulin strongly depends on the class of nutrients ingested [94], [95].

2.3.1 Model of glucagon kinetics to assess α-cell insulin and glucose sensitivity

Mathematical models accounting for glucagon contribution have been proposed, few having potential application to the clinical practice [96], [97], [98], [99], [100], [101], [102]. Among these, the models by Kelly et al. [102] and Subramanian et al. [101] were based on intravenous tests, which however are more difficult to perform compared to an OGTT. Instead, our group proposed a mathematical (compartmental) model for the description of glucagon kinetics during an OGTT for the estimation of α-cell insulin sensitivity [103]. The model presented in this thesis has been developed starting from such a model, and includes two differential equations, one for plasma

glucagon and one for C-peptide (marker of insulin secretion). In the new model formulation, plasma glucose is included as model input in addition to plasma C-peptide. The model provides two parameters of possible clinical relevance, namely S_{GLUCA} and k_G (α-cell insulin and glucose sensitivity, respectively).

Model formulation

The proposed model considers inhibition of glucagon secretion during an OGTT as controlled by both insulin (C-peptide) and glucose-based mechanisms. The latter, being the novelty with respect to the previous formulation, accounted for glucokinase activity[104], and was modelled considering glucagon inhibition controlled by the rate of change in plasma glucose. The former, exploited plasma C-peptide as a marker of insulin secretion as already done in the previous formulation The compartmental description is depicted in Figure 7.

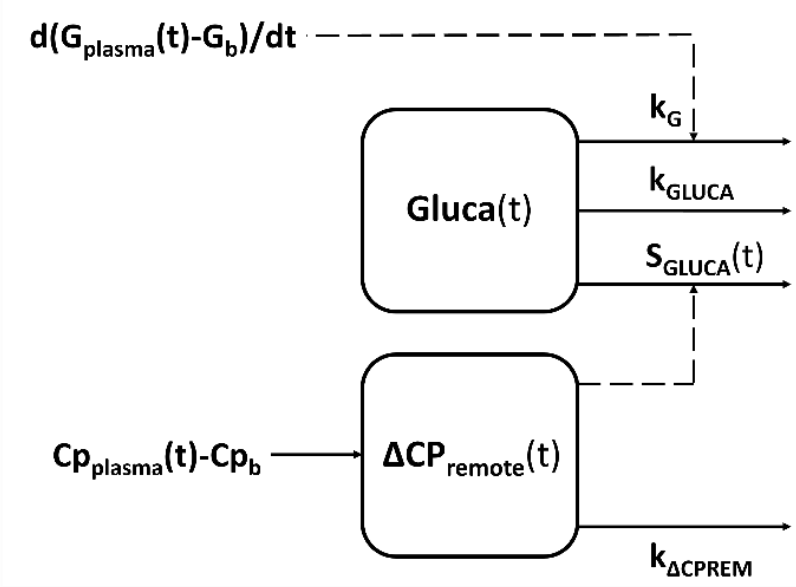

Figure 7. Schematic representation of the compartmental model. The two compartments of the model are the plasma glucagon compartment, Gluca(t), and a delayed version of remote (from plasma) C-peptide, $\Delta CP_{remote}(t)$; the suprabasal C-peptide concentration in the remote compartment ($Cp_{plasma}(t)$-Cp_b) and the rate of change of suprabasal plasma glucose concentration ($G_{plasma}(t)$-Gb) exert a control action on Gluca(t) through the parameters $S_{GLUCA}(t)$ and k_G, respectively. k_{GLUCA} denotes glucagon elimination rate from plasma and $k_{\Delta CPREM}$ is the C-peptide elimination rate from the remote compartment.

Two compartments, one for plasma glucagon and one for remote (from plasma) C-peptide, are used for model representation, as for the following two differential equations:

$$\frac{dGluca(t)}{dt} = -k_{GLUCA}(t) \cdot Gluca(t) - k_G \cdot \frac{dG_{plasma}(t)}{dt} - S_{GLUCA}(t) \cdot \frac{d\Delta CP_{remote}(t)}{dt} \quad Gluca(t) = Gluca_b \tag{12}$$

$$\frac{d\Delta CP_{remote}(t)}{dt} = -k_{\Delta CPREM} \cdot \Delta CP_{remote}(t) + \left(CP_{plasma}(t) - CP_b\right) \quad \Delta CP_{remote}(0) = 0 \tag{13}$$

where Gluca(t) ($ng \cdot L^{-1}$) is glucagon concentration in the plasma compartment and $\Delta CP_{remote}(t)$ ($nmol \cdot L^{-1}$) is suprabasal C-peptide concentration in a compartment remote from plasma. The clearance-rate parameter k_{GLUCA} (min^{-1}) accounts for glucagon elimination from plasma due to clearance; the parameter k_G accounts for glucagon inhibition due to mechanisms controlled by the rate of change in plasma glucose (G_{plasma}, $mmol \cdot L^{-1}$) and represents the glucagon-inhibition sensitivity to glucose (i.e., α-cell glucose sensitivity); the time-varying parameter $S_{GLUCA}(t)$ (ng of glucagon·nmol of C-peptide^{-1}) accounts for glucagon inhibition due to paracrine mechanisms controlled by suprabasal C-peptide in a compartment remote from plasma and represents glucagon-inhibition sensitivity to glucose-induced insulin secretion (i.e., alpha-cell insulin sensitivity). Parameter $k_{\Delta CPREM}$ (min^{-1}) is the C-peptide elimination rate from the remote compartment; CP_{plasma} represents plasma C-peptide concentration (with CP_b as basal value). G_{plasma} e CP_{plasma} are the model inputs.

Parameter estimation

Model parameter vector p=[k_{GLUCA}, $k_{\Delta CPREM}$, k_G, $S_{GLUCA}(t)$] was estimated using the *lsqnonlin* MATLAB function, solving the following nonlinear least-squares curve fitting problem:

$$\min_P \|f(p)\|_2^2 = \min_P \left[RSS + k_{GLUCA} + \frac{1}{k_G} + w1 \cdot S''_{GLUCA}(t) + w2 \cdot count(S_{GLUCA}(t) < 0)\right] \tag{14}$$

where RSS is the residual sum of squares, with residuals being the differences between model response and glucagon experimental measurements, and the other terms are added constraints that have been used to introduce further information to the problem: k_{GLUCA} denotes glucagon clearance and it should be small during an OGTT, during which the main contribution to glucagon suppression is given by insulin and glucose-based mechanisms; the term $1/k_G$ is used to prevent excessively small parameter

values; S_{GLUCA}''(t), the second derivative of the parameter S_{GLUCA}(t), is used to penalize abrupt changes of the parameter during the test; similarly, the term *count*(S_{GLUCA}(t)<0) acts to reduce the number of samples where the parameter assumes negative values. Value for w1 and w2 weights was manually adjusted, the trust-region-reflective algorithm was chosen, and function and step-size tolerances were set to 10^{-6}. Lower and upper bounds of parameter ranges were: (0,1) for k_{GLUCA} and $k_{\Delta CPREM}$; (-∞, +∞) for kG and S_{GLUCA}(t); 95% confidence intervals (CIs) for all the model parameter estimates have been computed by means of the *nlparci* function.

2.3.2 Declination of the research question

Glucagon relationship with glucose and insulin is highly heterogenous and an attempt to capture such heterogeneity may lead to the importance of a model including different contributors of glucagon secretion. In addition, this may be of impact in understanding how postprandial response and other mechanisms may change in relation to T2D state, to different macronutrients ingestion, or both. Thus, this study aimed at providing an improved formulation of the previously proposed mathematical model to describe glucagon kinetics (especially, its inhibition) during an OGTT, by accounting for the two (insulin and glucose-based) mechanisms.

2.3.3 Model validation on mean experimental data

Mean experimental data used to validate the model are those reported in the study by Sonne et al. [105] involving 15 subjects having T2D and 15 healthy control subjects (CNT), all of which underwent a 75 g OGTT with blood samples drawn at [-20, -10, 0, 15, 30, 45, 60, 90, 120, 180, 240] min and with glucose ingestion at 0 min. Mean plasma glucose, C-peptide and glucagon concentrations in the two groups of the study by Sonne et al. [105] have been considered. Results are reported as means±SD. unless otherwise stated.

2.3.4 Results

The parameter estimates with related confidence intervals are reported in Table V and best fit on mean experimental data reported by Sonne et al. [105] for CNT and T2D groups are shown in Figure 8. Trends of S_{GLUCA}(t) for CNT and T2D during the test is

reported in Figure 9. According to the 95% CIs, 4 out of 8 time points in the CNT group showed estimates of $S_{GLUCA}(t)$ significantly different from zero, whereas in the T2D group the same parameter did not show values significantly different from 0 throughout the whole test. As for k_G, lower values were found in T2D than in CNT; in the latter a significant difference from 0 was found.

Table V. Values and 95% confidence intervals (CI) for the estimates of K_{GLUCA} (min^{-1}), $K_{\Delta CPREM}$ (min^{-1}), K_G (min^{-1}), S_{GLUCA} (ng of glucagon·nmol of C-Peptide^{-1}) on reference mean experimental data by Sonne et al. [14] for the control group and for the T2D group.

	Estimated parameter	Value	95% CI [a]
CNT [b] Group	k_{GLUCA}	$4.6673\ 10^{-6}$	-0.0073 – 0.0073
	$k_{\Delta CPREM}$	0.0342	0.0290 – 0.03945
	k_G	2.8302	1.1973 – 4.4632
	S_{GLUCA1}	-0.7993	-0.7994 – -0.7993
	S_{GLUCA2}	-0.1515	-0.5332 – 0.2302
	S_{GLUCA3}	0.4620	0.1819 – 0.7420
	S_{GLUCA4}	0.4449	0.2228 – 0.6670
	S_{GLUCA5}	0.2375	-0.1428 – 0.6177
	S_{GLUCA6}	0.4780	-0.3364 – 1.2924
	S_{GLUCA7}	0.7629	0.1537 – 1.3720
	S_{GLUCA8}	0.2069	-0.6035 – 1.0174
T2D [c] Group	k_{GLUCA}	$9.1763\ 10^{-6}$	-0.0139 – 0.0139
	$k_{\Delta CPREM}$	0.0096	-0.0078 – 0.0270
	k_G	0.9913	-0.5559 – 2.5386
	S_{GLUCA1}	-5.5602	-12.9854 – 1.8651
	S_{GLUCA2}	-2.8988	-7.6482 – 1.8506
	S_{GLUCA3}	-0.3694	-3.1971 – 2.4583
	S_{GLUCA4}	1.1067	-0.5668 – 2.7802
	S_{GLUCA5}	0.8949	-0.1576 – 1.9473
	S_{GLUCA6}	0.1305	-0.8600 – 1.1210
	S_{GLUCA7}	0.7260	-0.6903 – 2.1423
	S_{GLUCA8}	0.2069	-4.1746 – 3.1374

[a] CI: Confidence Interval; [b] CNT: Control; [c] T2D: Type 2 Diabetes.

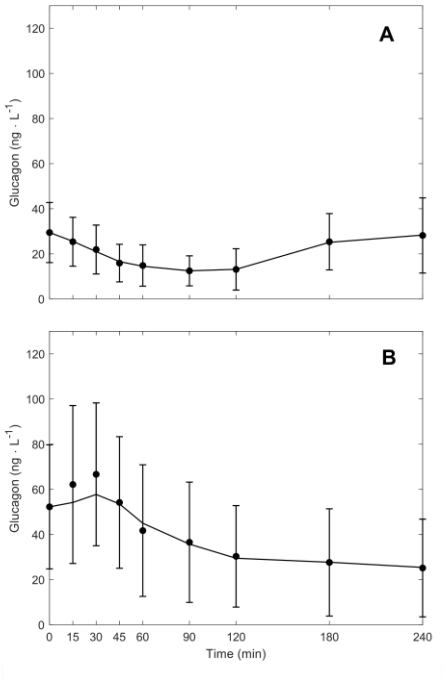

Figure 8. Best fit of the model validated on mean experimental data by Sonne et al for the control group (panel A) and for the T2D group (panel B). Closed circles are the reference experimental values (mean ± SD); the continuous line is the model prediction.

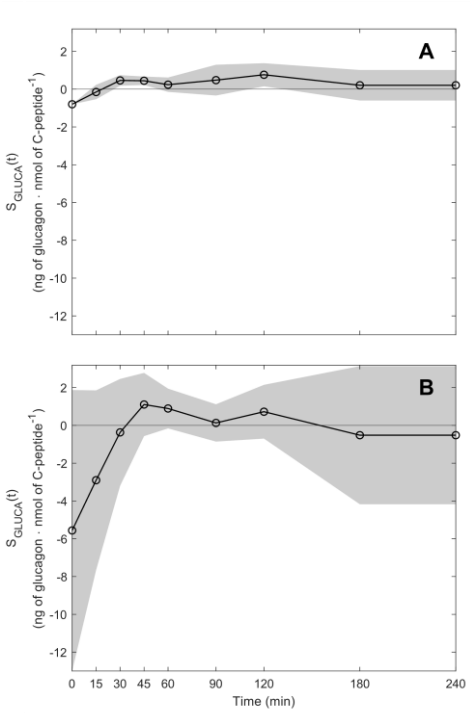

Figure 9. $S_{GLUCA}(t)$ temporal estimates on reference mean experimental data for the control group (panel A) and for the T2D group (panel B) are shown with open circles and continuous line. Dashed lines represent related 95% CIs.

2.3.5 Discussion

This study proposed a mathematical model derived from a former formulation proposed by our group and able to describe sensitivity of the α-cell to insulin and glucose in the single individual during an OGTT. Thus, the main improvement of this new model formulation, was to include the contribution of mechanisms related to α-cell glucose sensing. This is of impact for understanding how mechanisms change in relation to T2D state and/or to different macronutrients ingestion. Indeed, paracrine control of glucagon secretion in T2D is compromised and shows a V-shaped non-physiological dose response to glucose with maximal exocytosis at hyperglycemia [106].

Results of model validation on mean data of healthy and T2D subjects demonstrated that:

- consistently with physiological and clinical observations, both insulin and glucose-based mechanisms may play a noticeable role in determining glucagon secretion or inhibition (thus, glucagon time course), as demonstrated by k_G and $S_{GLUCA}(t)$ values significantly different from zero in the healthy group;
- in contrast, in the T2D group, both glucagon regulation controls are impaired (S_{GLUCA} (t) and k_G not significantly different from zero), resulting in a defective glucagon inhibition.

Modeling and methodological choices were done to maintain the model as simple as possible:

- no additional compartment was added for glucose, which contribution was represented as an input
- glucose regulation mechanism was modelled as dependent on glucose-concentration rate of change rather than the absolute value, consistently with studies on animal models showing that in the α-cell the regulation of glucose sensing is operated by glucokinase [104], whose activity is driven by changes in plasma glucose [107].

- the addition of penalties in the form of constraints in the parameter estimation procedure was necessary to overcome the ill-posed problem and prevent overfitting; in particular, constraints on $S_{GLUCA}(t)$ were already included in the former model formulation with the aim of preventing excessively rapid variations and favoring the occurrence of positive rather than negative values (considering that suppression during OGTT is more likely than stimulation), while one further constraint has been added, related to k_G, to avoid its contribution being excessively small and possibly collapsing into other parameters. In addition, k_G was allowed to assume positive and negative values, indicating that, in principle, glucose may either inhibit or stimulate glucagon secretion.

As a fact, factors that have been shown to possibly modulate glucagon secretion from alpha cells are many, including nutritional, chemical and environmental factors [108], [109]. Future studies may consider the role of these other factors in the model that, as for its intended purpose, in the present model were disregarded.

2.4 Concluding remarks

The developed modeling approaches are tools that allowed representation and quantification of important metabolic processes that show different roles in diabetes pathophysiology, some of which still need to be elucidated. In particular, focus was on insulin clearance (in its hepatic and extrahepatic components) and on α-cell sensitivity to glucose and insulin. One of the main advantages of using this kind of approaches is the individual estimation of such parameters, that allow to better characterize the metabolic status in the single individuals. Indeed, being diabetes a multifaceted disease, by deconvolving the main processes behind its pathophysiology (e.g., β-cell function and insulin sensitivity) it is possible to recognize subgroups that could be object of tailored treatment and management strategies[110]. Thus, in this thesis we decided to focus on processes such as insulin clearance and α-cell sensitivity instead of the more studied ones mentioned just above, to gain further insights on the so-called “component pathways” of the disease.

For what concerns insulin clearance assessment, the novel mathematical modeling approach presented in Section 2.2 exploited adding to the Polidori et al. other independent equations linking hepatic and extrahepatic components to the total insulin clearance. In this way it was suitable for application to IVGTT test, differently from Polidori's approach, that was conceived to work with IM-IVGTT since this kind of test allows to better separate the two insulin clearance components. Of note, data derived by tests with slower dynamics as OGTTs may be not adequate to be analyzed with the modeling approach proposed in this study, since the estimates for model parameters may exhibit insufficient accuracy.

On the other hand, the modeling approach for the assessment of glucagon kinetics instead applies to a more physiological test, i.e., the OGTT, and was maintained as simple as possible as for its previous version, limiting the number of compartments and adding constraints in the parameter estimation procedure to overcome the problem of ill-posedness, very likely when relying on time varying parameters.

Overall, in addition to having potential as tools applicable in clinical contexts, constituting decision support tools themselves, system models can also:

- help in the field of investigation of new scientific evidence that can constitute an expansion of the knowledge base;
- generate parameters that can be used as features for machine learning applications.

This latter point will be further described in the next chapter (Chapter 3) through an example of application of ML to data coming from the model-based assessment of significant metabolic quantities.

3 Model-based data-driven analysis

[2]As discussed in Chapter 2, physiological system modeling allow to assess metabolic parameters that would not be directly measurable, unless in some cases applying invasive procedures sometimes not compatible with life. Such parameters may offer the opportunity to adopt the information they carry and use this information to feed machine learning algorithms. Indeed, the rationale behind the use of model-based methodologies and machine learning approaches based on features rely on the fact that, starting from not very large but well-characterized datasets, this type of approach allows obtaining reliable and more easily interpretable results compared to the use of raw data, together with the advantage of having lower computational costs and therefore being suitable for real-time applications.

To give an example of this kind of approach, this chapter propose an application of machine learning techniques to develop a framework that starting from model-based parameter assessment is intended to shed light on the factors determining the development of T2D in women who had GD during pregnancy.

3.1 Machine learning applications in type 2 diabetes and gestational diabetes and research question

As previously mentioned, gestational diabetes is a diabetes diagnosed in the second or third trimester of pregnancy that was not clearly overt diabetes prior to gestation and even if it resolves after delivery, it is associated with a high risk to develop T2D later in their life [111]. Recently, research on T2D has exploited the use of ML techniques to handle large amount of data and automatically extract knowledge from them [112]. and pursuing different purposes, including early diagnosis investigation [113], [114], [115], [116], [117], [118], [119], estimation of T2D risk [120], [121], [122], detection of subjects affected by T2D or prediabetes from the general population [123], T2D characterization, classification [124], [125] and care [126].

[2] This chapter contains material published in [283].

However, the application of such techniques to determine factors influencing development of T2D in women with a previous history of GD has still been scarcely explored and the few studies addressing this topic have focused on "omics" approaches (i.e., metabolomics, lipidomics) [127], [128], [129], which consist in the identification and determination of metabolites in biological samples of altered states promoted by disease or specific stimuli (e.g. drug or environmental modulation) in comparison to normal states [130]. Although this field is promising to allow personalized approaches, limitations and challenges need to be addressed before the translation of the research outcomes into clinical settings [131].

As far as we knew, application of ML techniques to analyze dataset containing model-based features describing parameters of physiological interest was never been performed in women with a history of GD at risk to develop T2D. Thus, aim of this chapter is to set up an ML framework to unveil the factors, among those quantifying specific metabolic processes, which determine the development of T2D in such women at risk. The rest of the chapter is structured as follows. Section 3.2 presents the methodology, including the clinical dataset used, the feature extraction step and how the classification problem was formulated; Section 3.3 presents the obtained results and, finally, in Section 3.4 the main results are discussed.

3.2 Machine learning framework based on model-based parameters to unravel the factors determining development of type 2 diabetes in women with a history of gestational diabetes

ML techniques were applied to a dataset appropriately generated by including features quantifying specific metabolic processes such as insulin sensitivity, β-cell function and insulin clearance, which are all relevant processes underlying T2D development [2]. The workflow for data analysis is reported in Figure 10.

3.2.1 Clinical data

Data used in this work were previously analyzed in the studies [53], [59]. A group of 78 women who experienced a history of GD were analyzed early postpartum (4 to 6 months after delivery) and after a period of follow-up lasting up to 7 years. During the

follow-up women were screened for diabetes and some of them had a diagnosis of T2D (n=19), whereas the others did not develop the disease (n=59). Of note, all women were nondiabetic early postpartum nor were treated with antidiabetic agents before T2D diagnosis.

Both early postpartum and at the end of the follow-up period the group of women underwent a frequently sampled insulin modified intravenous glucose tolerance test (IM-IVGTT). Glucose (300 mg/kg) was injected at time 0-0.5 min and insulin (0.03 IU/kg) was infused intravenously at time 20 for 5 min. Samples were analyzed at fasting and for 180 min following glucose injection at [3, 4, 5, 6, 8, 10, 14, 19, 22, 27, 30, 35, 40, 50, 70, 100, 140, 180] min for glucose ($mmol \cdot L^{-1}$), insulin ($pmol \cdot L^{-1}$) and C-peptide ($pmol \cdot L^{-1}$) plasma concentrations.

3.2.2 Feature extraction and dataset generation

Features were extracted by applying mathematical models and methods to the IM-IVGTT data collected early-postpartum. The newly generated dataset included anthropometric data (age, height, body weight, and body mass index) and the extracted model-based features together with other computed parameters of physiological interest. In the generated dataset, women were labelled as progressors (PROG) if progressed to T2D during the follow-up period, while as non-progressors (NONPROG) if they did not progress to T2D.

In detail, extracted features included: i) computed mean areas under the glucose, insulin and C-peptide curves (G_{MEAN}, I_{MEAN}, Cp_{MEAN}), divided by the test duration [51]; ii) area under the insulin curve during the first ($AUC_{INS\text{-}1P}$) and second phase ($AUC_{INS\text{-}2P}$) of the test; iii) glucose disappearance rate before (K_{G1}) and after (K_{G2}) insulin infusion, computed as the absolute slope value of $\log_e$ of glucose multiplied by 100 in the 10–20- and 20–40-minute intervals, respectively [62]; iv) insulin-dependent and insulin-independent glucose disappearance, S_I and S_G, assessed by the minimal model of glucose kinetics, which also provides an estimate of glucose distribution volume (V) [132]; v) both S_G components i.e., basal insulin effect (BIE) and glucose effectiveness at zero insulin (GEZI) [133]; vi) first-phase insulin secretion, as for the acute insulin response (AIR) [134] and the acute C-peptide response (ACPR) indexes, computed as the mean of suprabasal insulin and C-peptide curves,

respectively, in the time interval 3–8 min during the IM-IVGTT; vii) disposition index (DI) computed as the product between S_I and AIR to provide combined contribution of insulin action and β-cell function [83].

Moreover, a model-based methodology has been used to derive insulin secretion rate (ISR(t)) by deconvolution of plasma C-peptide concentrations during IM-IVGTT [51] and has allowed to extract the following features: i) area under the curve of ISR(t) for the whole test (AUC_{SECR}) and also for the first ($AUC_{SECR\text{-}1P}$) and the second ($AUC_{SECR\text{-}2P}$) phase of the test; ii) basal secretion rate (BSR) and β-cell responsivity to glucose (Φ_{1c}); iii) total insulin clearance during the whole test (CL_{MEAN}) and also first ($CL_{MEAN\text{-}1P}$) and second ($CL_{MEAN\text{-}2P}$) phase [51]; iv) insulin clearance with separation of the hepatic (FE_L) and extra-hepatic (CL_P) contribution, derived by applying the approach proposed by Polidori et al. [54] and described in section 2.1.1.

Insulin peak after glucose injection ($I_{PEAK\text{-}FIRST}$) and after insulin injection ($I_{PEAK\text{-}INJESTION}$), C-peptide peak ($C_{PEAK}$) and glucose injected dose (DOSE) have been also included in the dataset. Fasting plasma glucose (g_b) has also been included being the most important clinical marker for the diagnosis of glucose tolerance deterioration [111]. A summary of the features included in the generated dataset with the related measurement units is described in Table VI.

3.2.3 Classification problem and data analysis

The classification problem consisted in classifying PROG vs. NONPROG considering as input the complete generated dataset described above. Data analysis has been performed in Orange Data Mining (v. 3.28), an open-source data visualization, data mining and machine learning toolkit which enables visual programming through the front-end Orange Canvas. This tool shows power for explorative rapid qualitative data analysis and interactive data visualization [135].

Table VI Description of all the features included in the generated dataset.

Acronym	Description	Units
age	Age	years
BW	Body weight	kg
h	Height	cm
BMI	Body mass index	kg/m^2
g_b	Basal glucose	mg/dL
G_{MEAN}	Mean area under the glucose curve	mmol/L
I_{MEAN}	Mean area under the insulin curve	pmol/L
Cp_{MEAN}	Mean area under the C-peptide curve	pmol/L
AUC_{INS-1P}	Area under the insulin curve during the 1st phase of test	$pmol/L \cdot min^{-1}$
AUC_{INS-2P}	Area under the insulin curve during the 2nd phase of test	$pmol/L \cdot min^{-1}$
K_{G1}	Disappearance rate of glucose before insulin injection	%/min
K_{G2}	Disappearance rate of glucose after insulin injection	%/min
S_I	Insulin sensitivity	$10^{-4} \cdot min^{-1}/(\mu U \cdot mL^{-1})$
S_G	Glucose effectiveness	min^{-1}
V	Distribution volume of glucose	L
BIE	Basal insulin effect of glucose effectiveness	$10^{-3} \cdot min^{-1}$
GEZI	Glucose effectiveness at zero insulin	$10^{-2} \cdot min^{-1}$
AIR	Mean of suprabasal insulin in the time interval 3-8 min	pmol/L
ACPR	Mean of suprabasal C-peptide in the time interval 3-8 min	pmol/L
DI	Disposition index	min^{-1}
BSR	Basal secretion rate	pM/min
Φ_{1c}	β-cell responsivity to glucose	pM/min/(mg/dL)
AUC_{SECR}	Area under the secretion curve during the entire test	pmol
$AUC_{SECR-1P}$	Area under the secretion curve during the 1st phase of test	pmol
$AUC_{SECR-2P}$	Area under the secretion curve during the 2nd phase of test	pmol
CL_{MEAN}	Mean insulin clearance during the entire test	$L \cdot min^{-1}$
$CL_{MEAN-1P}$	Mean insulin clearance during the 1st phase of test	$L \cdot min^{-1}$
$CL_{MEAN-2P}$	Mean insulin clearance during the 2nd phase of test	$L \cdot min^{-1}$
CL_P	Extra-hepatic insulin clearance	$L \cdot min^{-1}$
FE_L	Hepatic insulin clearance	%
$I_{PEAK-FIRST}$	Peak insulin after glucose injection	μU/mL
$I_{PEAK-INJECT}$	Peak insulin after insulin injection	μU/mL
C_{PEAK}	Peak C-peptide	ng/dL
DOSE	Glucose dose injected per kg of body weight	g/kg

The input dataset has been preprocessed by firstly detecting and removing outliers among PROG and NONPROG through Local Outlier Factor (LOF), a measure of the local deviation of the density of a given sample with respect to its neighbors [136]; settings for the LOF algorithm were: “Contamination” = 4%, “Neighbors” = 20, “Metric” = Euclidean. Feature selection, consisting in the selection of a subset of pertinent features, aims to reduce the dimensionality of the model without compromising classification performances. Keeping irrelevant features might also degrade classification accuracy by introducing noise in the model. Thus, the preprocessed dataset has been given as input to a classification algorithm based on decision tree, which is suitable for feature selection since it determines the best predictive features considering class purity to split the data into nodes; information gain ratio was the score used by the tree to evaluate features for splitting instances in a node. Parameters of the decision tree were set as follows: “Induce binary tree”, which means that the generated tree will be a binary tree; “Minimum number of instances in leaves” = 3, meaning that the algorithm does not undertake a split which would put less than 3 training samples into any of the branches; “Do not split subsets smaller than” = 5, which inhibits splitting the nodes with less than 5 instances; “Maximal tree depth” = 100, which limits depth of the tree to 100 node levels; and “Stop when majority reaches 95%”, indicating that the algorithm stops splitting the nodes after reaching 95% of the classified sample.

To evaluate the predictive power of the selected features in solving the classification problem, they were given as input to different classification algorithms, namely Naïve Bayes (a probabilistic classifier based on Bayes’ theorem with the assumption of feature independence), which did not require any parameter setting, and penalized logistic regression, whose parameters were set as follows: “Regularization type” = RIDGE (L2), Cost strength (C) = 1. L2 regularization has been used since it was seen that penalized regression models show advantages in scenarios with small sample size and multiple highly correlated metabolic variables [137]. All the classification algorithms have been built by using a 5-fold cross validation; features given as input of the classification algorithms have been normalized to zero mean and unit variance to adjust their values to a common scale. Performance evaluation was done on the average across the 5 folds.

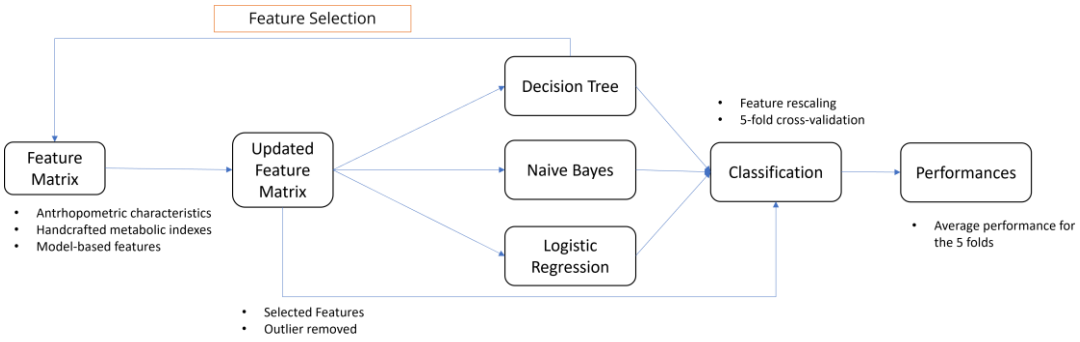

Figure 10. Workflow used for data analysis.

3.2.4 Performance measures

By considering PROG class as positive and NONPROG class as negative, the following definitions apply: the PROG cases classified as PROG by the classification algorithm were considered as true positive (TP); the NONPROG cases classified as NONPROG by the classification algorithm were considered as true negative (TN); the NONPROG cases classified as PROG by the classification algorithm were considered as false positive (FP) and the PROG cases classified as NONPROG by the classification algorithm were considered as false negative (FN).

The performance of each classification algorithm has been evaluated by computing the following measures: the area under the curve (AUC) of the receiver operating characteristics (ROC), the classification accuracy (CA, i.e., the proportion of cases correctly identified by the classification algorithm); the precision (PR, i.e., the proportion of TP among cases classified as positive); the sensitivity (SE, also indicated as recall, i.e., the proportion of positive cases that are correctly classified); the specificity (SP, i.e. the proportion of negative cases that are correctly classified); the F1 (i.e. the weighted harmonic mean of PR and SE).

3.2.5 Classification algorithms comparison

Venn diagrams were used for comparison of classification algorithms in terms of correctly classified and misclassified cases. Moreover, comparison of the performance measures (AUC, CA, PR, SE, SP and F1) has been performed through the Bayesian interpretation of the pairwise Student's t-tests [138].

3.3 Results

Characteristics of the pre-processed dataset are reported in Table VII and 25 out of 34 have been found statistically different. Removed outliers were 3 (1 NONPROG and 2 PROG), thus resulting in a total of 75 cases. Feature selection performed through decision tree provided 6 features for the classification and the identified thresholds were 0.3 min^{-1}, 28.7 kg/m^2, 32.4 pM/min, 39 years, 95 mg/dL and 240 pmol/L for DI, BMI, BSR, age, g_b and Cp_{MEAN}, respectively (Figure 11). The selected features have been found to be significantly different between PROG and NONPROG, but in Cp_{MEAN} significance was weak (p=0.04, see Table VII).

Confusion matrices for decision tree, Naïve Bayes and penalized logistic regression are reported in Figure 13, where correctly classified cases by each classification algorithms resulted to be 62, 61 and 63, respectively. The related ROC curves are reported in Figure 12. Performance of each classification algorithm in terms of AUC, CA, PR, SE, SP and F1 and comparison among algorithms are reported in Table VIII and IX, respectively. Penalized logistic regression outperformed tree and Naïve Bayes in terms of AUC, CA, SE and F1 but not in terms of PR and SP (in which Naïve Bayes was superior). The Venn diagrams for comparison among models of correctly classified/misclassified cases are shown in Figure 13; correctly classified or misclassified cases by all the classification algorithms where 53 and 5, respectively.

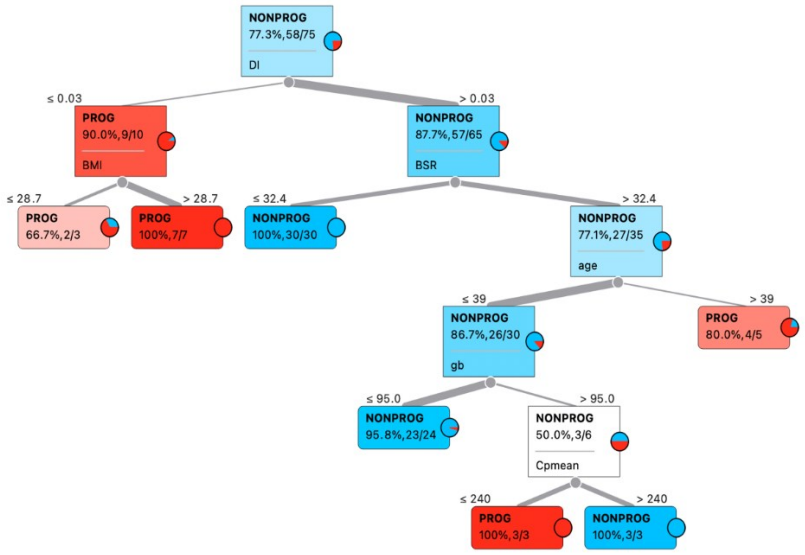

Figure 11 Best predictive features selected by decision tree.

Table VII. Characteristics of the pre-processed dataset.

Characteristics	PROG (n=17)	NONPROG (n=58)	p-value
age	36.6 ± 4.7	33.3 ± 4.2	<0.01
BW	75.0[18.8]	65.8[15.0]	0.03
h	158[12]	164[12]	0.04
BMI	30.6 ± 6.4	25.4 ± 3.9	<0.001
g_b	96 [11.50]	84 [8]	<0.001
G_{MEAN}	5.9[0.8]	5.1[0.7]	<0.001
I_{MEAN}	211.9[102.8]	201.8[78.3]	n.s.
Cp_{MEAN}	240.9[65.4]	182.4[97.2]	0.04
$AUC_{INS\text{-}1P}$	1520.9[1120.0]	2125.5[1053.2]	<0.01
$AUC_{INS\text{-}2P}$	36992.9[18872.1]	34468.1[1417.8]	n.s.
K_{G1}	1.56 [0.63]	1.93 [0.88]	<0.001
K_{G2}	3.4 ± 1.8	4.7 ± 1.8	0.01
SI	3.1 [2.0]	4.7 [2.7]	0.02
S_G	0.018[0.008]	0.022[0.005]	<0.01
V	13.9 [1.00]	13.4 [1.36]	n.s.
BIE	2.4 [1.5]	3 [2.4]	n.s.
GEZI	1.7 [0.6]	1.9 [0.7]	n.s.
AIR	132.8[103.0]	194.4[126.5]	<0.01
ACPR	158.2[150.0]	254.0[138.8]	<0.01
DI	0.52 [0.76]	1.36 [1.25]	<0.001
BSR	39.6 [10.9]	31.8 [10.4]	<0.001
Φ_{1c}	42.02 [33.31]	67.80 [31.90]	<0.01
AUC_{SECR}	32324.0[11317.6]	24734.9[15607.7]	0.03
$AUC_{SECR\text{-}1P}$	6252.9[3285.6]	7146.2[3591.8]	0.02
$AUC_{SECR\text{-}2P}$	27324.0[9849.6]	17450.7[15298.7]	<0.01
CL_{MEAN}	0.78[0.47]	0.69[0.42]	0.03
$CL_{MEAN\text{-}1P}$	4.17[1.76]	3.30[0.92]	n.s.
$CL_{MEAN\text{-}2P}$	0.68[0.35]	0.53[0.39]	<0.01
CL_P	0.56 ± 0.53	0.39 ± 0.42	n.s.
FE_L	0.50 [0.13]	0.53 [0.14]	n.s.
$I_{PEAK\text{-}FIRST}$	36.0[39.3]	53.2[39.5]	<0.01
$I_{PEAK\text{-}INJECT}$	559[150]	493[281]	n.s.
C_{PEAK}	380[140]	465[197]	0.04
DOSE	22.5[5.6]	19.7[4.5]	0.02

Data are presented as mean ± standard deviation or median [interquartile range]. Significance level: p-values < 0.05. n.s. not significant.

Table VIII Performances measures obtained for the three classification algorithms.

Performance measures	Classification algorithm		
	Tree	**Naïve Bayes**	**Logistic regression**
AUC	0.795	0.831	0.884
CA	0.827	0.813	0.840
Precision	0.830	0.854	0.834
Sensitivity	0.827	0.813	0.840
Specificity	0.700	0.821	0.662
F1	0.828	0.824	0.836

Table IX Comparison of the performance measures among the classification algorithms through Bayesian interpretation of the pairwise Student's t-tests. Percentage probabilities that the score for the classification algorithm in the row is higher than that of the classification algorithm in the column are reported.

		AUC	
	Tree	Naïve Bayes	Logistic regression
Tree		26.2	11.3
Naïve Bayes	73.8		28.3
Logistic regression	88.7	71.7	
		CA	
	Tree	Naïve Bayes	Logistic regression
Tree		57.5	42.5
Naïve Bayes	42.5		38.0
Logistic regression	57.5	62.0	
		Precision	
	Tree	Naïve Bayes	Logistic regression
Tree		35.9	42.0
Naïve Bayes	64.1		54.0
Logistic regression	58.0	46.0	
		Sensitivity	
	Tree	Naïve Bayes	Logistic regression
Tree		57.5	42.5
Naïve Bayes	42.5		38.0
Logistic regression	57.5	62.0	
		Specificity	
	Tree	Naïve Bayes	Logistic regression
Tree		13.3	57.6
Naïve Bayes	86.7		86.6
Logistic regression	42.4	13.4	
		F1	
	Tree	Naïve Bayes	Logistic regression
Tree		52.0	47.2
Naïve Bayes	48.0		46.0
Logistic regression	52.8	54.0	

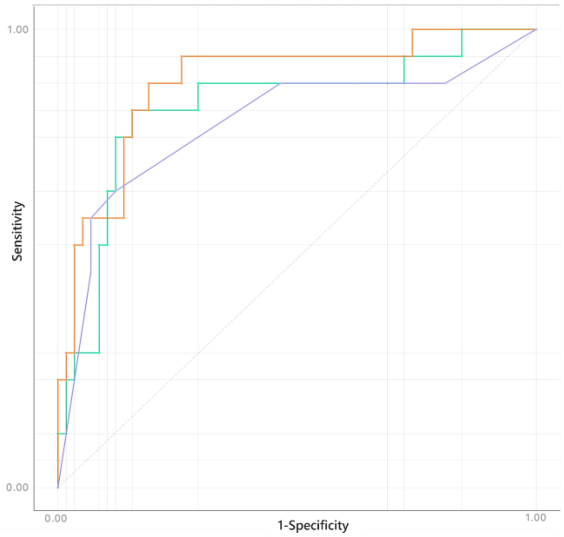

Figure 12 Receiver Operating Characteristics (ROC). Line for decision tree is in purple, for Naïve Bayes in green and for logistic regression in orange. Default threshold = 0.5.

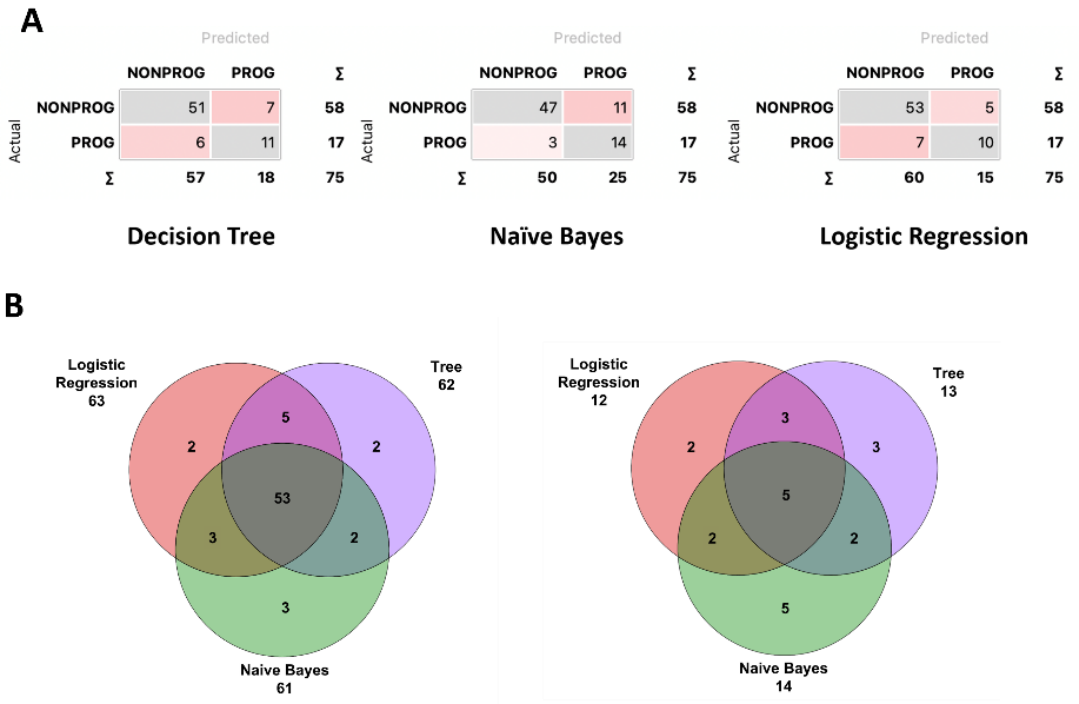

Figure 13. A) Confusion matrix for decision tree, Naïve Bayes, and logistic regression; B) Venn diagrams; left: correct classifications; right: misclassifications.

3.4 Discussion and conclusions

The feature extraction instead of the use of raw data such as plasma concentrations of glucose, insulin and C-peptide measured during the IM-IVGTT allowed a deeper interpretability of the findings.

The main novelty of this study was the application of machine-learning techniques to such a kind of database and in the specific context of T2D risk assessment in women with history of GD. Indeed, previous studies in the same context have focused on lipidomics or metabolomics [127], [128], [129]. In particular, the study by Lappas et al. [127] aimed to determine whether circulating lipid levels 12 weeks following pregnancy with GD were associated with an increased risk of T2D development and identified CE 20:4, PE(P-36:2) and PS 38:4 lipid species as significant risk factors. The other two studies (by Kahn et al. [128] and Allalou et al [129]) proposed different predictive signatures including different metabolites; moreover, reduced sphingolipids have been associated with the transition from GD to T2D [128]. Such "omics" approaches, however, are still not typically used in clinical practice, thus making our study an easier alternative from the technical point of view. It is worth noting that metabolomics/lipidomics predictive power could be enhanced complementing it with classical clinical and biochemical markers [139], therefore our approach could be seen as complementary with respect to omics approaches once they will reach clinical settings.

The main result here is the identification of disposition index, basal secretion rate of insulin and mean area under the C-peptide concentration curve among the most relevant features for the progression to T2D. Among indexes quantifying specific metabolic processes, basal secretion rate of insulin and mean area under the C-peptide concentration curve provide a quantification of insulin secretion, while disposition index represents the combined contribution of insulin secretion and insulin sensitivity and its importance is supported by evidence since it was already found to predict conversion to T2D in a large epidemiological study [140]; besides such indexes, also age, body mass index and fasting glycemia have been selected.

Comparisons between the tested classification models were based on AUC, CA, precision, sensitivity, specificity and F1 and showed that logistic regression

resulted the best model for the classification of progression to T2D since it reported higher values than Naïve Bayes and decision tree in 4 out of 6 measures, specifically AUC, CA, sensitivity and F1, while Naïve Bayes performed better only in precision and specificity, and decision tree reported lower values than the other models in all the measures. Logistic regression presented higher value of correct classification and lower value of misclassification followed by decision tree and Naïve Bayes. Moreover, being inclusion of penalized regression (L1 or L2, as in this study) characterized by the fact that it may include a small bias into the maximum likelihood estimation, we could claim that this helps to reduce the variance and improves the generalization of results [141].

Machine-learning methodologies have been extensively explored in the field of T2D prevention and management [113], [114], [119], [120], [121], [123], [124], [125], [126] but also showing possible critical issues. In fact, the analysis on large amounts of heterogeneous data is affected by the presence of spurious correlations [142], which indicate that the creation of appropriate fine phenotyped databases as done in this study is of primary importance to achieve reliable results. Even though the population under study was constituted by a limited number of subjects, they have been strictly controlled and monitored during a long follow-up period. Moreover, the subjects have been carefully screened to detect outliers and these were dropped out from the dataset before the analysis; the choice of dropping out the outliers instead of performing data imputation only for specific features was taken to reduce as much as possible bias and uncertainty. Thus, on one hand the use of machine-learning techniques, usually involving large amounts of data, is justified in this study by the high number of features included in the generated dataset, from which machine-learning may allow determination of the most relevant ones. On the other hand, with a low number of subjects and a high number of features, overfitting may occur and achieved results may be a little optimistic, especially when using decision tree algorithm also used for feature selection. It has to be acknowledged that this may be a risk of this study; however, the adoption of well-known strategies such as pruning (through which the redundant branches can be cut beforehand) and k-fold cross validation allowed us to mitigate such risk [143].

In this study, data analysis has been performed by using Orange Data Mining [135], a Python based tool that show the advantage of providing a visual programming front-end for explorative rapid qualitative data analysis and interactive data visualization; on the other side, even if the program is under continuous update, it may happen that possibilities in data analysis are limited by the procedures implemented in the "building blocks". Further studies may explore different and more customizable learning algorithms starting from the results of this study.

In conclusion, this was the first study applying machine-learning techniques to a database that contain features quantifying metabolic processes based on challenge test in women with a history of GD at risk to develop T2D. We found that disposition index, basal secretion rate of insulin, mean area under the C-peptide concentration curve, age, body mass index and fasting glycemia were identified as the most relevant features for the progression from GD to T2D. This result is of impact since the information provided from this pattern could be of interest for the study and characterization of diabetes pathophysiology and could shed light on GD, potentially accelerating opportunities for prevention and treatment [5].

4 Standardization of CGM data analysis

[3] The advancement in CGM technology raised the need of interpreting the large amount of produced data which in turn has led to the definition of lots of metrics useful to assess glycemic control [144], [145], accompanied by data display modalities to assist clinicians and patients in the management of therapy and in tracking their progresses. As a consequence, CGM data interpretation has been suffering from a lack of standardization, even though in the last ten years much work has been done to overcome this limitation [146]. A first important achievement was represented by the recommendation by the ADA for the adoption of a template report named Ambulatory Glucose Profile (AGP) [147], which nowadays is currently adopted by the majority of CGM devices manufacturers; a second achievement was reached in two steps, happened in 2017 and 2019 (ADA 2017 international consensus on CGM data analysis and ADA 2019 international consensus on time in range), when was reached international consensus on CGM data analysis, which recommended standard metrics that should be computed in clinical care [148], [149].

This chapter aims to make a step toward standardization of CGM data analysis, by investigating the agreement between metrics computed by different available software and tools in an effort to identify which would be the most reliable and suited one to be used in the next steps of the research involving CGM data analysis. Section 4.1 will review 12 software packages that have been identified from the literature, namely: Glyculator, EasyGV, CGM-GUIDE©, GVAP, Tidepool, CGManalyzer, cgmanalysis, GLU, CGMStatsAnalyzer, iglu, rGV, cgmquantify. Section 4.2 will then summarize the main findings.

4.1 Software packages and tools for the analysis of CGM data

CGM data interpretation is facilitated by software solutions, which have different characteristics in relation to the intended users (i.e., researchers, clinicians and/or patients) and provide partially different reports of CGM data with also different

[3] This chapter contains material published in [169], [284].

metrics. Ascertaining which functionality fits for each user requirement, however, is sometimes not so straightforward.

Being our focus on non-commercially available solutions, 12 software packages published until December 2021 have been identified from the literature. The timeline of their first publication is shown in Figure 14. Comparison has been done in terms of:

- main characteristics (i.e., presence of a Graphical User Interface (GUI), availability, presence of open-source code, programming language, supported CGM devices, data upload and download, supported data format and organization of the data structure, documentation, presence of a toy example, video tutorial, measurement-units conversion);
- preprocessing procedures;
- data display options;
- computed metrics (also analyzed in terms of adherence to the ADA 2017 and the ADA 2019 international consensus) and agreement between metrics computed by different software and tools.

On the basis of such comparison, Section 4.2 will discuss the main findings in terms of usability and complexity of data management, as well as the possibility to perform customized or patients-group analyses, by highlighting limitations and strengths also in relation to possible different user categories (i.e., patients, clinicians, researchers).

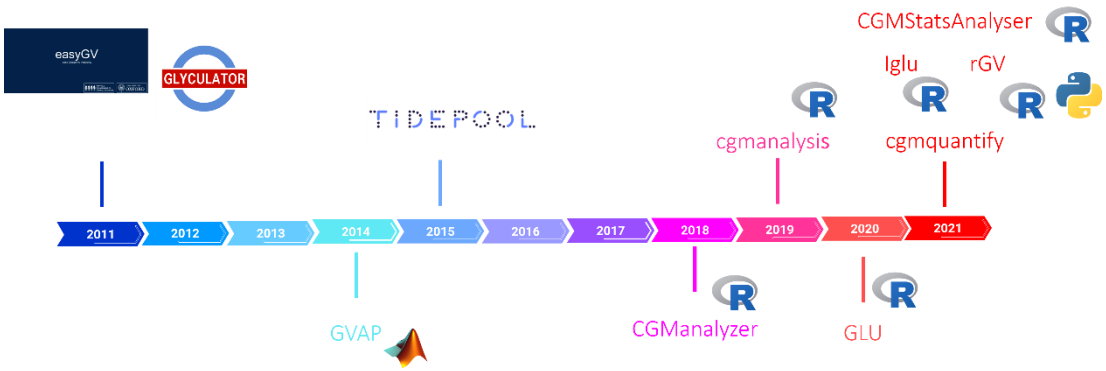

Figure 14. Timeline of the first publication of available software packages for CGM data analysis.

4.1.1 Standardization of CGM data analysis

Main characteristics of the available software packages and tools are summarized in Table X. Available display options for each software package are listed in Table XI. Introductory information for each of them is provided in the related subsections in the following.

GlyCulator

GlyCulator [150], [151], [152], is web application available in its latest version as Glyculator 3 (https://glyculator.btm.umed.pl/). However, the source code is available for the version Glyculator 2 (https://github.com/kpagacz/glyculator). It shows a large versatility, since dataset loading can be performed specifying the CGM manufacturer among those supported or choosing to import a generic data format. The computed metrics are easily accessible and downloadable in *.csv format from the online platform, together with the raw data file and the metadata file.

EasyGV

EasyGV [153], [154] (easy Glycaemic Variability) is a software application developed in Visual Basic and enabled in an Excel (Microsoft) workbook. The latest version EasyGV software v10 is freely available at the website: https://www.phc.ox.ac.uk/research/resources/easygv. It is largely used in research also thanks to its ease of use. One of its main characteristics is that time stamps are not mandatory for computations, thus if the user does not include them in the spreadsheet, the software does not allow to select specific time periods during the analysis.

CGM-GUIDE©

CGM-GUIDE©[155] (Continuous Glucose Monitoring GUI for Diabetes Evaluation) was designed using MATLAB environment version 2008b and has not been made publicly available.

GVAP

GVAP [156] (Glycemic Variability Analyzer Program) software package was developed in MATLAB environment version 2010b and it is open-source and freely available at https://sourceforge.net/projects/glyvariab/files/?source=navbar, providing

the instructions to build a standalone Windows-based application following a few steps in MATLAB environment. CGM data must be provided in a table with *.xls extension and containing four columns, Date, Time, Glu (glucose, expressed in $mg \cdot dl^{-1}$), Index (a counter associated with each glucose value), and at least 101 rows.

Tidepool

Tidepool Platform [157] is a cloud-based comprehensive platform for diabetes data management that integrates information from different applications and devices. The dashboard is named Tidepool Web, whose code is fully available on GitHub (https://github.com/tidepool-org/blip). It is free for clinicians and patients and by paying a fee, access to anonymized datasets is provided. A mobile app for data visualization and event tracking (i.e., meals, carbohydrate intake, insulin boluses, exercise) is included and a new one, the Tidepool Loop app, recently obtained Food and Drug Administration (FDA) clearance and is intended to connect via Bluetooth to commercially available insulin pumps and CGM devices to act as a controller.

CGManalyzer

CGManalyzer[158] is a free software package developed in R environment and available at: https://cran.r-project.org/web/packages/CGManalyzer/index.html. Among its features, it allows comparing data of different populations, such as T1D, T2D, pre-diabetes and healthy people.

cgmanalysis

cgmanalysis[159] is a free software package developed in R and available on the CRAN repository at https://cran.r-project.org/web/packages/cgmanalysis/index.html; its source code is also available on GitHub. It gives a list of supported CGM devices together with the possibility to provide a manually adjusted three-column *.csv file containing an identifier, ID, time stamp and glucose reading.

GLU

GLU[160] is a software package developed in R environment and is freely available on GitHub at https://github.com/MRCIEU/GLU. It gives a list of supported devices but in the case of devices other than those in the list a data analysis can be performed

through the conversion to a general format. Of note, data analysis may consider nighttime and daytime separately, or allow specifying pregnancy and diabetes conditions to consider populations specific characteristics and metrics settings.

CGMStatsAnalyser

CGMStatsAnalyser[161] is a freely available web-based application accessible at https://baker-biostats.shinyapps.io/CGMStatsAnalyser/. Multiple CGM data files can be uploaded into the software using the dedicated button to statistically compare the summary metrics between groups of subjects; it enables selecting the metric to test and the variable chosen among those of the subject characteristic file, also providing a displayed summary of the test results that can be downloaded as a *.csv file.

iglu

iglu [162] is a free open-source software package developed in the R environment and available at https://github.com/irinagain/iglu. The data accepted by the software can come from any device, given the three column format containing the identification of the subject (‘id’), date and time (‘time') and the measurement of blood glucose ('gl') expressed in $mg \cdot dl^{-1}$. Of note, it addresses the fact that time-dependent metrics requires evenly spaced data between glucose values by generating a grid of equidistant glucose measurements through the *CGMS2DayByDay* function.

rGV

rGV[163] is a free open-source software package developed in R environment with a GUI available at https://shiny.biostat.umn.edu/GV/. It supports any CGM device after using the function read.CGM, which enables data cleaning by formatting to a general two-column frame containing only time stamps and glucose readings.

cgmquantify

cgmquantify[164] is a free open-source software package, developed in both in Python programming language and R environment and is available at https://github.com/DigitalBiomarkerDiscoveryPipeline/cgmquantify. Some CGM devices are supported, but import functions are included to format data in a three-column frame: glucose, datetime, day.

Table X Overview information of software packages for CGM data analysis.

Name	Glyculator	EasyGV	CGM-GUIDE	GVAP	Tidepool	CGManalyzer	cgmanalysis	GLU	CGMStatsAnalyser	iglu	rGV	cgmquantify
Year of analyzed version	oct-21	oct-20	dec-11	apr-15	sep-15	gen-18	oct-19	feb-20	gen-21	apr-21	jul-21	aug-21
Citations	68	221	24	19	29	17	23	4	0	5	0	1
GUI	yes	yes	yes	yes	yes	no	no	no	yes	yes	yes	no
Available	yes	yes	no	yes	yes	yes	yes	yes	yes	yes	yes	yes
Open source	no‡	no	no	yes	yes	yes	yes	yes	no	yes	no	yes
Programming Language#	R	Mi	Mat 2008 b	Mat 2010 b	JS	R	R	R	app	R	R	R, Py
Supported devices§	any*	any*	any*	any*	11	AbF Glut Dex Med any*	Dia Dex Med iPro2 CL AbF any*	Med iPro2 AbF Dex G6 any*	Med iPro2 any*	Dex AbF AbP Med iPro any*	any*	Dex AbF any*
Data format	csv, txt, xls, xlsx	xlsm	xls	xls	d.s.	d.s.	csv	csv	csv	csv	csv	csv
Data frame	time, gl	gl	time, gl	date, time, gl, idx	d.s.	d.s.	id, time, gl	time, gl	time, gl	id, time, gl	time, gl	gl, time, day
Missing data imputation	yes	yes	no	yes	-	yes	yes	yes	-	yes	-	-
Preprocessing quality	med	med	med	med	-	high	high	high	med	high	med	med
Input units	both units	SI units	mg $\cdot dl^{-1}$	mg $\cdot dl^{-1}$	both	both	mg $\cdot dl^{-1}$	SI units	SI units	mg $\cdot dl^{-1}$	mg $\cdot dl^{-1}$	mg $\cdot dl^{-1}$
Complexity for data upload	low	low	-	med.	-	high	med.	med.	med.	med.	med.	med.
Download reports/data extraction	yes	yes	-	no	yes	yes	yes	yes	yes	yes	yes	yes
Units conversion	yes	to SI only	no	no	yes	no	no	no	no	n.a.	no	yes
Documentation	yes	yes	no	yes	yes	yes	yes	yes	yes	yes	yes	yes
Updating	yes	yes	no	no	yes	yes	yes	yes	new	yes	new	new
Toy example	yes	yes	no	yes	yes	yes	yes	yes	no	yes	no	yes
Video tutorial	yes	no	no	no	yes	no	no	no	no	no	no	no

Number of citations provided is based on Scopus (latest search May 2022).
* any device is accepted after conversion to a general format;
# Programming languages: R, Microsoft (Mi), Matlab (Mat), Javascript (JS), Java (J), Python (Py), Ruby (Ru);
§ Supported devices: Abbott FreeStyle Libre (AbF), Glutalor (Glut), Dexcom (Dex), Medtronic (Med), Diasend (Dia), Carelink (CL), Abbott FreeStyle Libre Pro (AbP);
- not available information;
‡ Glyculator source code available only for the previous versions;
gl:glucose; idx:index; d.s.: device specific; n.a: not available; med.: medium.

Table XI. Available display options for each software package.

Name	Display options
Glyculator	a) daily CGM graphs b) multi-patient time in range visualization (all downloadable analysis report in .pdf)
EasyGV	none
CGM-GUIDE	a) glucose trace with colored areas under hyper- and hypo-glycemic ranges b) transition density profile, which allows visualizing and evaluating the dynamics associated with frequency of glucose fluctuations across critical glycemic regions c) rate of change and histogram of the rate of change computed for every recorded time interval
GVAP	a) glucose curve b) mean amplitude of glycemic excursion (MAGE) curve
Tidepool	a) daily blood glucose readings (with colored lines depending on the target ranges set) b) CGM trends related to 1 up to 4 weeks (also with the possibility to select only weekend-related data) c) percentage spent in the selected ranges (represented through a bar graph) d) other information related to specific metrics and sensor usage (displayed through widgets)
CGManalyzer	a) glucose levels in several subjects at the same time b) glucose levels in time c) multiscale sample entropy (MSE[165]) both for each subject and for each group d) "antenna plot" to display, both for glucose levels and MSE at each scale, differences among pair of groups, reporting for each pair of groups the mean of difference and its confidence interval on the x-axis and the strictly standard mean difference (SSMD[166]) on the y-axis
cgmanalysis	a) Aggregate Daily Overlay (ADO), with Tukey smoothing version showing median, interquartile range and 5th and 95th percentiles of CGM values over the 24-hour period (similarly to the AGP report) b) ADO Loess smoothing version, showing all CGM data points and an overlapped curve representing the mean c) color-coded representation of mean glucose for each subject
GLU	a) glucose trace versus time, also including indicators of events (if provided) including meal times, exercise, use of relevant drugs, and capillary blood sugar measurement levels b) Poincare graphs, to visualize the blood glucose variation, in which each point on the graph is the glucose level of the sensor in the time point t compared to the glucose value of the sensor at time t + 1 c) histograms of glucose measurements distribution. SMG data are also visualizable
CGMStats Analyser	a) trace of glucose with respect to time represented by the median value and the 5th and 95th percentiles b) interactive visualization of metrics through violin plots, with the possibility to observe the different distributions according to a specified grouping variable

Name	Display options
	c) heatmap of the correlation between the computed metrics
iglu	a) glucose trace plot over time for each subject b) Lasagna plots, which allow visualizing data trends across different subjects or different days for the same subject by using color grids c) change in the variability of glucose as the rate of change shown through a time-series graph (in which each glucose measurement point is colored reflecting the corresponding rate of change value), or through a histogram plot d) an AGP report organized in three panels: glucose statistics and time in ranges in the first, CGM glucose profile (with the respective quantiles) in the central and daily glucose profile with colored hyperglycemic and hypoglycemic areas in the third
rGV	a) plots of glucose trace over time b) rate of change of glucose over specified time intervals c) a plot representing symmetrized blood glucose values over time, based on a function that transforms glucose readings to balance the amplitudes of hyper and hypoglycemic ranges and makes them symmetric around zero[167].
cgmquantify	a) longitudinal CGM data, including mean, standard deviation and hyper- and hypoglycemia according to personalized or standard clinical thresholds b) Locally weighted scatter plot smoothing (LOWESS) curves can also be displayed over the original CGM data to facilitate interpretation

4.1.2 CGM metrics

A comprehensive summary of the CGM metrics computed by the 12 software packages along with their description is given in Table XII. In order to perform a comparison of the available software packages and tools (with reference to their latest version) in terms of computable metrics, a standard CGM recording from the open D1NAMO dataset [168] was considered. The selected CGM recording pertains to a patient with type 1 diabetes (Subject 1) and was obtained through an iPro2 Professional CGM device. Results of the analysis are reported in Table XIII, which is also useful to check which are the metrics that can be computed by each tool. Results of the analysis for the whole D1NAMO dataset was reported in the published work supplementary material [169]. Further details about peculiarities in the modality of metric computation that may be useful from a practical point of view when using the different packages are provided Table XIV.

Table XII Description of all the metrics that can be found in at least one of the revised software solutions.

Metric	Description
eA1c†	Estimated HbA1c[170], [171]
%TAR†‡	Percentage of time spent above range (sometimes given in minutes)
%TBR†‡	Percentage of time spent below range (sometimes given in minutes)
%TIR†‡	Percent of time spent in the target range (sometimes given in minutes)
%of expected CGM readings†‡	Percentage of time the device was active with respect to the wearing time
ADRR	Average daily risk range, assessment of total daily glucose variations within risk space[172]
AUC†	Area under the glucose curve (eventually normalized to the duration of a measurement)
AUC-high/low	AUC above and below the hyper-/hypoglycemic limit
COGI	Continuous glucose monitoring index[173]
CONGA	Continuous overall net glycemic action[174]
CV†‡	Coefficient of variation of glucose trace (sometimes given in %)
daytime	Number of all sensor glucose values during specified daytime hours[159]
Distance Travelled	The sum of the absolute difference in glucose levels for one day of consecutive CGM readings[175]
EF	Excursion frequency, corresponding to the sum of all excursions
excursions_over/under	The number of local glucose peaks with an amplitude greater than a specifiable threshold [159]
Fasting Proxy	Measure of fasting glucose levels computed as the mean of the six lowest consecutive glucose values occurring during night[160]
FD	Fractal dimension[176]
GMI‡	Glucose management indicator [177]
GRADE	Glycemic risk assessment in diabetes equation[178]
GVP	Glycemic variability percentage[179]
HBGI/LBGI†	High blood glucose index/ low blood glucose index[172], [180]
Hyper/Hypo Index	Hyperglycemia/hypoglycemia index[146]
IGC	Index of glycemic control, equal to the sum of hyper index and hypo index[146]
IQR	Interquartile range of glucose
J-index	Measure of both the mean level and variability of glycemia[181]
LI	Lability Index[182]
MAD	Mean absolute deviation
MAG	Mean absolute glucose change per unit time[183]
MAGE	Mean amplitude of glucose excursions (default = 1SD)[184], [185], [186], [187]
max	Maximum glucose over all days
mean†‡	Mean glucose over all days
median	Median glucose over all days
MGE	Mean of glucose outside range (default = 1SD)[185]
MGN	Mean of glucose inside range (default = 1SD)[163]
min	Minimum glucose over all days
MODD	Mean of daily differences in glucose[188]
MSE	Multiscale sample entropy[165]

Metric	Description
M-value	Measure of variation of glucose values around a reference value[189]
nighttime	Number of all sensor glucose values during specified nighttime hours[159]
Number of days CGM worn†‡	Number of days the device was worn
number of episodes per day	Number of episodes (below 54 mg·dl^{-1} and above 70 mg·dl-1) per day
number of missing values	Number of missing glucose readings
PGS	Personal glycemic state; composite index that assesses four domains of glycemic control: mean glucose, glycemic variability, time in range and frequency and severity of hypoglycemia[190]
PIR	Percent of time spent inside range specified as multiple of SD (also in minutes), default = 1SD[191]
POR	Percent of time spent outside range specified as multiple of SD (also in minutes), default = 1SD[191]
Post-event AUC	Mean of the blood glucose measurements applied to the 15 minutes occurring 1-hour or 2-hour after meal, medication or physical exercise events[192]
Post-event time to peak	The number of minutes between the meal and the subsequent glucose peak value[192]
Q1	First quartile glucose value over all days
Q3	Third quartile glucose value over all days
Range	Range of glucose values
ROC	Rate of change of glucose
SD†	Standard Deviation of glucose trace
SD of ROC	Standard deviation of the rate of change of glucose
sGVP	Standardized glycemic variability percentage; length of the flattened glucose trace after being standardized, which reflects the degree of trace undulation[193]

Please note that in the original software name of the metric may slightly differ from the one here reported.
† Key metrics for CGM data analysis recommended by the 2017 international consensus on use of CGM[148];
‡ Standardized CGM metrics for clinical care recommended by the 2019 international consensus on time in range[149].

Table XIII. Compendium of metrics values computed on a single standard CGM recording according to the different software packages.

	Glyculator	**EasyGV**	**GVAP**	**CGManalyzer**	**cgmanalysis**	**GLU**	**CGMStats Analyser**	**iglu**	**rGV**	**cgmquantify**
Version used	3.0	10	1.1	1.3	2.7.3	0.2.0	0.1.0	3.3.1	0.0.1	0.1.0
eA1c (%)					**8.4**		**8.4**	**8.4**		**8.4**
TAR-level1‖ (%)	**49**	**49**	**49**#		**50**	**50**⁑#	**50**	**49**	**24**	
TBR-level1‖ (%)	**10**	**10**	**10**#		**10**	**10**⁑#	**4**	**10**	**4**	
TAR-level2 (%)	**25**	**25**	**25**#		**25**	**25**⁑#	**25**	**25**	**25**	
TBR-level2 (%)	**6**	**6**	**6**#		**6**	**6**⁑#	**6**	**6**	**6**	
TIR (%)	**41**	**41**			9^	**41**⁑	**41**	**41**	**41**	
Expected CGM readings (%)	**100**⁑				**100**§			**100**		
ADRR (d.n.)		**65.7**						54.6§	**65.7**	soon
AUC‡ (mmol·l^{-1})	**10.7**				**6.2 ·(10^4) *** ·min	**10.7**		**10.7***	**1.5 ·(10^4)*** ·min 24h AUC	
AUC-high/low‡ (mmol·l^{-1})			**2.4 /0.1***				**133.0 ·(10^2)** /- ·min			
COGI (%)								**36**⁑		
CONGA1 (mmol·l^{-1})		3.1¶	2.2*§	**2.5**	**2.5***		**2.5**	**2.5***	**2.5***	soon
%CV (%)	**48**	**48**⁑			**48**⁑		**48**	**48**	**48**	**48**
Distance Travelled (mmol·l^{-1})									**215.9 ***	
EF (count)			**20**							
Excursions over/under (count)					**7/ 3**					
Fasting proxy (mmol·l^{-1})						**5.8**				
GMI (%)	**7.9**				**7.9**			**7.9**	**7.9**	**7.9**
GRADE (d.n.)	**14.85**	**14.37**						**14.85**	**14.85**	
GRADE-Hypo (%)		**14**						**14**	**13**⁑	
GRADE-Eugly (%)		**3**						**3**	**3**⁑	

	Glyculator	**EasyGV**	**GVAP**	**CGManalyzer**	**cgmanalysis**	**GLU**	**CGMStats Analyser**	**iglu**	**rGV**	**cgmquantify**
GRADE-Hyper (%)		**83**						**84**	**83⁑**	
GVP (%)		**29.68**						1.29†	**29.68**	
HBGI (d.n.)	**14.22**	**14.23**			17.46 ^		**14.26**	**14.23**	**14.23**	5.54^
Hyper/Hypo Index (d.n.)								**3.66/ 3.13**		
IGC (d.n.)		**6.78**						**6.78**		
IQR (mmol·l^{-1})								**6.7***		
J-index (d.n.)	**81.60**	**81.44**			**81.44**		**81.44**	**81.44**	**81.46**	**81.44**
LBGI (d.n.)	**2.53**	**2.54**			13.75 ^		**2.54**	**2.54**	**2.54**	3.60^
LI (d.n.)		**6.3**							**6.3***	
MAD (mmol·l^{-1})				4.9†		**3.5**		**3.3***		
MAG (mmol·l^{-1})		**2.3**						**2.2**	**2.3**	
MAGE‡ (mmol·l^{-1})	**8.7**	**12.4**	**9.0***		**8.1***		**8.6**	**12.5***	n.a.	soon
MAGE+/ MAGE-‡ (mmol·l^{-1})			**9.1/ 8.9***					**12.6/ 12.5***	n.a.	
max/min (mmol·l^{-1})				**22.2/ 2.2**	**22.2/ 2.2***			**22.2/ 2.2***		**22.2/ 2.2***
mean (mmol·l^{-1})	**10.7**	**10.7**	**10.7***	**10.7**	**10.7***		**10.7**	**10.7***	**10.7***	**10.7***
median (mmol·l^{-1})	**9.9**			**9.9**	**9.9***			**9.9***		**9.9***
MGE (mmol·l^{-1})										**11.7***
MGN (mmol·l^{-1})										10.7^ *
MODD (mmol·l^{-1})		**4.4**	-1.0§	0.9§	**4.4***			**4.4***	**4.4***	soon
MSE (d.n.)				array						
M-value (d.n.)	294.8 ^	**47.5**						**47.5**	65.5†	
number of days CGM worn	**4**				**4**			**4**		
number of episodes per day									**0.5**	
number of missing values		**0**		**0**						
PGS (d.n.)		**26.99**								
PIR (%)										n.a.

	Glyculator	**EasyGV**	**GVAP**	**CGManalyzer**	**cgmanalysis**	**GLU**	**CGMStats Analyser**	**iglu**	**rGV**	**cgmquantify**
POR (%)										**33**
Post-event AUC						no event				
Post-event time to peak (min)						no event				
Q1/Q3 (mmol·l^{-1})				**7.2/ 13.9**	**7.2/ 13.9***			**7.2/ 13.9***		**7.2/ 13.9***
Range (mmol·l^{-1})								20.0*		
ROC (mmol·l^{-1} min^{-1})								array		
SD (mmol·l^{-1})	**5.1**	**5.1**	**5.1***	**5.1**	**5.1***		**5.1**	**5.1***	**5.1***	**5.1***
SD of ROC (mmol·l^{-1} min^{-1})								**0.05***		
sGVP (%)						**0.022**				
Total computed metrics	19	26	12	10	23	11	15	39	28	19
Total computed standard metrics	13	9	5	1	14	6	10	14	11	6
Total error and warning/Total metrics	1/19	1/26	2/12	1/10	4/23	0/11	0/15	1/39	0/28	3/19

Grey-color cells indicate consensus metrics (2017 and 2019); settings for the metrics are as follows: n=1 for CONGA, LLTR = 80, ULTR = 140, a = 1.1, b = 2, c = 30, d = 30 for IGC, Hyper and Hypo Index, M100 is considered for the M-value; d.n. stands for dimensionless number; n.a. indicates that the metric was not given as output when using the tool; "no event" indicates that the metric cannot be computed when event information is absent (as in the present case); "soon" means that the metric is only available in the Python-based version and, as declared by the software authors, will be made soon available in the R version (the one here used).
Metric values in agreement with the expected ones are marked in bold; errors/warnings/notes are marked with flags described below (detailed explanation is provided in SupplementaryInfo.docx).
Error/warning flags:
^ error in the computation;
§ warning on the code;
¶ warning on identified difference for no apparent reason that can be detected by the authors.
Note flags:
‡ difference due to the specific algorithm used and/or the time interval considered for metric computation;
‖ difference due to inclusion/not inclusion of level 2 values as part of level 1 (>180 mg·dl-1 or 181-250 mg·dl-1 for TAR-level 1 and <70 mg·dl-1 or 54-69 mg·dl-1 for TBR-level 1);
† difference in the interpretation;
* conversion from mg·dl-1 to mmol·l-1 using 18 as conversion factor;
# two-step estimation for level 1 and 2 of %TAR and %TBR; this estimation was not obtained directly from the software but off-line by the user as a result of a two-step running;
⁑ not directly provided as percentage by the software;
- no metric values can be obtained due to accessibility issues.

Table XIV. Observation on peculiarities in metric computations listed for each software package.

Name	Observations on computed metrics by each software
Glyculator	• M-value is computed as M100 (weighted average of transformed glucose with respect to the reference value 100 mg·dl-1); • MAGE is computed following Service et al., algorithm [184] • AUC is divided by the time in h • metrics are calculated in three day intervals: 12:00–6:00 AM, 6:00–12:00 AM, and the whole day
EasyGV	• M-value has the possibility to set the reference ideal glucose value (default is 120 leading to M-120 index) • CONGA[174] has specifiable time window (default value is 60 min) • MAGE has the possibility to compute a modified version, MAGE-CGM, for peak-to-trough or trough-to-peak identification[185] • %TIR, %TAR, %TBR allow customizable thresholds • LI [182] has the possibility to define the interval (default is 60 min)
CGM-GUIDE	• CONGA has specifiable time window • MAGE is computed according to the Fritzsche algorithm[186] • TIR, TAR, TBR allow customizable thresholds • AUC-high/low allow customizable thresholds
GVAP	• CONGA has a fixed time window of 60 min • MAGE algorithm slightly modified and separately considers the mean of the upward excursions (MAGE+), or downward excursion (MAGE-)[187] the meaningful excursions value can be set within 30-500 $mg \cdot dl^{-1}$ • %TBR and %TAR customizable • AUC-high/low is divided by time in min • for CONGA and MODD only result from whole days are included
Tidepool	• TBR, %TAR, % TIR default thresholds are based on the recommended are 54, 70, 180 and 250 $mg \cdot dl^{-1}$, and for % TIR thresholds can be customized
CGManalyzer	• CONGA has specifiable time window • Groups comparison computes: mean difference, CI, SSMD, p-value of two-sided t-test and a feature based on SSMD, named class of effect size [194], representing the strength of the difference between groups
cgmanalysis	• CONGA has specifiable time window • MAGE follows the Baghurst et al. algorithm [187] and allow customizable time threshold values for excursions (defaults are 35 and 10 minutes for upper and lower, respectively) and of a value defining how large an excursion must be to be considered in the MAGE computation • %TAR, %TBR, %TIR thresholds can be customized • metrics are provided separately for daytime, nighttime and whole day

Name	Observations on computed metrics by each software
GLU	• %TAR, %TBR, %TIR computed with specific threshold values depending on particular conditions of glucose tolerance (using the arguments diabetes and pregnancy, whose values follow those recommended by the consensus) or customizable.
CGMStats Analyser	• CONGA has specifiable time window • MAGE follows the Service et al. algorithm [184], • %TIR, %TAR, %TBR computed using the thresholds recommended in the consensus[148]. • AUC-high computed with the option of selecting 10 $mmol \cdot l^{-1}$ or 15 $mmol \cdot l^{-1}$ as threshold
iglu	• CONGA has specifiable time window • MAGE follows the Service et al. algorithm [184] with the possibility to choose an alternative version implemented in iglu which emulates the manual MAGE computation • TAR, TBR, TIR default thresholds are the recommended ones[148], but can also be customized.
rGV	• CONGA has specifiable time window • MAGE follows the Service et al. algorithm [184], • %TIR, %TBR, %TAR have customizable thresholds, • LBGI and HBGI have the option of using their corrected version[180] • compute metrics also based on EasyGV to allow comparisons
cgmquantify	• CONGA24 with n fixed to 24 hours • MAGE follows the Service et al. algorithm [184] • computation of SD and CV considering the entire CGM trace and separately for each day and computes the mean, median and standard deviation of all the SD and CV obtained for each separate day

4.2 Summary of the main findings

This review outlined the 12 available software packages and tools for the analysis of CGM data, by highlighting their characteristics. Among them, the pioneers EasyGV and Glyculator, together with the more recent ones, such as cgmanalysis, GLU, and iglu, have been continuously updated (non-necessarily with an accompanying paper), while CGM-GUIDE is not fully available anymore. Of note, there were some packages that were excluded from our analyses for different reasons: the MAGE software package [186], which takes its name from the homonymous metric, was not considered because it relates to the calculation of a single metric; other packages that are branching out from existing ones were also excluded, as for the case of Continuous

Glucose Data Analysis (CGDA [195]), an R package (also available at https://github.com/EvdVossen/CGDA) that has been developed starting from the source code of the existing package cgmanalysis. Even though the analysis was focused on the software solutions available in the public domain, the main characteristics of commercial/proprietary software solutions have been summarized in the reference article [169].

In the following sections, some considerations that were drawn by our analyses are here summarized from the point of view of different "shades" of user expertise, starting from those with no technical programming skills until arriving to software developers on one direction, and pitting clinicians against researchers on the other direction

Usability and data management complexity

For basic users, software packages that provide a GUI (such as cgmanalysis, CGManalyzer, GLU and cgmquantify), that make available video tutorials (as in the case of Glyculator and Tidepool), in addition to detailed documentations, may represent an important advantage. For those who can engage in simple instructions in programming language, the choice of the tool will rely on their specific programming-language skills and the availability of the platform; indeed, accessibility is an issue: in the case of MATLAB and Excel-based packages, for instance, the respective license is required, while in the case of web-based solutions that does not provide a downloadable version such as CGMStatsAnalyser, an internet connection is required and analysis is not allowed when the website changes domain or when is under maintenance. Considering the point of view of developers, often in strict contact with the community of users represented by researchers and clinicians, packages providing open-source scripts are very important since they allow for interoperability and standardization of the analyses, two necessary aspects when one aspire to obtain comparable and reliable results.

As for the complexity of data management, the most impactful factor is time: packages that directly support the data format downloadable from popular CGM devices will be more desirable since they reduce time for dataset preparation. However, this aspect is not the only one that determines level of complexity for data

management. Indeed, CGManalyzer seems to be characterized by a higher level of complexity in data management with respect the other solutions, although it supports data format from popular CGM devices; conversely, EasyGV showed very low level of complexity albeit it does not. Indeed, from the point of view of citations, Glyculator and EasyGV appeared as the most used in scientific literature and this could be ascribed to their simplicity in data management and use.

Standardization of CGM data analysis

The lack in standardization is the result of the high number of metrics proposed in the literature and the variety of available data display options that are growing with the spread of CGM use. Realistically, clinicians that are willing to monitor their patients, to adjust and personalize their therapies and track their improvements, will prefer those software packages that provide metrics and data visualization options recommended by the international consensus [148], [149]; from the analysis here carried on it resulted that the highest number of standard metrics is provided by cgmanalysis and iglu. The AGP report, by displaying multiple intuitive information at the same time, represents a powerful visualization modality, which could even be enhanced taking its basic version as starting point [196], [197]. In particular, the stacked bar charts used to represent time in range, also part of the AGP report, have shown to be a powerful representation as they are compact and fast in performing comparisons [198]. The iglu package provides a rather faithful reproduction of this display mode, similarly to all the proprietary software solutions. The software solutions Glyculator, Tidepool and iglu provide stacked bars for time in range visualization; however, none of them account for the automatic adjustment of different thresholds in different categories of patients (i.e., older patients, pregnant women and different diabetes type).

On the opposite side, researchers interest is more focused on all the metrics and display options that best meet the needs of the analyses relatively to the research question they want to address. In the case of advanced statistical analysis, i.e., applying machine learning methods, having a high number of computable metrics could be desirable and in this regard, iglu provides a total of 39 metrics, a very high number compared to the proprietary solutions, and the highest among the non-commercial ones. Thus, incorporating in the software packages all the metrics that are continuously

coming out would allow their evaluation, considering possible correlations with existent ones and their usefulness in characterizing glycemic control. In this regard, software authors should consider including metrics such as COGI (that uses TIR, TBR and CV) and is available in iglu, and the more recent Glycemia Risk Index (GRI) [199], a composite metric that uses both level 1 and 2 of TBR and TAR in its computation. It is worth noting that, currently, not all the packages include the possibility to compute time in ranges with both level 1 and level 2 breakout thresholds at the same time, which would be required for computation of GRI. In this case, if the software allow to set customizable thresholds, the only way would be using a two-step running and then computing difference between the values obtained by the two runs. However, this option may be not immediate for all the users.

Quality assessment and agreement in metrics computations

To assess the quality of glycaemic control evaluation an adequate sampling duration is required in order to achieve an appropriate level of accuracy in the derived metrics. Indeed, some metrics (i.e., MAGE) may become unreliable in the presence of significant data loss or low sampling frequency [200]. Consensus recommendations dictate a CGM data length higher than 70% over 14 days, which has been shown sufficient to compute TIR in presence of small data loss [201]; metrics that assess hypoglycemia, especially in populations characterized by high glycemic variability, are quite unstable and require longer window lengths [202]. This set the importance to include as a best practice the use of data quality control metrics in CGM data analysis (as already provided by EasyGV, Glyculator, CGManalyzer, cgmanalysis and iglu), helping the user be aware of the presence of missing data and of the number of days available for the analysis. Moreover, discriminating differences between subjects represent another important point and MAG and M-value were shown able in attenuating the influence of within subject variability [203]. On the other hand, packages that provide the possibility to compute metrics both inter- and intra-day (single day, daytime and nighttime) allow to account for differences not only inter- but also intra-person.

The assessment of equivalence among CGM metrics computed by different software solutions is not so straightforward. For metrics having adjustable parameters

such as for IGC and M-value, it is obvious that the same settings among the various software solutions are required for comparison purposes. Apart from this, there are other possible source of discrepancies in computation of metrics i.e., differences in raw data manipulation/transformation, performed in different ways by different software during preprocessing phase; however, including some preprocessing is an important quality control feature, since the use of raw CGM data could lead to unmeaningful results. A second important source of discrepancies may be the existence of plural ways to compute quantities having the same meaning, and even maintaining the same names and acronyms. An example is the case of the MAGE, which requires an algorithm for peak definition and detection and has plural implementation versions; indeed, it showed poor agreement among different software solutions [204], as confirmed by results of this study. Another example of discrepant computation that we found out is that of the AUC, since often units differ and sometimes normalization is performed across different time intervals. Thus, the best way to avoid miscalculations is to rely on those tools that provide open-source code or at least a detailed package documentation. There are also packages, such as cgmanalysis, that are trying to gain validation against metrics obtained by proprietary tools of CGM devices [205]; however comparison is possible only in terms of final results.

Which is the best solution?

Overall, the study here performed helped to shed light on which kind of differences may be found in metric computations across different software packages and offered a simple and fast tool to magnify possible faults and advantages of each of the analyzed solutions. Depending on the use, each of the reviewed solutions has some peculiarities that can be exploited while performing CGM data analysis. It has to be noted that the Tidepool platform presents additional services whose investigation was out of the scope of this analysis. In particular, it enables the patient to integrate data from all his/her devices (not only CGM but also insulin pumps, glucometers and ketone meters) in a single app and to share them directly with the clinician, thus representing a powerful solution for telemedicine practice; however, this rises the need of standardization of metrics related to insulin, as proposed in a very recent study [206]. Research studies analysis could also benefit from those packages, such as

CGManalyzer and CGMStatsAnalyzer, that allow performing group analyses across different populations.

However, choosing among all the available solutions, one could quickly realize that he/she may need more than one at the same time and that there is no one-size-fits-all solution to answer the question. Moreover, a great need to collaborate on software coding, formulation of consensus and standards, improvement of software quality control, documentation, and maintenance has arisen.

Conclusions

To conclude, an overview of the available software packages for the analysis of CGM data has been provided. Reported information could be useful to researchers interested in working in CGM data analysis, as to clinicians and endocrinologists needing tools capable of handling CGM data effectively.

5 Feature-based CGM data-driven analysis

[4]In Chapter 4, evaluation of the available tools for the extraction of CGM metrics was carried out in both qualitative and quantitative terms; this analysis gave as result that depending on the user expectations and requests, there may be a tool that is more suited than another when dealing with CGM data analysis. For research contexts, as for the one in which this thesis is placed, the choice can fall into something which allow the computation of a sufficiently high number of metrics, including those approved by the 2017 [148] and 2019 [149] consensus, and at the same time computed in a reliable way. This is particularly desirable if the application of machine learning methods is expected. The software package iglu showed optimal features and advantages with respect to other available packages, thus it will be the CGM metrics calculator of choice for almost all the applications presented below.

This chapter will present a series of feature-based machine learning applications that will exploit CGM computed metrics as input to the various ML algorithms that will be selected for the data analyses. Indeed, CGM metrics can be classified into different domains that allow obtaining interpretable results with respect to using raw CGM data. More specifically, Section 5.1 aims to show approaches in the field of innovative diagnosis and early identification of diabetes complications; in one case, a precise CGM data time window, i.e., the postprandial glycemic response, will be exploited for feature extraction to set up a classification task able to identify individuals with T2D or prediabetes from individuals with normal glucose tolerance; in the other case, focus will be in the early identification of subjects affected by diabetic retinopathy starting from CGM metrics only. Sections 5.2 and 5.3 instead will show the development of a ML framework for the prediction of impending hypoglycemia; this will be applied to the case of exercise induced hypoglycemia in individuals having type 1 diabetes; from here, a novel metric to assess the risk of hypoglycemia before the start of exercise will be proposed. Finally, a similar approach will be then applied in the context of hemodialysis induced hypoglycemia.

[4] This chapter contains material published in [285] and in press in [286], [287] and [288], [289].

5.1 Innovative diagnosis and early identification of complications

The diagnosis of diabetes, as previously mentioned, is still based on plasma samples from which fasting glucose or HbA1c or 2h-PG during OGTT have to be measured; the early characterization of T2D in its early phase relies on model based methodologies and in recent years the design of CDSS based on routine general practitioner data [119], [125] is under investigation. Although CGM was typically used to monitor glucose levels in T1D [207] or GD [208], it has been a while now that researchers are also interested in investigating possible applications of CGM to study glycemic variability in T2D [209] or to characterize progression from normal condition to prediabetes condition [210]. CGM information has been exploited in classification models based on ML approaches to distinguish among different categories of subjects, such as normal, prediabetic and diabetic subjects [211], [212], [213]. However, those studies considered fluctuations over several days and not within-day fluctuations such as the postprandial window. Thus, this represent the firs gap in the literature that is highlighted and addressed in this section.

On the other hand, early detection is of utmost importance also in the case of complications. A very common complication of diabetes is the retinal microvascular dysfunction known as Diabetic Retinopathy (DR), a condition that progressively lead to blindness [214]. It affects more than 100 million people and it is estimated that its burden will rise to 160 million in 2045 [215]. Timely treatment is fundamental to decelerate DR progression before irreversible vision loss. At present, frequent retinal assessment has to be scheduled for an early detection and this is done through the analysis of fundus photography [216], a time-consuming task performed by ophthalmologists. ML and AI based approaches demonstrated useful for automatic screening without human input, starting from fundus images, socio-demographic and genetics data [217]. Solutions such as smartphone-based fundus camera imaging or teleophthalmology have been also proposed to increase the screening rate [218]; however, compliance to the ophthalmic examinations is still low and many individuals fail to achieve timely diagnosis and treatment [219]. This opens another gap for which new technologies such as CGM devices and smartphone apps may help improve early DR detection by broadening the access to screening [220].

5.1.1 Identification of differences in postprandial glycemic responses of normal subjects versus subjects with type 2 diabetes/prediabetes

On the basis of the considered time frame, a definition that is not rigorous but may help subdivide different cases is that of short-term and long-term glycemic variability. In particular, short-term glycemic variability refers to within or between days fluctuations, whereas long-term glycemic variability considers fluctuations over several weeks or even months [221]. Thus, the research question in this study is about exploring the possibility of using fluctuations measured in a shorter period, such as in response to a standardized meal, to create a classification model able to identify differences in the postprandial response between subjects having T2D/prediabetes and normal subjects. Workflow of the used methodology is shown in Figure 15.

Dataset preparation

Data used in this paper have been taken from a freely available dataset [222] and pertain to 30 participants that have been screened for T2D and a diagnosis was given based on ADA guidelines as described in section 1.1. Participants have been classified as normal vs having T2D or prediabetes as reported in Table XV. Each participant underwent 3 standardized meals with similar calories but with varying amounts of proteins, fat, and fibers and received each meal twice, on separate days and always at breakfast. Participants wore a Dexcom G4 CGM device (sampling intervals of 5 minutes) from 30 minutes before the meal intake of until 2.5 hours after.

Table XV. Participants' characteristics.

Participants' Characteristics	all	normal	T2D/prediabetes
n	30	20	10
Age (years)	42±14	38±13	50±12
BMI ($kg \cdot m^{-2}$)	26±6	23±3	32±5
Fasting insulin ($\mu U \cdot mL^{-1}$)	6.8± 4.1	4.8±2.0	10.4±4.2
Fasting glucose ($mg \cdot dL^{-1}$)	94±14	87±5	108±15

T2D: type 2 diabetes; BMI: Body Mass Index; 2h-OGTT: 2-hour plasma glucose after Oral Glucose Tolerance Test; HbA1C: glycated hemoglobin; Tri/HDL: triglyceride concentration divided by high-density lipoprotein concentration, an approximation of insulin resistance. Values are expressed as mean ± standard deviation.

Data inspection and preprocessing revealed that some CGM recordings were shorter or longer than expected (3 hours). Acquisitions that were at least 25 minutes shorter than expected were discarded, while the remainder were adjusted to the correct length by removing and/or adding samples (computing the mean value between previous and following sample or repeating the last available sample in case of last sample missing). On the basis of participants classification, each CGM recording has been labelled as CNT if belonging to a subject classified as normal, or as T2D/prediabetes if belonging to a subject classified as having prediabetes or diabetes. Finally, a total of 151 CGM-recording observations, 105 of which are labelled as CNT and 46 as T2D/prediabetes, has been included in the dataset.

Classification problem

A classification model has been designed to classify each CGM recording as CNT or T2D/prediabetes class. The classification model was based on a logistic regression model, implemented by fitting data to a generalized linear model (GLM) with binomial distribution of the error around the response variable and logit function as link function. The function used to fit the GLM was *fitglm* (MATLAB). The decision threshold for classification was set to 0.5.

Feature extraction and selection

From each CGM recording, 19 features were extracted and are reported in Table XVI.

Table XVI Extracted CGM metrics divided according to the related feature domains.

Domain	CGM Metrics
Descriptive statistics	mean , median, min (i.e., minimum), max (i.e., maximum), SD , range, skew (i.e., skewness).
Meal related handcrafted features	maxGidx (i.e., timing of the peak after the meal) [223], prePmean and postPmean (i.e., preprandial and postprandial mean) [224], prePtime and postPtime (i.e., fraction of time spent below the preprandial mean and above the postprandial mean) [225], slope [225], AUCG [224]
Spectral features	meanFFT, medianFFT, minFFT, maxFFT and SDFFT of the Fast Fourier Transform of the CGM recording [226].

Feature selection was carried out in two steps. The first was application of a filter type feature selection and it was performed by visually inspecting the scatterplot matrix, reporting pairwise relationships between any combination of features. For a given pair of highly correlated features, point biserial correlation (equivalent to the Pearson's correlation) to class was computed and the one showing the highest correlation was retained, while the other discarded.

The second step of feature selection was a wrapper type (or sequential) feature selection, based on the classification model performances. It was conducted through a recursive algorithm based on the evaluation of the deviance of the fit, a generalization of the residual sum of squares [227]. Starting with the feature subset selected in the previous step, the deviance of the fit was computed and used as reference (dev0); one feature at a time was removed from the model, the deviance of the reduced model (devR) was calculated and compared with the deviance of the full model and the following rules were applied: if devR was higher than dev0 augmented by a tolerance value, the feature just excluded was considered significant for the classification task and was reintroduced in the model, otherwise it was considered irrelevant and discarded. The tolerance value was set to the 95th percentile for the chi-square distribution with 1 degree of freedom, i.e., tolerance equal to 3.84 [227].

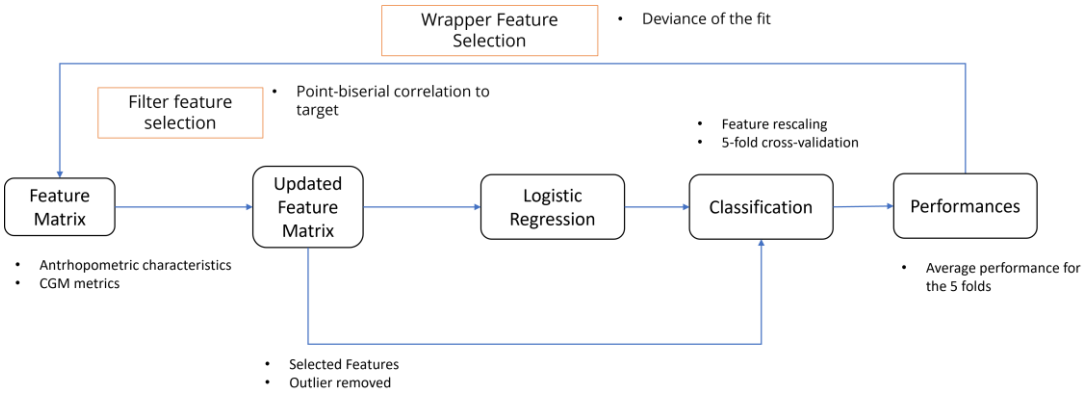

Figure 15. Methodology workflow.

Model validation

A logistic regression model, fed either with the features selected after the filter type or those selected after the wrapper type feature selection, has been validated using a 5-fold cross-validation. The resulting two classification models have been indicated as M_{FT} in the first case and M_{FT+WT} in the second case. Given that there were multiple recordings for each participant and that they were assumed as distinct observations in the dataset, whenever the dataset was split into training and validation sets during cross-validation, the observations of the same subject were included in either the training set or the validation set and not split between them.

Performance evaluation

T2D/prediabetes and CNT classes were considered as positive and negative classes, respectively. The T2D/prediabetes cases correctly classified as T2D/prediabetes were defined TP; the CNT cases correctly classified as CNT were defined TN; the T2D/prediabetes cases incorrectly classified as CNT were defined FN; eventually, the CNT cases incorrectly classified as T2D/prediabetes were defined FP.

Evaluation of the performance for both MFT and MFT+WT was accomplished by AUC of ROC, CA, SE, SP, and by positive predictive value, and negative predictive value defined as:

- PPV = TP / (TP + FP);
- NPV = TN / (TN + FN).

5.1.2 Results

After the filter type feature selection, 14 features out of 19 were retained and the rest were discarded. The wrapper type feature selection, furtherly dropped 5 features, hence arriving to 9 features. The timeline of feature selection is schematized in Table XVII. ROC curves and the mean AUC across the 5 folds for M_{FT} and M_{FT+WT} are depicted in Figure 16. M_{FT} and M_{FT+WT} deviance of the fit was found equal to 89.44 and 93.21, respectively. Performance measures for each of the 5 folds and averaged across them are shown in Table XVIII for M_{FT} and M_{FT+WT} .

Table XVII. Feature selection timeline. M_{FT} selected 14 features after filter type feature selection; M_{FT+WT} selected 9 features after wrapper type feature selection.

Features	**Description**	**M_{FT}**	**M_{FT+WT}**
mean	Mean glucose	X	X
median	Median glucose	X	
min	Minimum glucose	X	
max	Maximum glucose	X	X
maxGidx	Timing of peak after meal	X	X
SD	Standard deviation of glucose	X	X
range	Difference between max and min glucose		
prePmean	Pre-prandial mean glucose	X	X
postPmean	Post-prandial mean glucose		
prePtime	Percentage of time below prePmean	X	
postPtime	Percentage of time above postPmean	X	X
slope	Slope between meal and peak	X	
AUCG	Area Under glucose Curve		
skewness	Skewness	X	
$mean_{FFT}$	Mean of Fourier transform	X	X
$median_{FFT}$	Median of Fourier transform	X	X
min_{FFT}	Minimum of Fourier transform	X	X
max_{FFT}	Maximum of Fourier transform		
SD_{FFT}	Standard deviation of Fourier transform		

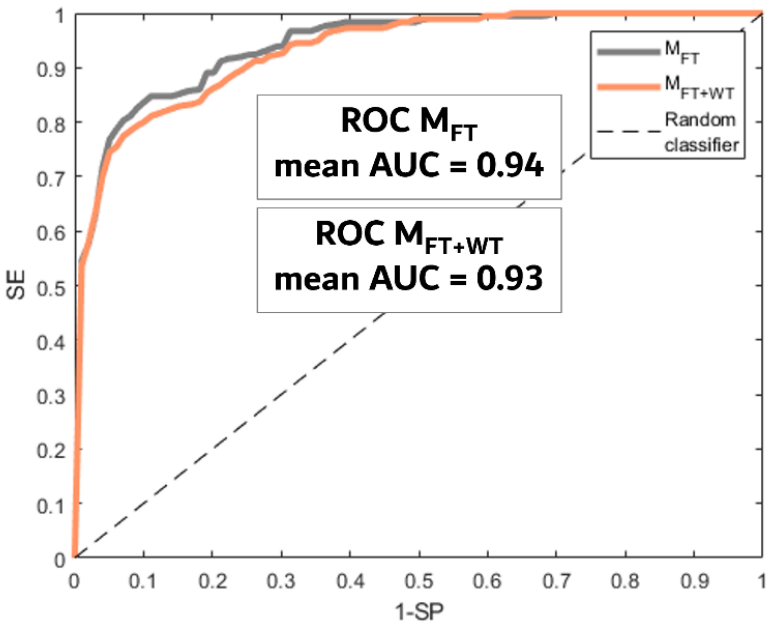

Figure 16. Average ROC curves computed across the 5-fold cross-validation and their mean AUC for the model before wrapper type feature selection (M_{FT}) and after it (M_{FT+WT}).

Table XVIII. M_{FT} and M_{FT+WT} performance measures across the 5 folds of the cross-validation.

		Fold 1	Fold 2	Fold 3	Fold 4	Fold 5	Mean ± sd
CA	$\mathbf{M_{FT}}$	0.89	0.86	0.94	0.79	0.65	0.82 ± 0.10
	$\mathbf{M_{FT+WT}}$	0.85	0.86	0.91	0.82	0.74	0.84 ± 0.05
SE	$\mathbf{M_{FT}}$	0.84	0.63	0.95	0.96	0.73	0.82 ± 0.13
	$\mathbf{M_{FT+WT}}$	0.84	0.63	0.95	1.00	0.82	0.85 ± 0.13
SP	$\mathbf{M_{FT}}$	1.00	0.95	0.91	0.40	0.44	0.74 ± 0.26
	$\mathbf{M_{FT+WT}}$	0.88	0.95	0.82	0.40	0.56	0.72 ± 0.21
PPV	$\mathbf{M_{FT}}$	1.00	0.83	0.95	0.79	0.76	0.87 ± 0.09
	$\mathbf{M_{FT+WT}}$	0.94	0.83	0.91	0.79	0.82	0.86 ± 0.06
NPV	$\mathbf{M_{FT}}$	0.73	0.86	0.91	0.80	0.40	0.74 ± 0.18
	$\mathbf{M_{FT+WT}}$	0.70	0.86	0.90	1.00	0.56	0.80 ± 0.16

CA: Classification accuracy; SE: Sensitivity; SP: Specificity; PPV = Positive Predictive Value; NPV = Negative Predictive Value.

5.1.3 Discussion

The proposed classification model identified differences in postprandial glycemic response of subjects having T2D/prediabetes with respect to that of normal subjects based on CGM data recorded during a standardized meal test. The main novelty of this work is that the window of the CGM signal from which the features are extracted is related to a standardized meal test and not to a signal lasting several days. Indeed, post-prandial glucose response in individuals with T2D differs significantly from the response of a healthy subject, for example in magnitude and peak delay [223], therefore it can be indicative of the health status of the person being analyzed. In this investigation features were handcrafted and not computed using iglu nor any other of the packages presented in Chapter 4. This is because we tried to consider features capable to enhance information in relation to the short postprandial time window considered. Future studies introducing different CGM metrics, including standardized ones, are however desirable.

Despite a multinomial classification (i.e., normal vs prediabetes vs diabetes) would be preferable, technical problems arise when it comes to a highly imbalanced dataset such this one. Indeed, class imbalance has a negative impact on classification performances and, although there exist techniques to overcome this issue [137] this was a first attempt and further investigation should be done. Similarly to other studies in the same context [211], as also in Chapter 3, a simple logistic regression model has been proven adequate to perform this classification task, with the advantage of

granting interpretability of the results which is a desideratum in the biomedical context. When considering more difficult classification tasks as for example differentiating between prediabetes and diabetes more sophisticated techniques may be necessary [212], [213]. The presence of different CGM recordings of the same subject could represent a further limitation in this study, however, for each fold, these were not considered simultaneously in the training and validation set.

The deviance of the fit, which quantifies the goodness-of-fit of the model, was equal to 89.44 for M_{FT} and 93.21 for M_{FT+WT}. This meaning that M_{FT+WT} "fits worst" than M_{FT}, but its deviance is still within the allowed value which is 93.28 (= 89.44 + tolerance, where tolerance = 3.84). Mean AUC resulted to be 0.94 for M_{FT} and 0.93 for M_{FT+WT}, revealing that in both cases, the positive and negative classes are well separable, and the models are robust with respect to the choice of the decision threshold of 0.5. Comparison between M_{FT} and M_{FT+WT} in terms of performance measures (see Table XVIII), shows that M_{FT+WT} represents the optimal choice. Indeed, besides an improvement of M_{FT+WT} compared with M_{FT} in terms of mean CA, SE and NPV, a lower standard deviation across the folds in almost all M_{FT+WT} measures (except SE) can be observed, indicateing that in M_{FT+WT} the performances of the classifier are quite independent on the training and validation partitions used. In both models the lowest performances were in the SP. This may have two explanations: firstly, the positive class is the minority class, accounting for just the 30% of the samples; secondly, the positive class exhibits a higher variance since it includes at the same time CGM-recording observations of subjects with prediabetes and with diabetes.

Along with the type of data used, an innovative aspect of this study is the two-steps feature selection. With respect to other systems based on physiological and anthropometric data [228], models that use metabolites' dynamic (such this one) can discover hidden patterns that are not present in static measurements [222], [224].

The use of such data to characterize the health status of a subject has the potential to account for individual differences that standard medical approaches might miss [229]. In this sense, this work can be framed in the domain of precision medicine, both because CGM allows for precision monitoring and because the logistic regression model implies a probability-based decision, thus reasonably compatible with a precision diagnosis [229].

In conclusion, the classification model here proposed based on CGM data recorded during a standardized meal test is able to identify differences in the postprandial glycemic response of subjects having prediabetes or diabetes from that of normal subjects.

5.1.4 Diabetic Retinopathy Detection

This study aimed to explore the potential of CGM and ML for DR detection. Workflow of the methodology is shown in Figure 17.

Database

[5]The cohort used in the present paper was derived from the REPLACE-BG study involving subjects having type 1 diabetes and under insulin pump treatment, who were monitored for 36 weeks using a CGM device (Dexcom G4) that recorded interstitial glucose every 5 minutes [11].

A total of 78 subjects (39/39 males/females, aged 43.9±13.9) were considered, of which, at the time of enrollment, 50 had various degrees of diabetic retinopathy (subset referred as DR group) and 28 had type 1 diabetes with no further complications (subset referred as NDR group). An inclusion criterion for both groups was having type 1 diabetes diagnosed for more than 10 years, time after which is more likely to develop DR. Characteristics of the two groups are reported in Table XIX.

Table XIX. Characteristics of the two groups.

Characteristic	**Groups**		
	DR	**NDR**	**p**
Age (years)	48.6± 12.6	35.4± 12.2	<0.01
Sex (M/F)	21M/29F	18M/10F	-
Hba1c (%)	7.1±0.7	7.2±0.7	n.s.
BMI (kg/m^2)	28.1± 4.7	26.0± 4.1	n.s.

Data are presented as mean±standard deviation. Statistically significant differences are set at $p<0.05$; n.s.: not significant; Hba1c: glycated hemoglobin; BMI: body mass index.

[5] The source of the data is the T1D Exchange, but the analyses, content and conclusions presented herein are solely the responsibility of the authors and have not been reviewed or approved by the T1D Exchange.

Data Preprocessing and Feature Extraction

To process CGM data the freely available R-based iglu software package was here used, which accurately allows both preprocessing and feature extraction as confirmed by our investigation performed in Chapter 4. CGM data were preprocessed to handle missing data points through linear interpolation of gaps lasting less than 45 minutes (i.e., 9 consecutive samples). Moreover, data were rearranged by performing the temporal alignment of each separate day of recording obtained from each subject to allow the correct computation of time-dependent CGM features; this was done through the iglu function *CGMS2DayByDay*.

Features included in the dataset were anthropometric characteristics (i.e., age, sex, BMI) and extracted CGM metrics, for a total of 54 features. Details on the computed CGM metrics and on the default settings for computation can be found in the iglu package documentation. Each CGM metric may describe glycemia trend according to one or more out of five different domains, namely descriptive statistics, hyperglycemia, hypoglycemia, glycemic control (i.e., glycemia maintenance inside optimal ranges) and glycemic variability (i.e., glucose fluctuations quantification), as detailed in Table XX.

Table XX. Extracted CGM metrics divided according to the related feature domains.

Domain	**CGM Metrics**
Descriptive statistics	CV*, SD*, minimum (Min.), maximum (Max), range, 1st and 3rd quartiles (1stQu, 3rdQu), Median, Mean, IQR
Hyper-glycemia	GRADE hyperglycemia contribution (GRADE_hyper), HBGI, hyperglycemia index (hyper_index), percentage of time above standard thresholds (above_140, above_180, above_250), area under glucose curve (AUGC)*, GRI*
Hypo-glycemia	GRADE hypoglycemia contribution (GRADE_hypo), LBGI, hypoglycemia index (hypo_index), percentage of time below standard thresholds (below_54, below_70), COGI*
Glycemic control	eA1C, GMI, GRADE and its euglycemia contribution (GRADE_eugly), IGC, M_value, percentage of time spent in reference ranges (TIR_63_140, TIR_70_180, TIR_70_140 aka TITR)
Glycemic variability	ADRR, J_index, MAD, MAGE, GVP, MODD, SD of glucose rate of change (SD.Roc), MAG, CONGA1, CONGA24, SD subtypes (SDw, SDwsh, SDbdm, SDhhmm, SDdm, SDb), CV subtypes (CV_Measures_Mean, CV_Measures_SD

*SD and CV must also be considered pertaining to glycemic variability domain; GRI also to hypoglycemia, AUCG also to hypoglycemia and glycemic control, COGI also to glycemic control and glycemic variability domains.

Formulation of the Classification Model

To fulfill the aim of the study of exploring the possibility to identify DR by exploiting information contained in CGM data a classification task was pursued, defining the DR class based on data from the DR group (50 instances) and the NDR class based on data from the NDR group (28 instances). The analysis was performed in Orange Data Mining environment (version 3.30.2).

Outliers detected through LOF were then excluded from the analysis. After outlier removal, the dataset was split into training and test sets with a 70%-30% partitioning by random sampling and maintaining the same proportion of DR and NDR cases in both sets. The test was left apart to be used at the end of the modeling process for performance evaluation. Feature selection also in this case was carried out in two steps: a filter type feature selection method was used to address collinearity among features, by retaining those that were highly correlated to the target (point-biserial correlation to class as in 5.1.1); then, ReliefF ranking method was used to further reduce the feature set by retaining features with best ReliefF score and keeping the number of selected features as low as possible. The obtained feature set was then given as input to four different classification models, namely, Logistic Regression, kNN, Random Forest and Naïve Bayes. Hyperparameter tuning was performed during Leave One Out (LOO) cross validation. Model hyperparameters settings were as follows: for Logistic Regression "Ridge (L2)" regularization was used and cost strength "C" = 10; for kNN "Number of neighbors" = 6, "Metric" = Manhattan, for Random Forest "Number of trees" = 10, "Number of attributes considered at each split" = 5, "Do not split subsets smaller than" = 5, "Limit depth of individual trees" = 35. Of note, training set only was used for both feature selection and models training. Features were normalized to have zero mean and unit variance.

Performance Evaluation

Considering DR class as positive and NDR class as negative, the DR and NDR cases correctly classified by the classification algorithm were considered TP and TN, respectively; the DR cases identified as NDR by the classification algorithm were considered FN, while the NDR cases identified as DR by the classification algorithm

were considered FP. Performance metrics that were selected to evaluate each classification algorithm were AUC of ROC, CA, PR, SE, SP and F1.

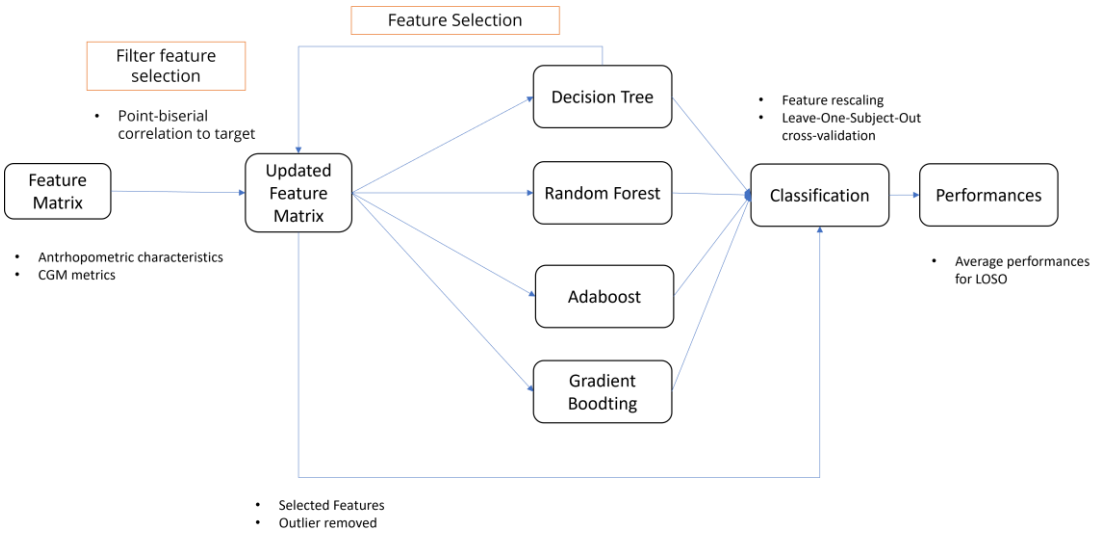

Figure 17. Methodology workflow. Of note, testing was done after model assessment.

5.1.5 Results

Feature values differences for the two groups are not shown, but significantly different features were 27 out of 54. Outlier detection resulted in 2 instances removed from the dataset, leading to a total of 76 final instances. After feature selection, the final feature set included 5 features that were Sex (ReliefF=0.24), Age (ReliefF=0.08), SDdm (ReliefF=0.05), SDb (ReliefF=0.04) and CV_Measures_SD (ReliefF=0.04). Inclusion of features with a ReliefF score lower than 0.04 resulted in lower performances and thus was not pursued. Performance metrics for both LOO validation and testing are reported in Table XXI. Confusion matrices for the test set (panel A) and Venn diagrams of correctly classified and misclassified cases (panel B) are shown in Figure 18.

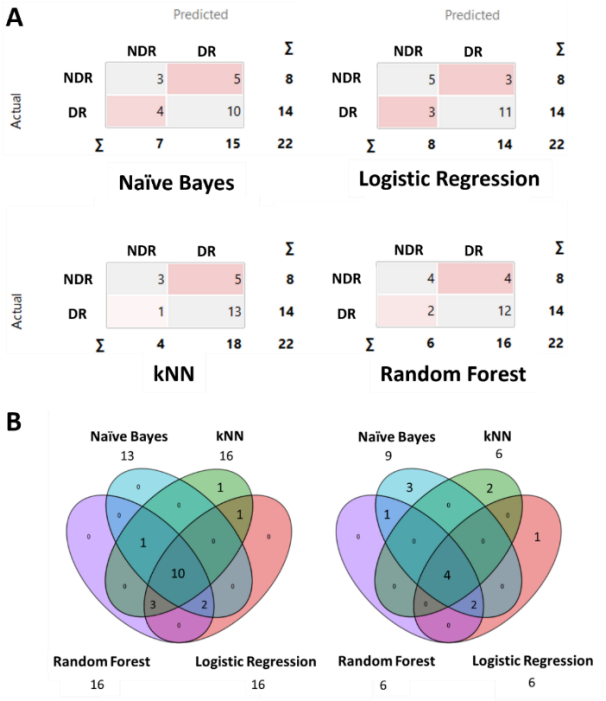

Figure 18. A) Confusion matrices for the four models in the test set; B) Venn diagrams for the correct (left) and misclassified cases (right) obtained for the four models in the test set.

Table XXI. Performances

Model	**Performance Evaluation**		
	Performances (%)	**LOO set**	**Test set**
Logistic Regression	AUC	82.2	77.7
	CA	83.3	72.7
	PR	83.2	72.7
	SE	83.3	72.7
	SP	79.9	68.3
	F1	83.2	72.7
kNN	AUC	78.1	74.1
	CA	81.5	72.7
	PR	82.0	73.2
	SE	81.5	72.7
	SP	80.9	57.6
	F1	81.6	69.9
Random Forest	AUC	86.8	79.5
	CA	83.3	68.2
	PR	83.5	66.7
	SE	83.3	68.2
	SP	82.0	55.0
	F1	83.4	66.1
Naïve Bayes	AUC	86.9	71.0
	CA	70.4	59.1
	PR	76.1	58.0
	SE	70.4	59.1
	SP	76.4	49.8
	F1	70.8	58.4

CA: classification Accuracy; LOO: Leave One Out.

5.1.6 Discussion

A ML approach based on CGM for DR detection have been presented. Being a feature-based approach (use of CGM metrics instead of raw CGM time series) it reduces the computational load, making it suitable for real-time applications and granting interpretability. Suitability of the selected metrics was also confirmed in previous studies [230].

Among the four ML algorithms used, Logistic Regression performed better in testing, with a balanced number of misclassifications accounting for less than 30% of misclassified cases. Compared to studies using electronic health records instead of CGM data [231], this approach achieved similar AUCs and lower SPs counterbalanced by higher SEs, which are desirable in biomedical context and suggest the potential of integrating both data sources. The main advantage of relying only on CGM for DR detection is in the opportunity to ensure wide screening, thanks to the growing diffusion of CGM use among patients with diabetes. Future studies examining different time windows (instead of all the 26 weeks at the same time as done here) for CGM metrics extraction will be an opportunity for improvement.

5.2 A machine learning framework based on CGM to prevent the occurrence of hypoglycemia: the case of exercise-induced hypoglycemia

Physical exercise is highly encouraged in the management of T1D since it was shown to improve cardiovascular health and glycemic control [232], ant to have beneficial effects in maintaining good fitness, healthy body weight and composition together with psychosocial wellbeing [233]. However, physical activity, especially prolonged aerobic exercise, causes changes in blood glucose levels which determine a high risk of hypoglycemia occurrence both during and after the exercise session. This increased risk discourages patients in engaging the recommended regular exercise, which in children and adolescents coincides with the recommendation for healthy children, of at least 60 min of moderate- or vigorous-intensity physical activity per day. Although guidelines have been provided to help combine meal timing, insulin therapy and

physical activity [233], [234], intersubject and intrasubject variability affects glucose changes during exercise and safe avoidance of exercise-induced hypoglycemia is still an open challenge. CGM devices real-time monitoring can be exploited in the context of exercise also in association with automated insulin delivery (AID) algorithms and insulin pumps to allow insulin to be automatically adjusted based on glucose levels and carbohydrate intake. However, AID accuracy decreases during exercise and thus is still not effective in preventing exercise-induced hypoglycemia [235]. A possible help may come from the use of CGM data before the exercise to predict incoming adverse events and provide the patient with information about the risk of hypoglycemia giving suggestions to counteract it before starting physical activity.

5.2.1 Exercise-induced hypoglycemia classification

Although there are a number of studies that have evaluated the use of ML techniques to predict hypoglycemia from CGM data [236], [237], [238], we are not aware of a prior study that exploited classification based on CGM metrics to reveal pre-exercise characteristics associated with hypoglycemia during and after exercise. Thus, this section aim is to investigate application of ML to distinguish whether a specific configuration of CGM metrics evaluated before starting of exercise could be more prone to induce hypoglycemia after the start of the exercise session until the following day (to account also for nocturnal hypoglycemia).

Clinical Studies

Two different datasets from children with T1D were investigated separately: the first in which exercise was performed in controlled conditions and the second in which was performed in free-living conditions. Subjects details are reported in Table XXII.

The first study included freely available data from the Diabetes Research in Children Network (DirecNet) multi-center study group (https://public.jaeb.org/direcnet/stdy/160), involving 50 young subjects with T1D, average age being 14.8 ± 1.7 years, with 22 females and 28 males and average glycated hemoglobin (HbA1c) of 7.8 ± 0.8% [239]. Each subject had a 24-h inpatient stay with a 75-minute exercise session in the late afternoon. On the morning of the inpatient stay, the subjects were asked to walk on a motorized treadmill for 5 to 15 minutes until

achieving a heart rate of 140 beats per minute (equivalent to 55% maximum effort, i.e., VO2 max) to record treadmill settings and use them as the start settings of the exercise session. The CGM device was the Medtronic MiniMed (5-minute sampling) and it was worn throughout the day until the morning of the following day.

The second study involved children from the freely available T1-DEXIP dataset (https://public.jaeb.org/dataset/590) involving 51 subjects with T1D, average age being 13.7 ± 1.7 years, with 33 females and 18 males and average glycated hemoglobin (HbA1c) of 6.8 ± 1.1%. In a 10 days study period subjects underwent different types of exercise including individual and group forms of exercise, in both competition and non-competition settings. For the purpose of the analyses, running activity was selected and one day of exercise was considered in order to avoid subject dependent bias in classification. Subjects used their personal Dexcom G6 CGM, or a blinded Dexcom G6 CGM if they did not use a personal Dexcom G6 CGM.

Preprocessing and Labelling

Pre-exercise data, i.e., the available portion (ranging from 2 to 5 hours) of CGM recording that preceded the start of the exercise session have been used to extract relevant CGM metrics as described below.

Post-exercise data, i.e., the portion of CGM recordings following the start of the exercise session have been used for post-exercise hypoglycemia screening. In case of pre-exercise acquisitions lasting less than 2 hours or of missing samples in post-exercise acquisitions, the related subjects have been excluded from the analysis. In case of missing samples in pre-exercise data, linear interpolation was used if the maximum gap was lower than 45 minutes. In the first study all interventions during the study were done considering a threshold of 60 mg/dl to define hypoglycemia, thus the same definition was maintained in the labelling [239]. For the second study, instead, hypoglycemia threshold was the standard one of 70 md/dl.

On the basis of hypoglycemia screening, pre-exercise acquisitions were labelled as HYPO, if belonging to subjects who experienced hypoglycemia, or as NO-HYPO, if belonging to subjects who did not experience any hypoglycemia during the time period following exercise.

Table XXII Characteristics of the two datasets.

	First study	Second study
Age (years)	14.8 ± 1.7	13.7 ± 1.7
Sex (M/F)	28/22	33/18
HbA1c (%)	7.8 ± 0.8	6.8 ± 1.1
Therapy	27 pump 23 MDI	51 pump/Closed loop
CGM device	Medtronic MiniMed	Dexcom G6
Exercise	Controlled conditions (inpatient stay) 75-minute exercise session (treadmill) at 55% VO2 max	Free daily living (running)
Hypoglycemia threshold used for labeling HYPO/NO-HYPO	60 mg/dl (as for the study protocol [1])	70 mg/dl for at least 15 minutes (as for consensus [2])
HYPO/NO-HYPO evaluation window	From start of exercise until following morning	From start of exercise until following morning

Feature Extraction and Dataset Construction

Features included in the dataset for each subject were both anthropometric characteristics (i.e., weight, height, BMI) and CGM metrics. A total of 43 CGM metrics have been extracted from pre-exercise CGM data by using either the R package iglu [162], and custom made R functions. GRI index was computed separately since iglu did not provide it at the time of the analysis. Metrics for which parameters are not reported were computed using iglu default settings. CGM metrics available in iglu but for which a minimum of 2 days of recording is needed for computation were not considered for the analysis. A summary of all the features included in the dataset according to the same CGM metrics domains described in 5.1.4 is shown in Table XXIII.

Classification Problem and Data Analysis

The classification problem has been designed to classify subjects as those who experienced versus those who did not experience hypoglycemia after the start of the

exercise session. Thus, starting from each subject single pre-exercise data previously labeled as HYPO and NO-HYPO, the respective homonymous classes (HYPO and NO-HYPO) have been defined. Data analysis was performed in Orange 3.30.2.

Features selection has been performed in two steps, belonging to the category of filter and intrinsic feature selection, respectively. Filter type feature selection through point biserial correlation (as in 5.1.1) was used to retain the best feature set with a reduced collinearity. The second step exploited a decision tree-based feature selection to determine the more relevant predictive features by splitting data into more homogeneous partitions in relation to the class, as done instead in 3.2.2. Parameters of the decision tree-based classification algorithm were set as follows: “Minimum number of instances in leave” = 2; “Do not split subsets smaller than” = 10; “Limit maximal tree depth to” = 10. Moreover, the option “Induce binary tree”, was selected and “Stop when majority reaches 90%” was chosen. The final feature set thus obtained was then further evaluated with respect to the classification problem by providing it as input to three other classification models: random forest, adaboost and gradient boosting. Hyperparameter tuning was performed heuristically during training and set as follows:

- random forest: “Number of trees” = 25, “Number of attributes considered at each split” = 2, “Do not split subsets smaller than” = 5, “Limit depth of individual trees” = 15;
- adaboost: “Number of estimators” = 100, “Learning Rate”= 1, SAMME.R classification algorithm as boosting method which updates base estimator's weight with probability estimates, and selecting “Exponential” as regression loss function;
- gradient boosting: “Number of estimators” = 100, “Learning Rate”= 0.3, “Lambda” = 0.05, “Limit depth of individual trees” = 3, “Fraction of features for each tree”=1 and catboost as method.

All features were normalized to have a common scale (mean equal to zero and unit variance).

Leave-One-Out Cross-Validation and Performance Evaluation

All the classification algorithms (decision tree, random forest, adaboost and gradient boosting) were validated through leave-one-out cross-validation procedure. By considering HYPO class as positive and NO-HYPO class as negative, the HYPO cases correctly classified were considered TP; the NO-HYPO cases correctly classified were considered TN; the HYPO cases classified as NO-HYPO were considered FN; and the NO-HYPO cases classified as HYPO were considered FP. Performance metrics considered were AUC of the ROC, CA, PR, SE, SP, and F1.

Table XXIII. Summary of features: CGM metrics grouped according to the different domains.

Domain	**CGM Metrics**
Descriptive statistics	CV*, SD*, Min, Max, range, 1st and 3rd quartiles (1stQu, 3rdQu), Median, Mean, IQR
Hyperglycemia	GRADE_hyper, HBGI, hyper_index, above_140, above_180, above_250, AUGC*, GRI*
Hypoglycemia	GRADE_hypo, LBGI, hypo_index, below_54, below_70, COGI*
Glycemic control	eA1C, GMI, GRADE GRADE_eugly, IGC, M_value, TIR_63_140, TIR_70_180, TIR_70_140 aka TITR
Glycemic variability	ADRR, J_index, MAD, MAGE, GVP, SD.Roc, MAG, CONGA1, SD subtypes (SDw, SDwsh, SDbdm, SDhhmm, SDdm, SDb), CV subtypes (CV_Measures_Mean, CV_Measures_SD

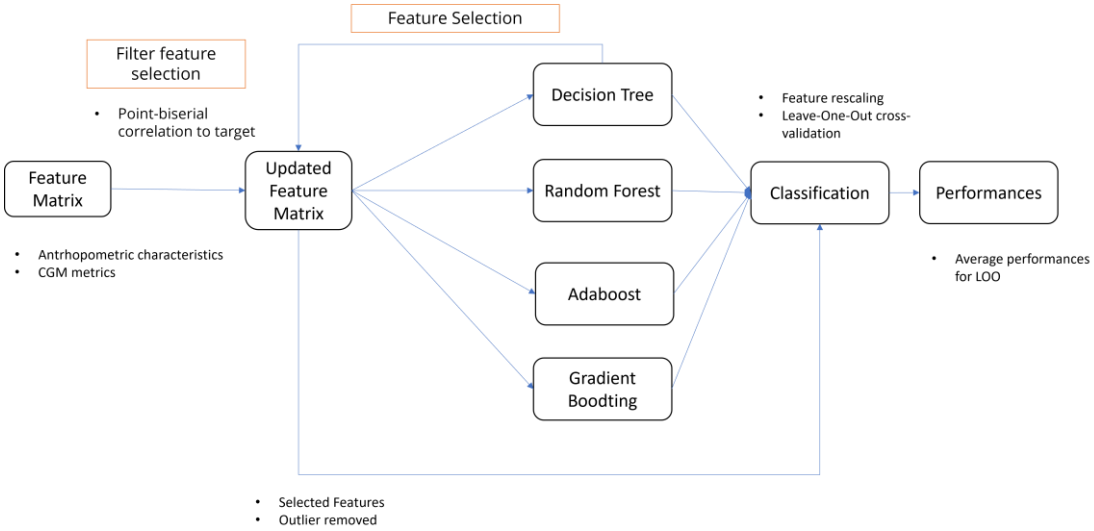

Figure 19. Workflow of the methodology.

5.2.2 Exercise-induced hypoglycemia index (HIKE)

HIKE (Hypoglycemia Index to Keep-a-check-on Exercise), a new composite index of hypoglycemia risk during and after exercise, based on CGM metrics evaluated in the pre-exercise phase, was formulated. HIKE was designed as detailed in equation 15 by combining a set of CGM metrics, whose role in predicting upcoming exercise-induced hypoglycemia was demonstrated in the results obtained for the first study dataset. CGM metrics selected by the second study dataset were not considered, since at present, results obtainable at free-living conditions (second study results) were slightly worse and need further investigation as will be discussed in the discussion section (5.2.4). Such results are presented in the following paragraphs (5.2.3).

$$\mathrm{HIKE} = \left(1 - \mathrm{mean}(\text{M-value}_{\mathrm{rescaled}}\mathrm{Max}_{\mathrm{rescaled}}, \mathrm{TAR180}_{\mathrm{rescaled}}, \mathrm{TAR250}_{\mathrm{rescaled}})\right) \times 100 \quad (15)$$

5.2.3 Results

A total of 47 CGM recordings (one for each subject and accounting for a total of 12081 glucose data points), 34 labelled as HYPO and 13 labelled as NO-HYPO were included in the analysis after preprocessing. Features computed for the preprocessed dataset for which 25 out of 43 features resulted statistically different between the two classes are not shown but can be found in the published work.

After the first step of feature selection, feature correlation to target was used to retain the best 36 features out of the 43 contained in the full dataset. With the second step of feature selection, the best predictive features obtained by the decision tree-based classification algorithm are shown in Figure 20. In case of the first study, high hypoglycemia risk after exercise, the M-value (i.e., the level of glucose deviation from the reference basal value) is more likely to distribute toward lower values, as shown by the first split of the decision tree. The other three selected metrics are instead associated with hyperglycemia. For the second study, selected metrics were instead more associated with glycemic variability. This may be explained by the better glycemic control that characterized this second group, as for the Hba1c in Table XXII. Performance results, obtained by all the used classification algorithms through leave one out validation, are reported in Table XXIV, and Figure 21 shows the related receiver operating characteristics (ROCs).

Table XXIV. Average performance metrics for leave-one-subject-out cross-validation on each classification algorithm

Algorithm	**First study performances (%)**					
	AUC	***CA***	***PR***	***SE***	***SP***	***F1***
Decision Tree	85.52	87.23	86.93	87.23	76.11	86.88
Gradient Boosting	82.13	78.72	78.72	78.72	68.11	78.72
Random Forest	78.05	74.47	74.47	74.47	61.73	74.47
Adaboost	74.32	76.60	78.56	76.60	72.05	77.27
	Second study performances (%)					
	AUC	***CA***	***PR***	***SE***	***SP***	***F1***
Decision Tree	80.48	80.39	80.62	80.39	76.27	79.97
Gradient Boosting	69.68	68.63	68.17	68.63	63.75	67.96
Random Forest	69.37	76.47	77.06	76.47	70.67	75.58
Adaboost	67.86	70.59	70.33	70.59	65.13	69.73

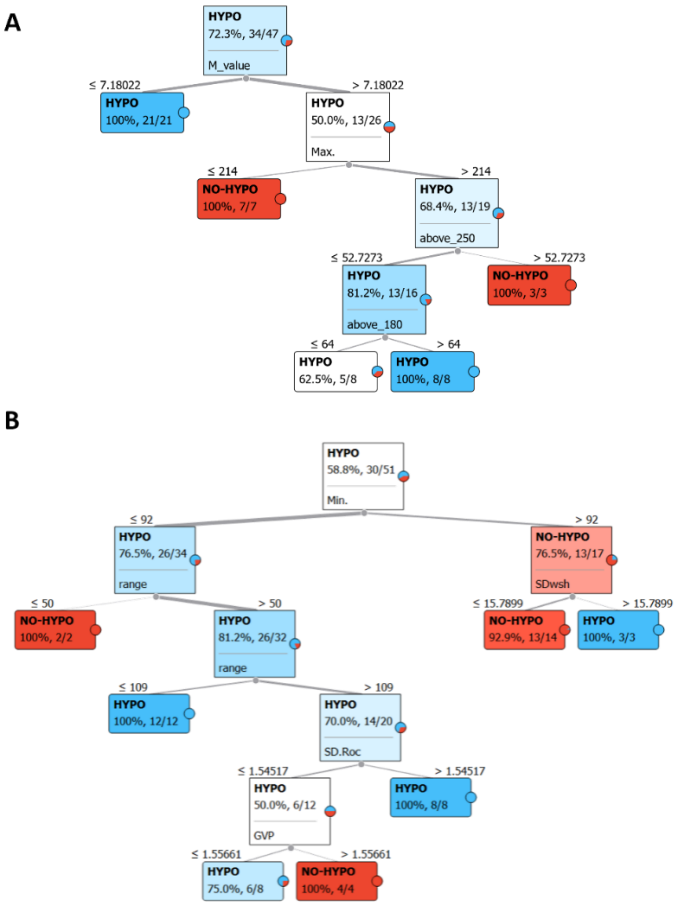

Figure 20 Decision tree classification algorithm based on the resulting best predictive features.

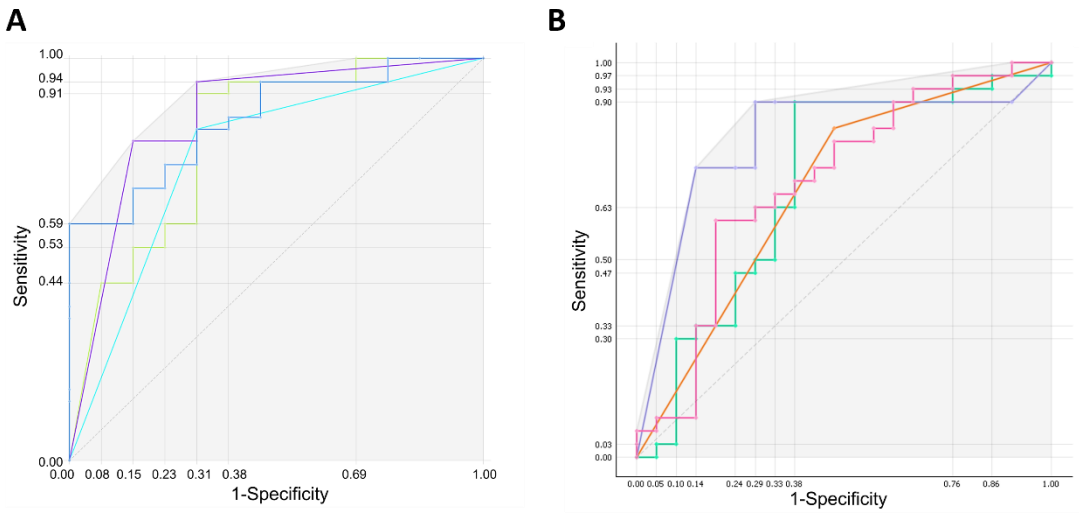

Figure 21 Receiver Operating Characteristics for decision tree (purple), random forest (green), adaboost (cyan), and gradient boosting (blue).

For HIKE metric, after outliers removal, a total of 47 subjects, i.e., those pertaining to the first study, were included. Considering those who experienced hypoglycemia (34 out of 47), HIKE classified 27 as high-risk and 6 as medium-risk. The 77% of cases classified by HYKE as subject at risk of exercise-induced hypoglycemia actually experienced hypoglycemia. Similarly, 75% of cases classified by HYKE as subject at low risk of exercise-induced hypoglycemia actually did not experience any hypoglycemia. Detailes are shown in Figure 22.

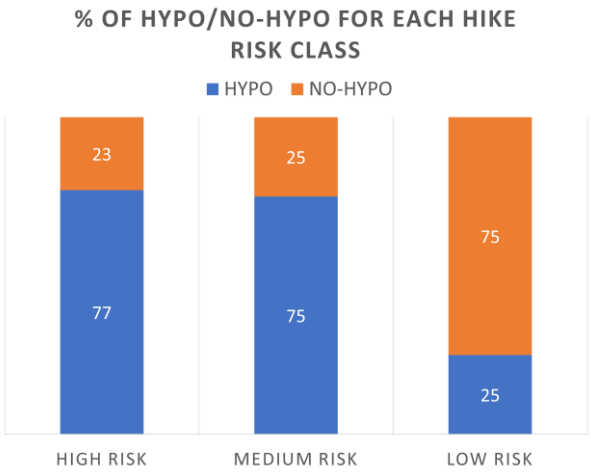

Figure 22 Percentages of HYPO and NO-HYPO cases that were classified at high, medium or low risk of exercise-induced hypoglycemia by the HYKE index.

5.2.4 Discussion

A ML framework based on CGM data to prevent the occurrence of exercise-induced hypoglycemia in children with T1D has been proposed. Results of this study provided insights on which specific configuration of CGM metrics evaluated before starting of exercise is more predictive of hypoglycemia occurrence during the period going from start of the exercise session until the following morning. The information provided by the proposed framework may suggest implementation of preventive actions that produce a "favorable" configuration for the CGM metrics; preventive actions may be taken by the subject (e.g., eating a snack) or by the clinician (e.g., adjusting medication regimens) based on the planned physical activity.

Of note, definition of standard metrics is usually confined to clinical care whereas metrics standardization related to exercise is underinvestigated both in adults and in children; thus, evaluation of the use of common metrics in different conditions (i.e., pre-exercise timestamps) and in specific time windows represents a novel aspect of the present study.

According to the proposed framework, the most informative CGM metric for the first study was M-value, and surprisingly, a lower M-value, which usually indicates better glycemic control, was associated with a higher risk of hypoglycemia after exercise. Moreover, the other three selected metrics are associated with hyperglycemia and not with hypoglycemia, as one could have expected. Indeed, subjects who did not report hypoglycemia showed a sort of "protective hyperglycemia" before exercise start. Of note, among the selected metrics only one was strongly statistically different between the two classes, while difference was less strong or not evident for the other metrics. This supports the usefulness of ML approaches in revealing hidden patterns that CGM information may show in different applications. Different metrics were instead selected in the second study, which were more related to glycemic variability. Indeed, evaluation of glycemic variability by a single CGM metric may be not sufficient, but when exploiting ML, the combination of features that account for glycemic variability into different ways may unveil significant pathways related to the specific problem.

Among the different ML algorithms used, decision tree achieved the highest performances in both cases. It has to be acknowledged pruning and leave-one -out cross-validation were adopted to prevent overfitting [143]. As already detected in applications above presented, also here SP was lower than SE in almost all the classifiers, meaning that models were prone to errors in classifying cases who did not have hypoglycemia as cases who had hypoglycemia after the start of exercise. Among previous studies concerning the prediction of hypoglycemia during exercise, the one by Reddy et al. [238] also used decision tree achieving similar or lower validation performances (78.0%, 79.3%, 66.7% and 86.5% for AUC, CA, sensitivity and specificity, respectively). They then improved those performances by using random forest with a different and more numerous feature set. Differently from the present study, however, the study by Reddy et al. [238] used features not only from blood glucose but also exercise intensity and hormone therapy, thus requiring a higher number of measures. Moreover, they used features from the beginning of the exercise session to predict hypoglycemia occurring during and not also after exercising as we did in our study. On the other hand, Jensen et al. [240] predicted nocturnal hypoglycemia with an AUC of 79.0% on testing, but their study was not focused on exercise-induced hypoglycemia. Several other studies were mainly focused on prediction of hypoglycemia by forecasting glucose levels, as reviewed by Mujahid et al.[241]. Even if we did not focus on prediction of glucose, we were able to discriminate the occurrence of hypoglycemia by using only pre-exercise CGM data.

The number of subjects included in the present study could seem low, thus representing a limitation; however, it is comparable with that of Reddy et al. [238] which is based on similar experimental conditions. A limitation of the present work could be found in the unbalanced dataset (HYPO class representing 72.34% of all samples); this, however, reflects a real-world scenario where hypoglycemia is likely to occur after exercise and because of this we chose to train the model on that dataset even though it may have resulted in lower specificity. Another limitation is that labelling did not distinguish between hypoglycemia occurred during and after exercise; however, even if these two hypoglycemic conditions originate from different physiological processes, they were considered together since both are induced by exercise. Moreover, the threshold used to define hypoglycemia may impact on

classification and this requires further investigation. Indeed, although the international consensus[148] provided 54 mg/dL and 70 mg/dL as threshold, different values (such as 60 mg/dl used in this study) are still used [242], as we did in the first study. Future studies examining at-home exercise sessions instead of a 24-h inpatient stay will be needed to confirm the results for a real-world scenario.

Regarding the HIKE composite metric evaluated in a 5-h window preceding the exercise session, it appeared to provide useful information on the risk of hypoglycemia when considering exercise performed in controlled conditions. Future work may aim to develop an automated CDSS based only on pre-exercise data, thus informing, at starting, on the existence of a "favorable configuration", with low probability of hypoglycemia during and after exercise. Moreover, further effort will be employed in the adjustment of HIKE definition and thresholds in relation to different exercises (i.e., intensity, duration, etc.), users (i.e., adults, children, adolescents) and therapeutic approaches (i.e., pump, MDI); indeed, data pertaining to adult subjects (T1DEXI data) have been provided to our research group as part of the T1D Exercise Initiative following the presentation of a project proposal (not funded); the HIKE metric would then have the potential to be tested in future clinical studies and to complement/summarize currently available recommendations.

5.3 A machine learning framework based on CGM to prevent the occurrence of hypoglycemia: the case of hemodialysis-induced hypoglycemia

Hemodialysis-induced hypoglycemia is not infrequent [243]. By using the same approach as above this section aims to setup a classification model based on CGM metrics to provide information about risk of hypoglycemia occurrence during hemodialysis, before the hemodialysis session starts.

5.3.1 Hemodialysis-induced hypoglycemia classification

The study considered a cohort of hemodialysis patients (10 of which with T2D) from the GIOTTO study (approval n. 2616, 28/09/2017) undergoing CGM (FreeStyle Libre) for two weeks [36]. Each hemodialysis session was labelled as HYPO/NO-HYPO

based on hypoglycemia occurrence (mild or severe); pre-session data was used to compute CGM metrics. A 70%-30% dataset partition for training/validation (LOSO, Leave One Subject Out cross-validation) and testing was used. After a multistep feature-selection process, the selected CGM feature set was evaluated through standard performance metrics by using different ML classification models. Dataset characteristics are described in Table XXV, dataset preparation is depicted in Figure 23 and classification procedure is the same of Figure 19, with the difference that instead of point biserial correlation, the filter type feature selection was performed by reducing the number of features by ranking those with highest content of information through gain ratio and retaining the best ranked to be given as input to the decision tree for wrapper-type feature selection.

Table XXV. Dataset characteristics.

Dataset	**Patients**	**HYPO/NO-HYPO Mild**	**HYPO/NO-HYPO Severe**
Whole	19	36/56	18/74
Training/validation	13	27/35	11/51
Testing	6	9/21	7/23

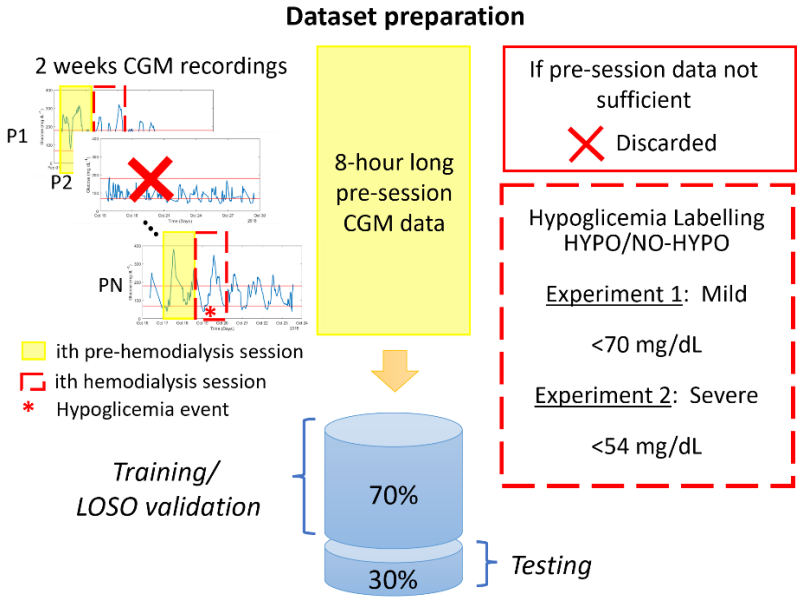

Figure 23 Dataset preparation.

5.3.2 Results

For brevity, ranges for performance metrics across the classification models and values for the best- model (i.e., Logistic Regression, in brackets) are in Table XXVI. Mild hypoglycemia prediction did not show satisfactory performances. On the contrary, severe hypoglycemia revealed promising results.

Table XXVI. Performances.

	Mild		**Severe**	
	LOSO	**Test**	**LOSO**	**Test**
AUC	0.45-0.64 (0.63)	0.50-0.71 (0.66)	0.78-0.94 (0.83)	0.57-0.77 (0.76)
CA	0.48-0.66 (0.60)	0.57-0.70 (0.67)	0.74-0.89 (0.74)	0.77-0.83 (0.80)
F1	0.49-0.66 (0.60)	0.57-0.69 (0.68)	0.77-0.89 (0.77)	0.74-0.82 (0.81)
SE	0.48-0.66 (0.60)	0.57-0.70 (0.67)	0.74-0.89 (0.74)	0.77-0.83 (0.80)
SP	0.48-0.68 (0.61)	0.43-0.60 (0.60)	0.53-0.94 (0.94)	0.43-0.74 (0.74)

5.3.3 Discussion

According to the proposed framework, CGM metrics can be exploited to detect conditions associated with a higher risk of severe hypoglycemia during hemodialysis. As a proof of concept study, testing was conducted, and among the different ML algorithms used in the present study, Logistic Regression achieved the highest performances with 76%, 80%, 81%, 80%, 74% for AUC, CA, F1, SE, SP, obtained for the test set in the case of severe hypoglycemia prediction. Of note, the number of subjects included in the present study could seem low, thus representing a limitation; however the total number of observed hemodialysis sessions was 92, including more than 5000 data points.

To conclude, the main results showed that CGM metrics measured prior the hemodialysis session have a role in predicting upcoming severe hypoglycemia.

5.4 Concluding remarks

For what concerned this chapter, focused on feature-based CGM data-driven analysis, some final consideration can be made:

- a simple logistic regression model has been proven adequate to perform a classification task to identify differences in postprandial glycemic response of subjects having T2D/prediabetes with respect to that of normal subjects;
- logistic regression also performed better in testing when used for DR detection, giving a balanced number of misclassifications accounting for less than 30% of misclassified cases; compared to studies using electronic health records instead of CGM data, we obtained similar AUCs and lower specificity counterbalanced by higher sensitivities, desirable in biomedical context and suggesting the potential of integrating both data sources;
- for exercise-induced hypoglycemia detection, we achieved similar performances compared to studies that required additional information coming from other measures such as heart rate or insulin level;
- the HIKE composite metric evaluated in a 5-h window preceding the exercise session appeared to provide useful information on the risk of hypoglycemia when considering exercise performed in controlled conditions;
- CGM metrics measured prior the hemodialysis session have a role in predicting upcoming severe hypoglycemia.

6 In-silico modeling approach to separate exogenous and endogenous plasma insulin appearance

[6] This chapter relies again on the use of mathematical models, but differently from Chapter 2 which focused on insulin clearance and glucagon suppression as determinants of diabetes pathophysiology, this methodological approach is framed in the field of pharmacological therapy, particularly focusing the attention on the open problem of quantifying the exogenous insulin that reaches the circulation (bioavailability). Investigation of such an aspect is carried on through the development of an in-silico approach based on dynamic modeling, performed using meal tolerance test data following inhaled insulin administration that were provided directly by MannKind, who, as far as we know is the only one productor of inhaled insulin approved for use by FDA in the United States.

Exogenous insulin administration is used to counteract hyperglycemia condition and is especially used for T1D [20] but also in T2D when oral antidiabetic medications fail to achieve adequate glucose control [21]. Despite the extant impairment, a variable residual endogenous insulin secretory capability exists in T2D [244] and there is increasing evidence that it also apply in cases of T1D [245], [246]. This residual endogenous component may contribute to the measured total plasma insulin in a non-negligible amount with respect to exogenous insulin; therefore, its correct quantification is important to provide a more reliable estimate of the expected exogenous insulin profile, as well as may eventually impact the decision on the adequate exogenous insulin administration considering the perspective of precision medicine [229]. Quantification of endogenous insulin secretion is also necessary in clinical trials for drug development. Indeed, when testing pharmacokinetic properties and dose ranging for safety of new exogenous insulin formulations, early phase clinical

[6] This chapter contains material that has been submitted for publication [290]

trials are performed in healthy individuals, who have a preserved endogenous secretion that may play an important role.

Model-based approaches have been extensively used to describe typical profiles of insulin concentration over time following exogenous administration of various insulin formulations [247], [248]. However, issues related to the quantification of endogenous insulin secretion were often ignored since suppression of this component can be obtained through experimental procedures (e.g., hyper-insulinemic clamp or somatostatin administration); such procedures, however, are complex to perform, present potentially harmful drawbacks for the individual and may be not fully effective in achieving adequate suppression [249]. When experimental conditions are more physiological and thus do not involve suppression (as in mixed meal tolerance test), simple "baseline correction" methods are nowadays exploited that assume a single value of plasma glucose, insulin or C-peptide reflecting the endogenous component and correct the total plasma insulin for this constant quantity [250], [251], [252]. Even though plasma C-peptide is commonly considered a more reliable marker with respect to insulin since it is co-secreted with insulin in equimolar amount, but it is not extracted to a significant extent by the liver, still the baseline correction represents a very rough quantification as it does not reflect the dynamic changes during the test. Some attempts to provide a more refined correction based on C-peptide were made that involve mixed effects regression equations [253] but such data-driven approaches act as a black box, disregarding the description of the underlying physiological processes; moreover, robustness of such approaches in individual estimation are strongly affected by statistical assumptions among which the choice of covariates [64]. For this reason, a dynamic model-based approach is desirable to overcome the limitations of the approaches previously proposed. On this basis, the aim of the present chapter is to develop a dynamic in-silico modeling approach that separates and quantifies the contributions of exogenous and endogenous insulin to measured plasma insulin in physiological conditions (i.e., meal test).

Although insulin is typically delivered through subcutaneous injection, alternate routes of administration are also used, including pulmonary delivery via inhalation, whose advantages were reported in section 1.2.3. As a secondary aim, application of the

proposed methodology to inhaled insulin administration was pursued to assess its effects on endogenous insulin secretion.

6.1 Materials and Methods

6.1.1 Experimental Protocol

A phase 1, single-center, open-label, randomized, crossover study in 21 healthy subjects (protocol number MKC-TI-141) was considered [253]. In summary, all subjects underwent two equivalent standardized meal tests (approximately 600 kcal to be completed within 20 minutes) on separate days, with one of the tests preceded by inhalation of a dose (22U or 20U) of Technosphere® Insulin through the Gen2B Inhaler. Blood samples were analyzed for glucose, insulin, and C-peptide obtained over a 6-hour period [0, 7, 15, 30, 60, 120, 240, 300, 360] min, thus providing one set of experimental data for the meal test ($G_{MT}(t_i), I_{MT}(t_i), CP_{MT}(t_i)$) and one set for the meal test with inhaled insulin ($G_{MT+I}(t_i), I_{MT+I}(t_i), CP_{MT+I}(t_i)$), with i indicating the i-th measurement time sample. Insulin and C-Peptide concentrations were determined using an electrochemiluminescence immunoassay and a competitive chemiluminescence immunoassay, respectively. The study design is summarized in Figure 24 and subjects characteristics are shown in Table XXVII.

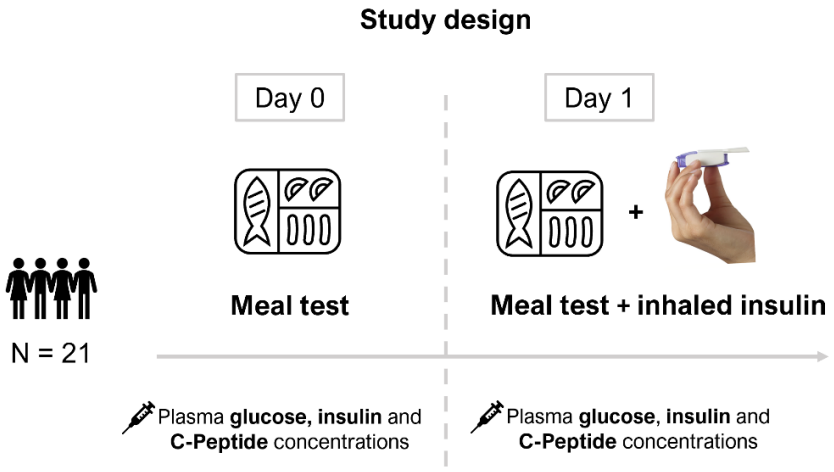

Figure 24. Graphical representation of the study design. Subjects underwent a standardized meal test on day 0 and a standardized meal test followed by Technosphere® Insulin inhalation on day 1.

Table XXVII. Subject's demographic and baseline characteristics and estimates for the C-peptide model parameters from Step 1 of the analysis (mean and standard deviation across subjects) and for the insulin model parameters from Step 2a (mean and standard deviation of individual estimates)

Subject characteristics	**Total (n=21)**
Sex	10M, 11F
Age (years)	28.1±8.5
BMI (Kg/m^2)	26.1±2.9
Ethnicity	14 C, 3 A, 2 B,1 H, 1 AI
G_b (mg/dL)	90.4±6.6
I_b (μU/mL)	10.2±11.2
Cp_b (ng/mL	1.6±0.7

Data are mean± standard deviation unless otherwise indicated. M: Male, F: Female, C: Caucasian, A: Asian, B: Black of African Heritage, H: Hispanic, AI: American Indian, Gb: Basal glucose, Ib: Basal insulin, Cpb: Basal C-peptide.

6.1.2 Modeling

The three-step dynamic model-based (DM) approach summarized in Figure 25 was used to estimate the exogenous and endogenous insulin contributions to total plasma insulin.

First step. Estimation of the C-peptide secretion rate ($CPSR\,(t)$, pmol·min^{-1}) was performed by solving a deconvolution problem with $CPSR\,(t)$ as the unknown input function and C-peptide kinetics described by the following two-compartment model, as initially introduced by Eaton et al. [254]:

$$\frac{d}{dt}A_{CP1}(t) = -(k_{21} + k_{01}) \cdot A_{CP1}(t) + k_{12} \cdot A_{CP2}(t) + CPSR\,(t),$$

$$A_{CP1}(0) = A_{CP1\,basal} = \mathrm{CP}_{basal} \cdot \mathrm{V}_{CP1} \qquad (16)$$

$$\frac{d}{dt}A_{CP2}(t) = k_{21} \cdot A_{CP1}(t) - k_{12} \cdot A_{CP2}(t),$$

$$A_{CP2}(0) = \frac{k_{21}}{k_{12}} \cdot A_{CP1\,basal} \qquad (17)$$

where $A_{CP1}(t)$ and $A_{CP2}(t)$ are the amounts of C-peptide (pmol) in the accessible and in the remote (from plasma) compartment, $A_{CP1\,basal}$ is the basal amount of C-peptide (pmol) in the accessible compartment, CP_{basal} is the basal plasma C-peptide concentration (pmol·L^{-1}) measured immediately before inhalation and meal intake, V_{CP1} is the C-peptide distribution volume (L) in the accessible compartment, and k_{12}, k_{21}, k_{01} are the transfer rate constants (min^{-1}). The model predicted C-peptide

concentration is $\frac{\mathrm{CP(t)=A}_{CP1}(t)}{\mathrm{V}_{CP1}}$. The parameters representing the three model rate constants and distribution volume were determined using each subject's anthropometric characteristics (age, sex and body surface area) by applying the formulas from Van Cauter et al.[57] .

Given that C-peptide and insulin are secreted equimolarly, and that C-peptide does not undergo hepatic extraction, insulin secretion rate can be assumed equal to $CPSR\,(t)$. This approach was applied to the meal test data without (1a in Figure 25) and with (1b in Figure 25) prior inhalation of exogenous insulin to obtain $CPSR_{\,MT}(t)$ and $CPSR_{\,MT+I}(t)$, respectively.

Second step. The following one-compartment model of insulin kinetics was used to obtain subject-specific estimates of insulin distribution volume V_I (L) and elimination rate constant n (min^{-1}) using plasma insulin concentration-time measurements [64] :

$$\frac{d}{dt}A_{Iendo}(t) = -n \cdot A_{Iendo}(t) + CPSR\,(t),$$

$$A_{Iendo}(0) = Iendo_{basal} \cdot \mathrm{V}_I \quad (18)$$

where $A_{Iendo}(t)$ is the amount of plasma insulin (pmol), $CPSR\,(t)$ is the insulin secretion rate (pmol·min^{-1}), and $Iendo_{basal}$ is the basal plasma insulin concentration (pmol·L^{-1}) measured immediately before meal intake. The model predicted endogenous insulin concentration is $Iendo^{DM}(t) = A_{Iendo}(t)\frac{}{\cdot \mathrm{V}_I}$. The model was first applied to the meal test data without prior inhalation of exogenous insulin (2a in Figure 25). The resulting subject-specific model was then used on meal test data with inhaled insulin to predict the plasma insulin component attributable to endogenous insulin $Iendo^{DM}_{MT+I}(t)$ (pmol·L^{-1}), as depicted in step 2b of Figure 24.

Third step. The contribution of exogenous insulin $Iexo^{DM}_{MT+I}(t)$ to plasma insulin was obtained by subtracting the predicted endogenous component $Iendo^{DM}_{MT+I}(t)$ from the total insulin concentration $I_{MT+I}(t_i)$ measured during the meal test with inhaled insulin:

$$Iexo^{DM}_{MT+I}(t) = I_{MT+I}(t_i) - Iendo^{DM}_{MT+I}(t) \quad (19)$$

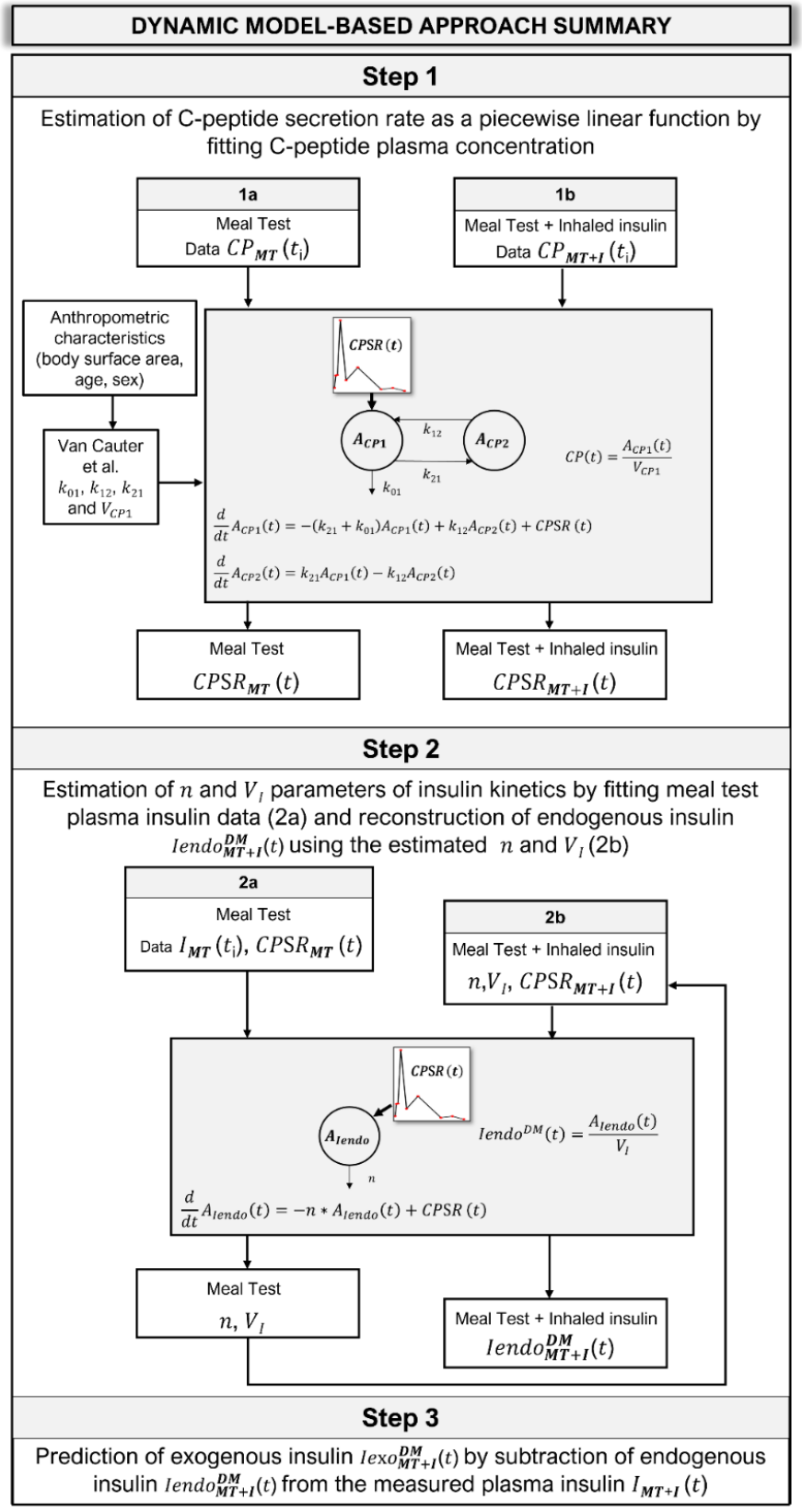

Figure 25. Flow chart of the three-step modeling approach.

6.1.3 Model implementation and parameter estimation

Model simulation and parameter estimation were performed using the ADAPT (version 5) software for pharmacokinetic/pharmacodynamic system analysis [255]. The deconvolution problem to estimate $CPSR\,(t)$ was solved by assuming $CPSR\,(t)$ as a piecewise linear function, as depicted in Figure 25, whose parameters (slopes of each line segment) were determined through maximum likelihood estimation using the measured plasma C-peptide measurements. Break points of the piecewise linear function corresponded to the measurement times [256]. Estimation of individual insulin kinetic parameters (V_I and n in Figure 25) was obtained using maximum likelihood estimation in ADAPT.

6.1.4 Comparison with other C-peptide-based methods

The dynamic model-based method for estimating endogenous plasma insulin proposed herein was compared to the "C-peptide correction" methods previously proposed by Owens [252] and by Marino et al. [253] These latter two methods attempt to correct the measured insulin concentration by removing the component (assumed constant) attributable to endogenous secretion, thus resulting in the isolated contribution of exogenous insulin.

Application of the method proposed by Owens [252] - also known as "baseline correction" (BC) - to the meal test with inhaled insulin data ($I_{MT+I}(t_i), CP_{MT+I}(t_i)$) results in the following predicted values of the endogenous ($Iendo^{BC}_{MT+I}(t_i)$) and exogenous ($Iexo^{BC}_{MT+I}(t_i)$) components of plasma insulin:

$$Iendo^{BC}_{MT+I}(t_i) = ICPR^{BC} \cdot CP_{MT+I}(t_i) \tag{20}$$

$$Iexo^{BC}_{MT+I}(t_i) = I_{MT+I}(t_i) - Iendo^{BC}_{MT+I}(t_i). \tag{21}$$

In equation (20), $ICPR^{BC}$ represents the Insulin-to-C-Peptide fractional temporal Ratio and is a constant value throughout the test, computed as follows:

$$ICPR^{BC} = \frac{I_{MT+I}(0)}{CP_{MT+I}(0)} \tag{22}$$

where $I_{MT+I}(0)$ and $CP_{MT+I}(0)$ are the plasma insulin and C-peptide concentrations measured at baseline (i.e., before starting the test), respectively.

The method proposed by Marino et al. [253], hypothesized the existence of a linear relationship between insulin and C-peptide time courses and exploited a linear

mixed effects (LME) modeling approach to predict the endogenous component, $Iendo_{MT+I}^{LME}(t_i)$, and the related exogenous component, $Iexo_{MT+I}^{LME}(t_i)$, from meal test with inhaled insulin data according to the following equations:

$$Iendo_{MT+I}^{LME}(t_i) = ICPR^{LME} \cdot CP_{MT+I}(t_i) + Intercept \quad (23)$$

$$Iexo_{MT+I}^{LME}(t_i) = I_{MT+I}(t_i) - Iendo_{MT+I}^{LME}(t). \quad (24)$$

In equation (8), $ICPR^{LME}$ is a constant value throughout the test computed as follows:

$$ICPR^{LME} = Slope + v_{subject} \quad (25)$$

where $Intercept$ and $Slope$ in equations (23) and (25) represent the mean values of the intercept and slope in the linear regression analysis across all subjects, thus accounting for the fixed effects; $v_{subject}$ is the subject specific deviation from the mean slope and represents the random effects. To estimate parameters of the linear mixed effect model ($Slope, v_{subject}$ and $Intercept$), meal test data [$I_{MT}(t_i)$ and $CP_{MT}(t_i)$] were used (analogous to Step 2a in Figure 25).

Each of these C-peptide correction methods was implemented in MATLAB 2019b (The Mathworks); the fitlme built in function was used to perform the required linear mixed effect modeling analysis. Our dynamic model-based estimation method and the two C-peptide correction method results were evaluated by comparing their respective insulin-to-C-peptide fractional temporal ratio values, which for our approach is given by the following equation:

$$ICPR^{DM}(t_i) = \frac{Iendo_{MT+I}^{DM}(t_i)}{CP_{MT+I}(t_i)} \quad (26)$$

6.1.5 Assessment of the percentage of exogenous insulin dose reaching the plasma

The percentage of initial exogenous insulin dose that reached the plasma (i.e., absolute bioavailability, $\%exo$) was obtained as follows:

$$\%exo = \frac{AUC_{Iexo}}{AUC_{IV}} \quad (27)$$

being AUC_{Iexo} (pmol·min/L) the area under the exogenous insulin concentration profile and AUC_{IV} (pmol·min/L) the area under the curve that would be obtained if the same dose was administered intravenously.

Assuming a single-compartment description, AUC_{IV} was computed as follows:

$$AUC_{IV} = \frac{V_I \cdot n}{Dose} \quad (28)$$

being V_I the insulin distribution volume and n the elimination rate constant estimated in the second step of Fig. 2; $Dose$ is the dose of inhaled insulin administered to each subject (20 or 22 U).

6.1.6 Statistical analyses

Statistical analysis was performed using the MATLAB 2019b (The Mathworks). The Lilliefors test was used to evaluate if variables come from a normal distribution. Differences in measured glucose, insulin and C-peptide concentrations between meal test and meal test with inhaled insulin were assessed using the nonparametric Wilcoxon signed rank test. The model performance was evaluated in terms of goodness of fit (coefficient of determination, R^2). Results are presented as mean ± standard deviation unless otherwise designated. Statistical comparisons of the endogenous insulin predicted for both meal test without ($Iendo_{MT}^{DM}$) and with ($Iendo_{MT+I}^{DM}$) prior inhalation of exogenous insulin were evaluated at each sampling time and in terms of supra-basal area under the curve using the nonparametric Wilcoxon signed rank test.

6.2 Results

The plasma glucose, C-peptide and insulin concentrations measured during the meal test with and without prior inhalation of exogenous insulin are summarized in Figure 26. The bottom panel of Figure 26 shows the higher insulin concentration observed in the first hour of the meal test with inhaled insulin. From the central panel, it can be noticed that the observed C-peptide (a marker of endogenous insulin secretion) is lower in the meal test with inhaled insulin during the 30-to-120-minute interval following the meal test.

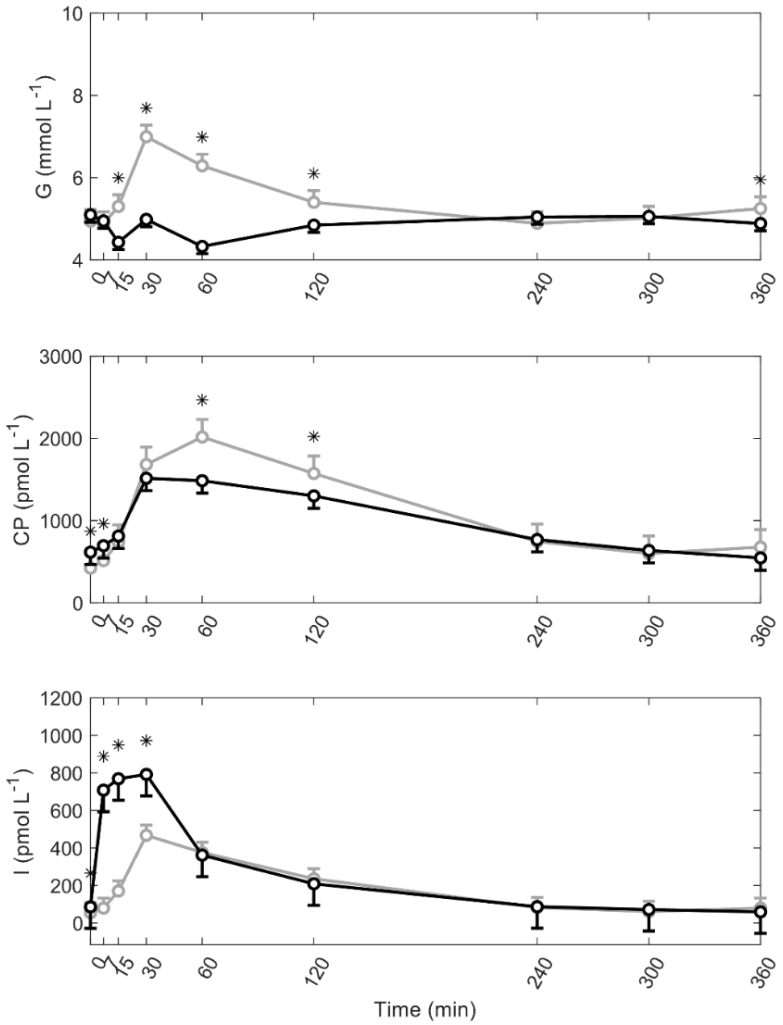

Figure 26. Average plasma glucose (G), C-peptide (CP) and insulin (I) concentrations measured during meal test without (grey line) and with prior inhalation of exogenous insulin (black line). * p<0.05. Vertical bars represent SE.

Estimates for the C-peptide model parameters from Step 1 of the analysis (V_{CP1}, k_{12}, k_{21}, k_{01}) and for the insulin model parameters from Step 2a (V_I and n) are given in Table XXVI. Plots of the individual subject's model predicted plasma insulin concentrations from Step 2a are shown in Figure 27, and result in an overall goodness of fit $R^2 = 0.919$. Individual subject's predicted endogenous insulin $Iendo_{MT}$ versus measured total plasma insulin concentrations $I_{MT}(t)$ are shown in Figure 28.

Table XXVIII. Estimates for the C-peptide model parameters from Step 1 of the analysis (mean and standard deviation across subjects) and for the insulin model parameters from Step 2a (mean and standard deviation of individual estimates)

Calculated parameters_Step 1	**Mean±Standard Deviation**
$V_{CP1}(L)$	4.223±0.350
k_{12} (min^{-1})	0.050±0.001
k_{21} (min^{-1})	0.052±0.001
k_{01} (min^{-1})	0.059±0.001
Estimated parameters_Step 2a	Mean±Standard Deviation
V_I (L)	15.680±5.740
n (min^{-1})	0.120±0.050

Data are mean± standard deviation unless otherwise indicated.

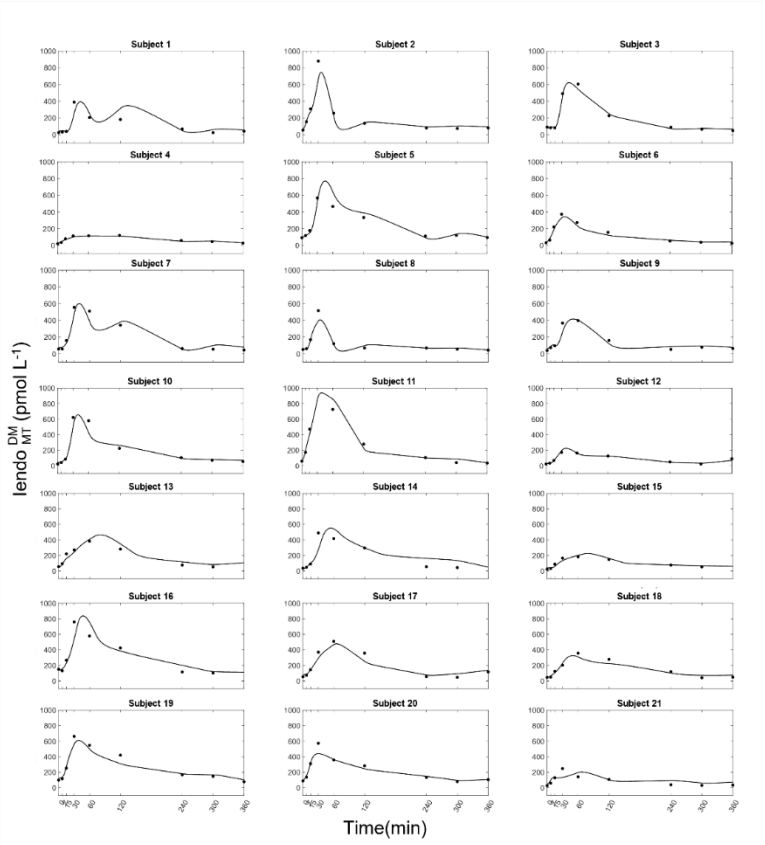

Figure 27. Individual fits for each of the 21 subjects from meal test data; continuous black lines show the model fit; black dots represent meal test measured plasma insulin concentration ($pmol \cdot L^{-1}$).

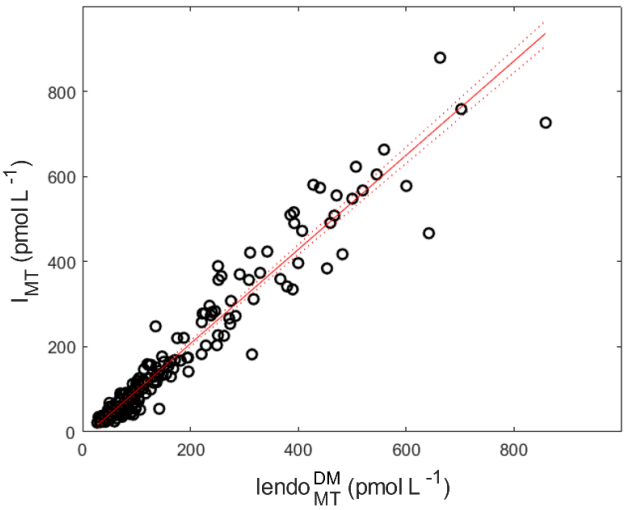

Figure 28. Goodness-of-fit plot showing the individual subject predicted endogenous insulin ($Iendo_{MT}^{DM}$) vs. measured plasma insulin concentrations of the meal test (I_{MT}). The line of identity is represented as a solid black line. Dotted lines represent 95% confidence bounds. $R^2 = 0.919$.

The endogenous insulin profiles, $Iendo_{MT}^{DM}$ and $Iendo_{MT+I}^{DM}$, predicted based on each subject's model parameters were averaged and shown in Figure 29 (panel A). A statistically significant difference in endogenous insulin with and without inhaled insulin was found at the 60 min sample time ($p<0.01$) and a divergence (accounting for a statistically significant difference according to Wilcoxon signed rank test) in the time course of endogenous insulin between the two tests was present between 30- and 120-min following insulin delivery. Moreover, the supra-basal area under the curve of $Iendo_{MT+I}$ was significantly lower than that of $Iendo_{MT}$ (sAUC_$Iendo_{MT+I}^{DM}$ = 2.1±1.7·10^4 pmol·min/L, sAUC_$Iendo_{MT}^{DM}$ = 4.2±1.8·10^4 pmol·min/L, $p<0.001$). For the meal test with inhaled insulin, the predicted exogenous insulin contribution to the total plasma insulin is shown in Figure 29 (panel B) and accounts for on average 34±18% of total plasma insulin. Average of Insulin-to-C-Peptide fractional temporal Ratio (ICPR) across subjects obtained for the baseline correction and linear mixed effect methods ($ICPR^{BC}$ and $ICPR^{LME}$, respectively) are displayed in Figure 30, along with the estimated $ICPR^{DM}$ obtained from the dynamic model-based method. The latter shows a rapid increase followed by a rapid decrease during the first hour of test, peaking at 30 min (0.22±0.02), and falling between $ICPR^{BC}$ (0.16±0.05) and $ICPR^{LME}$

(0.23±0.01). The percentage of initial exogenous insulin dose that reached the plasma, $\%exo$, resulted to be 42±21% ranging from a minimum of 11% to a maximum of 77%.

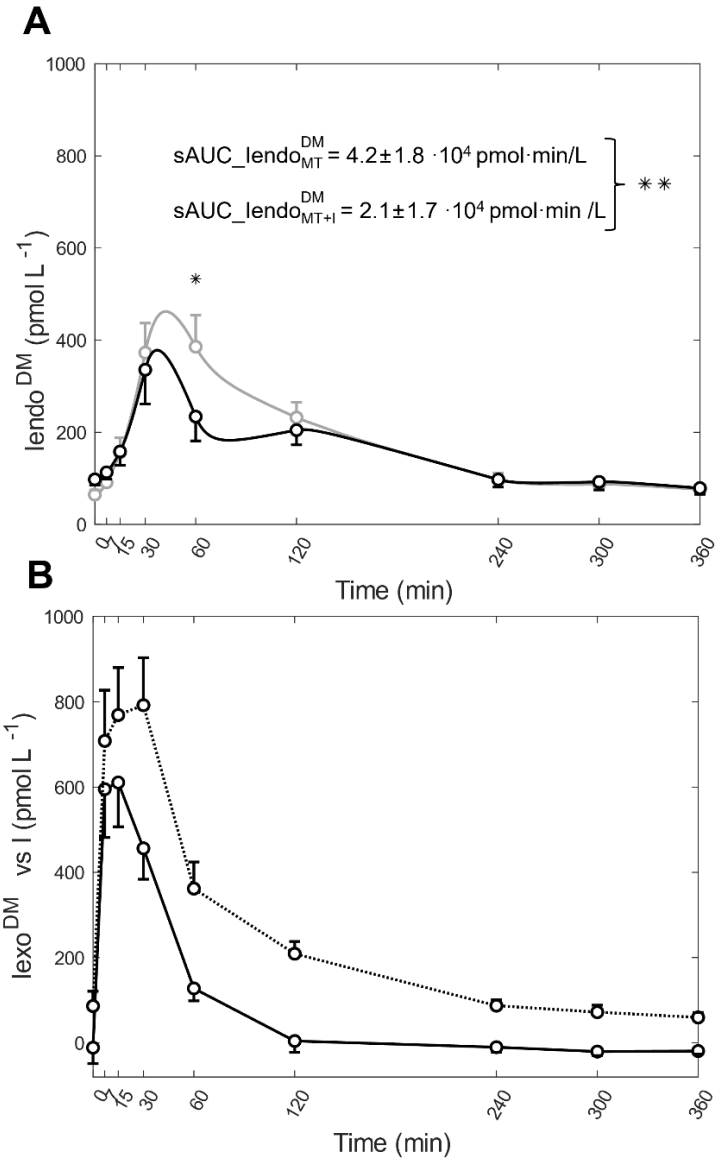

Figure 29.. (A) Average predicted endogenous insulin component for meal test ($Iendo^{DM}_{MT}$, grey line) and meal test with inhaled insulin ($Iendo^{DM}_{MT+I}$, black line); * p<0.01, ** p<0.001; (B) average total measured plasma insulin concentration ($Iexo^{DM}_{MT+I}$, dotted line) and average predicted exogenous component (I_{MT+I}, solid line). Vertical bars represent SE.

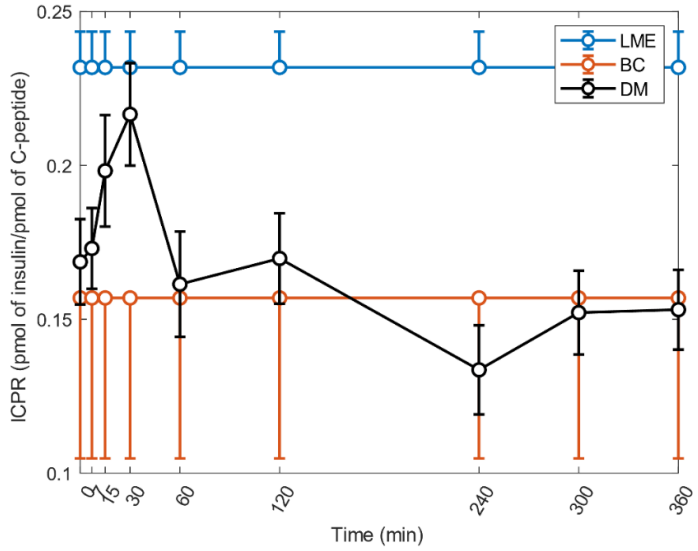

Figure 30. Insulin-to-C-Peptide fractional temporal Ratio (ICPR) between endogenous insulin estimates and measured C-peptide concentrations during the meal test with inhaled insulin obtained for baseline correction (BC, orange line) and linear mixed effect (LME, light blue line) methods and for the herein proposed dynamic model-based method (DM, black line). Vertical bars represent SE.

6.3 Discussion

6.3.1 Novelty, relevance, and clinical applications

A general model-based methodology has been developed that allows for quantification of the separate contributions of exogenous and endogenous insulin to total peripheral plasma insulin concentration following insulin administration. As first element of novelty, the methodology does not require complex experimental procedures to suppress the endogenous component as those traditionally used and can be applied to tests performed in more physiological conditions (i.e., meal tolerance test). Secondly, the procedure allows an easier quantification of percentage of exogenous insulin dose reaching the plasma, a concept usually indicated as absolute bioavailability and regarded as a pharmacokinetic feature of the drug. Determination of this feature usually requires a complex experimental setup, including intravenous drug administration and the suppression previously mentioned; however, the proposed approach not only overcomes the limitations of the traditional experimental setup but also facilitates determination of intra- and inter-individual variability in absolute bioavailability, thus broadening the perspective with respect to the potential of

bioavailability in the direction of "individual bioavailability". Eventually, the approach can be implemented in an easy-to-use integrated software tool for quantifying the exogenous component of systemic plasma insulin and the individual bioavailability, in an effort to assess patient-specific dose-response following insulin administration during a meal test.

Application of the proposed method to a clinical trial based on inhaled insulin administration in healthy subjects provided insight on the difference in endogenous contribution to plasma insulin following meal tests with and without inhaled insulin (see Figure 29 panel A). Indeed, the predicted time course of endogenous insulin showed a 18.2% reduction in its peak value and the overall endogenous insulin exposure, as assessed by the supra-basal area under the endogenous insulin curve, was reduced by a factor of two following inhaled insulin administration. This general action of exogenous insulin to reduce endogenous insulin secretion, which can be attributed to a negative-insulin-feedback loop mechanism, has been reported previously for other exogenous insulin formulations [257], [258], [259] and may contribute to preserving beta-cell function in patients with type 2 diabetes [260] and also type 1 diabetes [261]. The ability to separately quantify exogenous and endogenous contributions with their own dynamic behaviors while capturing the effect that one has on the other may open new scenarios in the field of precision medicine by designing tailored therapeutic regimens on the basis of the individual's residual capability to manage changes in blood glucose [262], [263], [264], [265]. Indeed, evidence showed the existence of a log-linear relationship between glycemic variability, a measure of glycemic control, and endogenous insulin secretion in insulin-treated and non-insulin-treated patients with type 2 diabetes [266]. However, studies were conducted exploiting fasting C-peptide as a marker of endogenous secretion and consideration of the time course of endogenous insulin, as done in the present study, may help to investigate how target trends in glucose response can be obtained and to modulate exogenous insulin doses accordingly. As for the case of inhaled insulin, there is evidence that Technosphere Insulin is beneficial to reduce daytime glycemic variability [267], thus the method proposed herein could be useful to elucidate the role of endogenous insulin in mediating this relationship.

Quantification of individual bioavailability obtained by the present approach may be also framed in the domain of personalized therapy; indeed, attempts have been recently made to design tools based on personalized bio-impedance modelling for real-time monitoring of the amount of bioavailable insulin, with the aim to achieve a more accurate insulin administration accounting for both the intra- and inter-individual variability in insulin bioavailability [268], [269]. Range of values of bioavailability obtained by the approach proposed in the present study furtherly supported the fact that a high variability exists among individuals and tools for real-time monitoring of the amount of bioavailable insulin may benefit from such an approach to improve their reliability (as for example, in calibration procedures).

6.3.2 Comments on the applied methodology

The proposed method for decomposing total plasma insulin into its endogenous and exogenous components involves the use of compartment models to describe the kinetics of C-peptide (Step 1) and the kinetics of insulin (Step 2). In contrast to other methods that attempt to determine insulin secretion using measured plasma insulin alone [270], our approach also requires measurement of associated C-peptide concentrations whose assessment in clinical practice is increasingly encouraged [271]. For C-peptide, the well-established two compartment model used by Eaton et al. [254] was adopted, with specific parameters determined based on each subject's body surface area, age and sex following Van Cauter's method[57]. Although the method is based on subject's specific estimates, the calculated C-peptide kinetic model parameters obtained in Step 1a are based on mean population information derived from anthropometric characteristics (e.g., body surface area, age, sex), reflecting the inter subject variability that can be explained based on these patient's specific covariates. It is correct that other factors contributing to inter subject differences, not explained by a subject's body surface area, age and sex, are not taken into account. On the other hand, determining unique subject specific C-peptide kinetic parameters would require complex experiments designed to estimate each subject's C-peptide kinetics. Therefore, C-peptide kinetic model parameters were obtained using the Van Cauter's method [57], extensively exploited for similar purposes. To represent the C-peptide secretion rate profile, a piece-wise linear function was assumed with the break points

corresponding to the measurement times, which allows easy estimation of the unknown slopes of each line segment using the measured C-peptide concentration data. The choice of piece-linear approximation to the C-peptide release rate has advantages over fully parametric methods that use a single overall function (e.g., Gaussian [272]) to represent C-peptide release rate. Moreover, despite we recognize that nonparametric deconvolution approaches could have some advantages (i.e., finer input discretization grids), we noted that the simplified approximation to the C-peptide release rate used in this work can adequately describe the time course of observed insulin data when used as the input to the insulin kinetic model, as shown in Figure 27 and Figure 28. A one-compartment model was then used to describe plasma insulin kinetics, parameterized in terms of distribution volume and rate constant of elimination, with the C-peptide secretion rate function determined in Step 1 serving as the input. The use of single compartment to represent insulin kinetics was deemed appropriate during a meal test, where insulin levels remain low enough to avoid saturable processes and hence maintaining linear dynamics [273]. Furthermore, since we were not interested in segregating hepatic and extrahepatic contributions to insulin elimination, hepatic extraction was not included in the model, and, therefore, the elimination rate constant n represents an overall measure of insulin clearance. The resulting estimates of the elimination rate constant (Step 2a) are in good agreement with those reported in other studies involving healthy subjects [64], [274], [275], further supporting the choice of C-peptide function approximation and insulin kinetic model. The individual subjects' estimates of both insulin distribution volume and elimination rate constant obtained from the meal test alone were assumed to be the same in each subject during the meal test with inhaled insulin. These estimates were then used in such meal test with inhaled insulin to determine the endogenous contribution to plasma insulin (Step 2b), and subsequently the exogenous component (Step 3).

As for the bioavailability estimation, to overcome the need to perform a second experiment involving intravenous insulin administration, we exploited each subject insulin pharmacokinetic estimated parameters in order to compute a surrogate area under the curve that would have been obtained if the same dose would have been injected intravenously. This assumption has been deemed appropriate since the insulin

kinetic parameters are estimated independently from the route of administration, being the description of the absorption bypassed.

6.3.3 Comparisons to other C-peptide based methods

The dynamic model-based methodology presented herein addresses some of the limitations of previously reported approaches for separating exogenous and endogenous contributions to plasma insulin following insulin administration. In the "baseline correction" or Owens method [252], the endogenous contribution to plasma insulin is calculated to be a constant fraction of total insulin based on a single baseline insulin sample, and thus ignores the systems dynamics included in Steps 1 and 2 in our proposed modeling framework (Fig. 2). Indeed, a recent study that evaluated C-peptide baseline correction method concluded that in the presence of unsuppressed endogenous insulin caution should be taken when using such methods for predicting exogenous insulin [276]. In contrast, the method proposed by Marino et al. [253] exploiting linear mixed effects modeling partially overcomes the limitations of the baseline correction method by considering measurement time points over the whole test. This method, however, again ignores the insulin dynamics included in Step 2 of our approach. The resulting differences in the three methods are illustrated in Figure 30, which shows the insulin-to-C-peptide fractional temporal ratio between the endogenous insulin component and the measured C-peptide. Results from the baseline correction and linear mixed effect methods indicate that they maintain a constant relationship throughout the test. The prediction obtained with the dynamic model-based method, in contrast, results in a time varying insulin-to-C-peptide fractional temporal ratio, which better reflects insulin dynamics; in this case, a fast change (rapid increase followed by rapid decrease) is observed in the first hour of the test.

It has to be acknowledged that comparison has been limited to methods relying on C-peptide, although other methods based on "glucose correction" have been proposed [250]. The reason for this choice relies on the fact that methods based on glucose were developed in applications devoted to glucose control, thus in conditions in which additional simplifying assumptions are needed.

6.3.4 Limitations and related comments

The study design required with the proposed method has some limitations. Primarily, the application of the proposed approach requires administration of two different meal tests, one with and one without inhaled insulin, which would need to be conducted so as to minimize any carryover effects, i.e., the influence of the first test on the second one; however, other methods based on meal test have the same requirements [253]. Moreover, the method has been evaluated in a relatively limited number of healthy subjects, and evaluation in diabetic patients is needed. Furthermore, another issue has to be acknowledged: indeed, it has to be noted that a direct evaluation of the quantities predicted by the model-based approach under experimental conditions similar to physiological ones (i.e., meal test), however, cannot be achieved by using Technosphere® Insulin. This is because, being its formulation based on regular human insulin, it is indistinguishable from that secreted endogenously. In future studies, this direct assessment could be evaluated across other insulin analogs that are distinguishable from regular human insulin by using assays based on specific monoclonal antibodies that have low cross-reactivity to insulin analogs but high reactivity to endogenously produced insulin. Nonetheless, as a proof of reliability of the proposed method, it can be noted that the predicted exogenous insulin time course shown in Figure 29 (panel B) is qualitatively comparable, in terms of onset and duration, to that previously reported for a dose of 24U of inhaled insulin [27]. Similarly, the time course is characterized by a fast onset (peak around 15 min) and a relatively short duration (baseline reached after 120 min, Figure 29 panel B); however, strict comparison is not possible since in this latter study a less refined method was used to quantify exogenous insulin. Lastly, the estimates here obtained for absolute bioavailability are not directly comparable to those previously reported in the literature for the case of Technosphere insulin (which provided lower values, usually not exceeding 15% [248], [277], [278]) for multiple reasons; indeed, previous estimates were obtained exploiting the baseline correction method, which could have produced underestimation of the exogenous insulin profile; moreover, in previous studies insulin was administered using different inhalation devices, which may be less efficient than the one here used [27].

6.4 Conclusions

A dynamic model-based approach has been developed to separate exogenous and endogenous insulin contributions to total plasma insulin during a meal. Application to the case of inhaled insulin showed an effect of exogenous insulin on the endogenous secretion, which can be potentially beneficial to preserve the latter. This methodology could be useful to assess the exogenous insulin profile in studies based on subjects with residual endogenous insulin and, when introduced in the framework of personalized therapy, to provide patient-specific dose-response following insulin administration. Finally, we noted that although exogenous insulin in this study was provided through inhalation, the proposed approach can be applied to other routes of administration.

7 Conclusions and future developments

The vast concept of digital health technology has started to permeate the field of diabetes prevention, management and treatment as various solutions have started popping up for their potential to revolutionize diabetes care. The proposal to offer solutions based on the transformation of information from measurable metabolic data seems promising in the perspective of developing CDSS. In fact, leveraging transformed information through techniques such as physiological system modeling or metric extraction, rather than raw data, offers certain advantages. It allows for the characterization and representation of a specific process from a metabolic point of view, and it does so conveniently in terms of computational expenses for real-time applications and interpretability. This is what has been attempted in this thesis work, developing model-based and feature-based data-driven approaches, sometimes resorting to machine learning techniques. Indeed, such kind of approach is quite innovative also considering that the related literature works published so far were more focused on blood glucose forecasting for the full-automation of insulin delivery and less on standalone CDSS. In this work we explored different applications moving from model-based towards the feature-based data-driven approaches, answering open research questions encompassing preventive screening, innovative diagnosis, hypoglycemia risk prediction and quantitative physiology for targeted-therapy, for individuals at different metabolic statuses. Summary of the specific addressed tasks, together with possible limitations and future developments are provided in the following sections. Findings are also discussed in relation to a recent review by Jacobs et al. [279], which provides consensus guidelines for machine learning practitioners in the field of diabetes.

7.1 Summary of main findings

In Chapter 2 physiological system modeling was exploited to assess: i) insulin clearance in its hepatic and extrahepatic components, firstly with the implementation of a previously proposed method enriched by the use of regularization techniques and

then by developing a novel approach; ii) α-cell sensitivity to glucose and insulin. The approaches were applied to different sets of data for each case and results showed that:

- a simplified version of the IM-IVGTT (1 hour) with the adoption of the assumption of a linear hepatic clearance dynamics proof reliable to assess hepatic and extrahepatic insulin clearance in women with a history of GD;
- the higher insulin clearance observed in DIRKO animal model compared to its WT counterpart during the IVGTT first phase may be due to its extrahepatic component, suggesting that in conditions of lack of incretin effect a compensatory response may take place at peripheral level;
- adding to the Polidori et al. other independent equations linking hepatic and extrahepatic components to the total insulin clearance profs suitable for application to IVGTT test, which for construction is a less appropriate test to separate the two insulin clearance components than the IM-IVGTT;
- for the glucagon model, the main improvement of the new formulation was to include the contribution of glucose to that of insulin when considering the mechanisms related to alpha-cell glucose sensing, which resulted in the presence of a dual regulation in the healthy group and impaired in the T2D group.

It is worth noticing that in this piece of the thesis we decided to focus on processes such as insulin clearance and α-cell sensitivity instead of considering the more studied processes of β-cell function and insulin sensitivity, and this was done precisely with the idea of guaranteeing an overall characterization of the pathology that takes into account its heterogeneous etiology. Indeed, there is evidence that response to treatment and progression of complications may be optimized by knowing all the different "component pathways" that may contribute to the disease, as for what theorized by McCarthy [280]. Thus, we used physiological system modeling to deepen into such specific processes offering tools for estimating parameters that allow fine phenotyping of the data. In general, besides having potential as tools applicable in clinical contexts,

constituting decision support tools themselves, physiological system models can help in the field of investigation of new scientific evidence that can constitute an expansion of the knowledge base of CDSS or generate parameters that can be used as features for machine learning applications. This is in line with one of the suggested best practices in the review consensus guidelines [279], there considered in the specific context of exercise, but that we can extend to other contexts.

In Chapter 3, the latter concept was investigated through the use of model-based parameters to feed machine learning algorithms in order to assess a ML-based framework capable to help preventing T2D development in women who had GD. In particular, the main result was the identification of features, namely disposition index, basal secretion rate of insulin and mean area under the C-peptide concentration curve among the most relevant features for the progression to T2D.

In Chapter 4 an analysis was performed before setting out approaches based on CGM data in order to determine which was the most appropriate tool to be used in subsequent analyses. Among the 12 tools that have been tested, results indicated that iglu software package was the right package showing a good trade-off between number of computable metrics and reliability of computations.

In Chapter 5 CGM computed metrics were given as input to various ML algorithms to build feature-based machine learning approaches in different fields: i) innovative diagnosis, ii) early identification of diabetes complications, iii) prediction of impending hypoglycemia in the case of exercise-induced hypoglycemia in individuals having type 1 diabetes, iv) and in the case of hemodialysis-induced hypoglycemia. Results showed that:

- a simple logistic regression model has been proven adequate to perform a classification task both to identify differences in postprandial glycemic response of subjects having T2D/prediabetes and to detect DR;
- good performance were obtained for T2D/prediabetes detection while for DR detection additional information may be required in addition to CGM data for reaching better performances;
- for exercise-induced hypoglycemia detection, we achieved similar performances compared to studies that required additional information coming from other measures such as heart rate or insulin level;
- decision tree resulted adequate for exercise-induced hypoglycemia detection in both controlled and free-living exercising conditions;
- CGM metrics measured prior the exercise session have a role in predicting upcoming exercise-induced hypoglycemia;
- The proposed HIKE composite metric evaluated in a 5-h window appeared informative on the risk of hypoglycemia when considering exercise performed in controlled conditions;
- CGM metrics measured prior the hemodialysis session have a role in predicting upcoming severe hypoglycemia;

A main advantage of relying only on CGM is in the opportunity to ensure wide screening, thanks to the growing diffusion of CGM use among patients with diabetes. For DR detection this would allow a pre-screening in people at risk, that would need to be confirmed going to fundus checks, which are very often postponed. For the early diagnosis of impaired glucose tolerance, feasibility of CGM based tolerance test would have many advantages if added to the standard diagnosing tests. Moreover, what the approach stands out for is that even if we did not implemented techniques for glucose forecasting, we were able to discriminate the occurrence of hypoglycemia by using only pre-event CGM data.

In relation to consensus-based best practices and pitfalls to avoid when developing ML-based applications in the field of diabetes, we can conclude that:

- the CGM datasets used were all open-source data, had good heterogeneity and glucose variance, ensuring a good representation of the population under study (i.e., T1D subjects under MDI or pump therapy were well balanced) and avoiding biased results;
- when partitioning the datasets, we ensured that samples coming from the same subject were not mixed among training, validation, test sets;
- when handling missing values, linear interpolation, which is considered a good choice since CGM data change rapidly, was adopted only in presence of gaps lasting less than 45 minutes;
- in line with the fact that simple models generalize better that complex models if trained on not so large datasets, as typically are CGM dataset, we avoided using deep learning-based algorithms and relied on simple ML well known models;
- the choice of windows from which computing CGM metrics was done in relation to the application: diagnosis based on postprandial glucose comprised the period until 3 hours after meal, in line with standard diagnosis test (OGTT); for identification of complications a long window was selected to take into account differences in glycemic control evaluated during the whole observation period (26 weeks); for induced hypoglycemia the window was shorter (i.e., 3-8 hours);
- CGM metrics extracted were not only those proposed in the review and standardized in the consensus but also those provided by the selected package, which were previously verified in chapter 4; our aim was to investigate the information in many forms in a way to take into account possible hidden patterns that may be present in relation to each evaluated research question.
- we did not include food and drug intake as features, nor heart rate and accelerometry signal based features, to make the approach suitable for a broader population;
- for long prediction horizons it is suggested to predict binary events, as we did in the case of induced hypoglycemia;

In general, the framework proposed in the guidelines supports the methodology we have developed.

Finally, in Chapter 6 we proposed an easier and less invasive quantification– with respect to the traditional experimental setup– of absolute bioavailability i.e., the percentage of exogenous insulin dose reaching the plasma. In particular, the methodology allow assessing individual bioavailability thus opening new scenarios in the field of precision medicine that would boost the design of tailored therapeutic regimens on the basis of the individual's characteristics. Moreover, when applied to inhaled insulin results showed that the overall endogenous insulin exposure, as assessed by the supra-basal area under the endogenous insulin curve, was reduced by a factor of two following inhaled insulin administration, thus proving the methodology useful to assess the effect of exogenously administered insulin on endogenous secretion.

7.2 Limitations and future developments

Concerning the number of subjects considered in each application, it seemed not large enough to justify the use of ML-based methods; however, if we look at the common datasets found in the field of metabolism, we can find that dataset dimensions used in this thesis are comparable with that of other works. Indeed, feature and metric extraction allow a dataset to be well characterized and representative, thus overcoming the initial problem. Data augmentation techniques were not employed since we preferred relying on data reflecting real-world scenarios and avoid introduction of bias. These consideration were all confirmed by the consensus guidelines we are making reference. According to the common pitfalls in the field of DSS in diabetes, one of the limitations of the thesis concerns the fact that the applications relating to the prediction of hypoglycemia, which in the case of exercise led to the formulation of a risk metric, however still represent an embryonic state of DSS, as validation requires comparison with the current recommendations proposed in the clinical guidelines. This may be focus for future work. Moreover, regarding the CGM-based approaches, future studies may include: i) examining different windows for CGM metrics extraction and different CGM metrics with respect to those considered at present; ii) examining smoothing

techniques to remove outlier samples from the CGM trace to reduce noise that is not physiologically possible (guidelines report that CGM does not typically change faster than ± 4 mg/dL/minute); iii) compare the approach with more complex models (i.e., deep-learning) based on raw CGM data. For what it concerns the direct evaluation of the model-based bioavailability prediction, since Technosphere® Insulin is indistinguishable from the insulin that is secreted endogenously, it was not possible in the experiment samples to trace the exogenous insulin. In future studies, this direct assessment could be evaluated across other insulin analogs that are distinguishable from regular human insulin i.e., by using assays based on specific monoclonal antibodies that have low cross-reactivity to such insulin analogs but a high reactivity to endogenously produced insulin, thus allowing its direct quantification. In conclusion, even if the present thesis addresses scattered problems and is characterized by a transversal nature, the integration of the different approaches in an integrated tool could be the object of interest for the future, with a general perspective of optimizing prevention, diagnosis and diabetes therapy.

References

[1] P. Saeedi *et al.*, “Global and regional diabetes prevalence estimates for 2019 and projections for 2030 and 2045: Results from the International Diabetes Federation Diabetes Atlas, 9th edition,” *Diabetes Res Clin Pract*, 2019, doi: 10.1016/j.diabres.2019.107843.

[2] R. Bizzotto *et al.*, “Processes Underlying Glycemic Deterioration in Type 2 Diabetes: An IMI DIRECT Study.,” *Diabetes Care*, vol. 44, no. 2, pp. 511–518, Feb. 2021, doi: 10.2337/dc20-1567.

[3] N. A. ElSayed *et al.*, “2. Classification and Diagnosis of Diabetes: Standards of Care in Diabetes—2023,” *Diabetes Care*, vol. 46, no. Supplement_1, pp. S19–S40, Jan. 2023, doi: 10.2337/dc23-S002.

[4] H. Sun *et al.*, “IDF Diabetes Atlas: Global, regional and country-level diabetes prevalence estimates for 2021 and projections for 2045,” *Diabetes Res Clin Pract*, vol. 183, p. 109119, Jan. 2022, doi: 10.1016/j.diabres.2021.109119.

[5] J. F. Plows, J. L. Stanley, P. N. Baker, C. M. Reynolds, and M. H. Vickers, “The Pathophysiology of Gestational Diabetes Mellitus.,” *Int J Mol Sci*, vol. 19, no. 11, Oct. 2018, doi: 10.3390/ijms19113342.

[6] D. Tomic, J. E. Shaw, and D. J. Magliano, “The burden and risks of emerging complications of diabetes mellitus,” *Nat Rev Endocrinol*, vol. 18, no. 9, pp. 525–539, Sep. 2022, doi: 10.1038/s41574-022-00690-7.

[7] G. Freckmann *et al.*, “Standardization process of continuous glucose monitoring: Traceability and performance,” *Clinica Chimica Acta*, vol. 515, pp. 5–12, Apr. 2021, doi: 10.1016/j.cca.2020.12.025.

[8] Z. Mian, K. L. Hermayer, and A. Jenkins, “Continuous Glucose Monitoring: Review of an Innovation in Diabetes Management,” *American Journal of the Medical Sciences*. 2019. doi: 10.1016/j.amjms.2019.07.003.

[9] J. Bolinder, R. Antuna, P. Geelhoed-Duijvestijn, J. Kröger, and R. Weitgasser, “Novel glucose-sensing technology and hypoglycaemia in type 1 diabetes: a

multicentre, non-masked, randomised controlled trial," *The Lancet*, vol. 388, no. 10057, pp. 2254–2263, Nov. 2016, doi: 10.1016/S0140-6736(16)31535-5.

[10] T. Haak, H. Hanaire, R. Ajjan, N. Hermanns, J. P. Riveline, and G. Rayman, "Use of Flash Glucose-Sensing Technology for 12 months as a Replacement for Blood Glucose Monitoring in Insulin-treated Type 2 Diabetes," *Diabetes Therapy*, vol. 8, no. 3, pp. 573–586, Jun. 2017, doi: 10.1007/S13300-017-0255-6.

[11] G. Aleppo *et al.*, "REPLACE-BG: A Randomized Trial Comparing Continuous Glucose Monitoring With and Without Routine Blood Glucose Monitoring in Adults With Well-Controlled Type 1 Diabetes," *Diabetes Care*, vol. 40, no. 4, pp. 538–545, Apr. 2017, doi: 10.2337/DC16-2482.

[12] D. Rodbard, "Continuous Glucose Monitoring: A Review of Successes, Challenges, and Opportunities," *Diabetes Technol Ther*, vol. 18, no. S2, pp. S2-3-S2-13, Feb. 2016, doi: 10.1089/dia.2015.0417.

[13] D. Rodbard, "Continuous Glucose Monitoring: A Review of Recent Studies Demonstrating Improved Glycemic Outcomes," *Diabetes Technol Ther*, vol. 19, no. S3, pp. S25–S37, Jun. 2017, doi: 10.1089/DIA.2017.0035.

[14] S. Ida, R. Kaneko, and K. Murata, "Utility of Real-Time and Retrospective Continuous Glucose Monitoring in Patients with Type 2 Diabetes Mellitus: A Meta-Analysis of Randomized Controlled Trials," *J Diabetes Res*, vol. 2019, pp. 1–10, Jan. 2019, doi: 10.1155/2019/4684815.

[15] I. Malandrucco, B. Russo, F. Picconi, M. Menduni, and S. Frontoni, "Glycemic Status Assessment by the Latest Glucose Monitoring Technologies," *Int J Mol Sci*, vol. 21, no. 21, p. 8243, Nov. 2020, doi: 10.3390/ijms21218243.

[16] K. M. Miller *et al.*, "Benefit of Continuous Glucose Monitoring in Reducing Hypoglycemia Is Sustained Through 12 Months of Use among Older Adults with Type 1 Diabetes," *Diabetes Technol Ther*, vol. 24, no. 6, pp. 424–434, Jun. 2022, doi: 10.1089/DIA.2021.0503/SUPPL_FILE/SUPP_TABLES6.DOCX.

[17] E. M. Scott, D. S. Feig, H. R. Murphy, and G. R. Law, "Continuous Glucose Monitoring in Pregnancy: Importance of Analyzing Temporal Profiles to Understand Clinical Outcomes," *Diabetes Care*, vol. 43, no. 6, pp. 1178–1184, Jun. 2020, doi: 10.2337/dc19-2527.

[18] A. A. Al Hayek, A. A. Robert, and M. A. Al Dawish, “Acceptability of the FreeStyle Libre Flash Glucose Monitoring System: The Experience of Young Patients With Type 1 Diabetes,” *Clin Med Insights Endocrinol Diabetes*, vol. 13, pp. 1–7, Jan. 2020, doi: 10.1177/1179551420910122.

[19] R. J. Galindo and G. Aleppo, “Continuous glucose monitoring: The achievement of 100 years of innovation in diabetes technology,” *Diabetes Research and Clinical Practice*. 2020. doi: 10.1016/j.diabres.2020.108502.

[20] R. I. G. Holt *et al.*, “The management of type 1 diabetes in adults. A consensus report by the American Diabetes Association (ADA) and the European Association for the Study of Diabetes (EASD),” *Diabetologia*, vol. 64, no. 12, pp. 2609–2652, Dec. 2021, doi: 10.1007/s00125-021-05568-3.

[21] M. J. Davies *et al.*, “Management of Hyperglycemia in Type 2 Diabetes, 2018. A Consensus Report by the American Diabetes Association (ADA) and the European Association for the Study of Diabetes (EASD),” *Diabetes Care*, vol. 41, no. 12, pp. 2669–2701, Dec. 2018, doi: 10.2337/dci18-0033.

[22] N. A. ElSayed *et al.*, “15. Management of Diabetes in Pregnancy: *Standards of Care in Diabetes—2023*,” *Diabetes Care*, vol. 46, no. Supplement_1, pp. S254–S266, Jan. 2023, doi: 10.2337/dc23-S015.

[23] N. Spaan, A. Teplova, G. Stam, J. Spaan, and C. Lucas, “Systematic review: continuous intraperitoneal insulin infusion with implantable insulin pumps for diabetes mellitus,” *Acta Diabetol*, vol. 51, no. 3, pp. 339–351, Jun. 2014, doi: 10.1007/s00592-014-0557-3.

[24] X. Jin, D. D. Zhu, B. Z. Chen, M. Ashfaq, and X. D. Guo, “Insulin delivery systems combined with microneedle technology,” *Adv Drug Deliv Rev*, vol. 127, pp. 119–137, Mar. 2018, doi: 10.1016/j.addr.2018.03.011.

[25] A. Gedawy, J. Martinez, H. Al-Salami, and C. R. Dass, “Oral insulin delivery: existing barriers and current counter-strategies,” *Journal of Pharmacy and Pharmacology*, vol. 70, no. 2, pp. 197–213, Jan. 2018, doi: 10.1111/jphp.12852.

[26] V. Sugumar *et al.*, “A Comprehensive Review of the Evolution of Insulin Development and Its Delivery Method,” *Pharmaceutics*, vol. 14, no. 7, p. 1406, Jul. 2022, doi: 10.3390/pharmaceutics14071406.

[27] L. Heinemann, R. Baughman, A. Boss, and M. Hompesch, “Pharmacokinetic and Pharmacodynamic Properties of a Novel Inhaled Insulin.,” *J Diabetes Sci Technol*, vol. 11, no. 1, pp. 148–156, Jan. 2017, doi: 10.1177/1932296816658055.

[28] K. Rave, T. Heise, L. Heinemann, and A. H. Boss, “Inhaled Technosphere® Insulin in Comparison to Subcutaneous Regular Human Insulin: Time Action Profile and Variability in Subjects with Type 2 Diabetes,” *J Diabetes Sci Technol*, vol. 2, no. 2, pp. 205–212, Mar. 2008, doi: 10.1177/193229680800200206.

[29] E. R. Seaquist *et al.*, “Hypoglycaemia is reduced with use of inhaled Technosphere® Insulin relative to insulin aspart in type 1 diabetes mellitus,” *Diabetic Medicine*, vol. 37, no. 5, pp. 752–759, May 2020, doi: 10.1111/DME.14202.

[30] A. Galderisi *et al.*, “Effect of Afrezza on Glucose Dynamics During HCL Treatment,” *Diabetes Care*, vol. 43, no. 9, pp. 2146–2152, Sep. 2020, doi: 10.2337/DC20-0091.

[31] P. Levin, B. J. Hoogwerf, J. Snell-Bergeon, T. Vigers, L. Pyle, and L. Bromberger, “Ultra Rapid-Acting Inhaled Insulin Improves Glucose Control in Patients With Type 2 Diabetes Mellitus,” *Endocr Pract*, vol. 27, no. 5, pp. 449–454, May 2021, doi: 10.1016/J.EPRAC.2020.10.004.

[32] C. K. Boughton and R. Hovorka, “New closed-loop insulin systems,” *Diabetologia*, vol. 64, no. 5, pp. 1007–1015, May 2021, doi: 10.1007/s00125-021-05391-w.

[33] M. Clements, N. Kaufman, and E. Mel, “Using Digital Health Technology to Prevent and Treat Diabetes,” *Diabetes Technol Ther*, vol. 25, no. S1, p. S-90-S-108, Feb. 2023, doi: 10.1089/dia.2023.2506.

[34] A. N. Klonoff, W.-A. (Andy) Lee, N. Y. Xu, K. T. Nguyen, A. DuBord, and D. Kerr, “Six Digital Health Technologies That Will Transform Diabetes,” *J Diabetes Sci Technol*, vol. 17, no. 1, pp. 239–249, Jan. 2023, doi: 10.1177/19322968211043498.

[35] R. T. Sutton, D. Pincock, D. C. Baumgart, D. C. Sadowski, R. N. Fedorak, and K. I. Kroeker, “An overview of clinical decision support systems: benefits,

risks, and strategies for success," *NPJ Digit Med*, vol. 3, no. 1, p. 17, Feb. 2020, doi: 10.1038/s41746-020-0221-y.

[36] American Diabetes Association Professional Practice Committee, "2. Classification and Diagnosis of Diabetes: *Standards of Medical Care in Diabetes—2022*," *Diabetes Care*, vol. 45, no. Supplement_1, pp. S17–S38, Jan. 2022, doi: 10.2337/dc22-S002.

[37] E. Eyth, H. Basit, and C. J. Swift, *Glucose Tolerance Test*. Treasure Island (FL): StatPearls Publishing, 2023.

[38] C. J. Greenbaum *et al.*, "Mixed-Meal Tolerance Test Versus Glucagon Stimulation Test for the Assessment of β-Cell Function in Therapeutic Trials in Type 1 Diabetes," *Diabetes Care*, vol. 31, no. 10, pp. 1966–1971, Oct. 2008, doi: 10.2337/dc07-2451.

[39] E. Carson and C. Cobelli, *Modelling Methodology for Physiology and Medicine*. Elsevier, 2014. doi: 10.1016/C2012-0-06031-0.

[40] J. Wang, Y. Li, R. X. Gao, and F. Zhang, "Hybrid physics-based and data-driven models for smart manufacturing: Modelling, simulation, and explainability," *J Manuf Syst*, vol. 63, pp. 381–391, Apr. 2022, doi: 10.1016/j.jmsy.2022.04.004.

[41] A. Mari, A. Tura, E. Grespan, and R. Bizzotto, "Mathematical Modeling for the Physiological and Clinical Investigation of Glucose Homeostasis and Diabetes," *Front Physiol*, vol. 11, Nov. 2020, doi: 10.3389/fphys.2020.575789.

[42] G. Cappon, F. Prendin, A. Facchinetti, G. Sparacino, and S. Del Favero, "Individualized Models for Glucose Prediction in Type 1 Diabetes: Comparing Black-Box Approaches to a Physiological White-Box One," *IEEE Trans Biomed Eng*, vol. 70, no. 11, pp. 3105–3115, Nov. 2023, doi: 10.1109/TBME.2023.3276193.

[43] K. Li, C. Liu, T. Zhu, P. Herrero, and P. Georgiou, "GluNet: A Deep Learning Framework for Accurate Glucose Forecasting," *IEEE J Biomed Health Inform*, vol. 24, no. 2, pp. 414–423, Feb. 2020, doi: 10.1109/JBHI.2019.2931842.

[44] R. N. Bergman, Y. Z. Ider, C. R. Bowden, and C. Cobelli, "Quantitative estimation of insulin sensitivity.," *American Journal of Physiology-Endocrinology and Metabolism*, vol. 236, no. 6, p. E667, Jun. 1979, doi: 10.1152/ajpendo.1979.236.6.E667.

[45] A. Caumo, R. N. Bergman, and C. Cobelli, “Insulin Sensitivity from Meal Tolerance Tests in Normal Subjects: A Minimal Model Index,” *J Clin Endocrinol Metab*, vol. 85, no. 11, pp. 4396–4402, Nov. 2000, doi: 10.1210/jcem.85.11.6982.

[46] C. Della Man, A. Caumo, and C. Cobelli, “The oral glucose minimal model: Estimation of insulin sensitivity from a meal test,” *IEEE Trans Biomed Eng*, vol. 49, no. 5, pp. 419–429, May 2002, doi: 10.1109/10.995680.

[47] A. Mari, A. Tura, A. Gastaldelli, and E. Ferrannini, “Assessing Insulin Secretion by Modeling in Multiple-Meal Tests,” *Diabetes*, vol. 51, no. suppl_1, pp. S221–S226, Feb. 2002, doi: 10.2337/diabetes.51.2007.S221.

[48] W. C. Duckworth, R. G. Bennett, and F. G. Hamel, “The Significance of Intracellular Insulin to Insulin Action,” *Journal of Investigative Medicine*, 1997.

[49] W. C. Duckworth, R. G. Bennett, and F. G. Hamel, “Insulin degradation: Progress and potential,” *Endocrine Reviews*. 1998. doi: 10.1210/er.19.5.608.

[50] K. Ohashi *et al.*, “Increase in hepatic and decrease in peripheral insulin clearance characterize abnormal temporal patterns of serum insulin in diabetic subjects,” *NPJ Syst Biol Appl*, 2018, doi: 10.1038/s41540-018-0051-6.

[51] M. Morettini, C. Göbl, A. Kautzky-Willer, G. Pacini, A. Tura, and L. Burattini, “Former gestational diabetes: Mathematical modeling of intravenous glucose tolerance test for the assessment of insulin clearance and its determinants,” *Mathematical Biosciences and Engineering*, 2020, doi: 10.3934/mbe.2020084.

[52] M. Morettini, C. Göbl, A. Kautzky-Willer, G. Pacini, A. Tura, and L. Burattini, “Insulin clearance in women with a history of gestational diabetes assessed by mathematical model analyses of intravenous glucose tolerance test,” in *IFMBE Proceedings*, 2020. doi: 10.1007/978-3-030-31635-8_61.

[53] A. Tura, C. Göbl, M. Morettini, L. Burattini, A. Kautzky-Willer, and G. Pacini, “Insulin clearance is altered in women with a history of gestational diabetes progressing to type 2 diabetes,” *Nutrition, Metabolism and Cardiovascular Diseases*, vol. 30, no. 8, pp. 1272–1280, Jul. 2020, doi: 10.1016/j.numecd.2020.04.004.

[54] D. C. Polidori, R. N. Bergman, S. T. Chung, and A. E. Sumner, “Hepatic and Extrahepatic Insulin Clearance Are Differentially Regulated: Results From a

Novel Model-Based Analysis of Intravenous Glucose Tolerance Data," *Diabetes*, vol. 65, no. 6, pp. 1556–1564, Jun. 2016, doi: 10.2337/db15-1373.

[55] R. N. Bergman, F. Piccinini, M. Kabir, C. M. Kolka, and M. Ader, "Hypothesis: Role of Reduced Hepatic Insulin Clearance in the Pathogenesis of Type 2 Diabetes," *Diabetes*, vol. 68, no. 9, pp. 1709–1716, Sep. 2019, doi: 10.2337/db19-0098.

[56] F. Piccinini and R. N. Bergman, "The Measurement of Insulin Clearance," *Diabetes Care*, vol. 43, no. 9, pp. 2296–2302, Sep. 2020, doi: 10.2337/dc20-0750.

[57] E. Van Cauter, F. Mestrez, J. Sturis, and K. S. Polonsky, "Estimation of Insulin Secretion Rates from C-Peptide Levels: Comparison of Individual and Standard Kinetic Parameters for C-Peptide Clearance," *Diabetes*, vol. 41, no. 3, pp. 368–377, Mar. 1992, doi: 10.2337/DIAB.41.3.368.

[58] A. Caumo, I. Florea, and L. Luzi, "Effect of a variable hepatic insulin clearance on the postprandial insulin profile: insights from a model simulation study," *Acta Diabetol*, vol. 44, no. 1, pp. 23–29, Mar. 2007, doi: 10.1007/s00592-007-0237-7.

[59] A. Tura *et al.*, "Progression to Type 2 Diabetes in Women with Former Gestational Diabetes: Time Trajectories of Metabolic Parameters," *PLoS One*, 2012, doi: 10.1371/journal.pone.0050419.

[60] C. S. Göbl, L. Bozkurt, T. Prikoszovich, C. Winzer, G. Pacini, and A. Kautzky-Willer, "Early possible risk factors for overt diabetes after gestational diabetes mellitus," *Obstetrics and Gynecology*, 2011, doi: 10.1097/AOG.0b013e318220e18f.

[61] A. Tura, S. Sbrignadello, E. Succurro, L. Groop, G. Sesti, and G. Pacini, "An empirical index of insulin sensitivity from short IVGTT: Validation against the minimal model and glucose clamp indices in patients with different clinical characteristics," *Diabetologia*, 2010, doi: 10.1007/s00125-009-1547-9.

[62] M. Morettini *et al.*, "Glucose Effectiveness from Short Insulin-Modified IVGTT and Its Application to the Study of Women with Previous Gestational Diabetes Mellitus," *Diabetes Metab J*, 2020, doi: 10.4093/dmj.2019.0016.

[63] M. Morettini *et al.*, “Assessment of glucose effectiveness from short IVGTT in individuals with different degrees of glucose tolerance,” *Acta Diabetol*, 2018, doi: 10.1007/s00592-018-1182-3.

[64] A. Tura, B. Ludvik, J. J. Nolan, G. Pacini, and K. Thomaseth, “Insulin and C-peptide secretion and kinetics in humans: direct and model-based measurements during OGTT.,” *Am J Physiol Endocrinol Metab*, vol. 281, no. 5, pp. E966-74, Nov. 2001, doi: 10.1152/ajpendo.2001.281.5.E966.

[65] A. Tura, G. Pacini, A. Kautzky-Willer, B. Ludvik, R. Prager, and K. Thomaseth, “Basal and dynamic proinsulin-insulin relationship to assess β-cell function during OGTT in metabolic disorders,” *American Journal of Physiology-Endocrinology and Metabolism*, vol. 285, no. 1, pp. E155–E162, Jul. 2003, doi: 10.1152/ajpendo.00104.2002.

[66] A. Tura and G. Pacini, “Comment on Piccinini and Bergman The Measurement of Insulin Clearance. Diabetes Care 2020;43:2296–2302,” *Diabetes Care*, vol. 44, no. 2, pp. e35–e35, Feb. 2021, doi: 10.2337/dc20-2444.

[67] S. Contreras, D. Medina-Ortiz, C. Conca, and Á. Olivera-Nappa, “A Novel Synthetic Model of the Glucose-Insulin System for Patient-Wise Inference of Physiological Parameters From Small-Size OGTT Data,” *Front Bioeng Biotechnol*, vol. 8, Mar. 2020, doi: 10.3389/fbioe.2020.00195.

[68] L. L. Del Giudice, A. Piersanti, L. Burattini, A. Tura, and M. Morettini, “Individual Estimation of Parameters Describing the Glucose-Insulin Regulatory System: a Modeling Approach with Regularization for Reduced-Sampling Oral Glucose Tolerance Test Data,” in *11th International Conference on E-Health and Bioengineering - EHB 2023*, Bucharest, Romania: in press.

[69] M. O. Goodarzi *et al.*, “Insulin Sensitivity and Insulin Clearance Are Heritable and Have Strong Genetic Correlation in Mexican Americans,” *Obesity*, 2014, doi: 10.1002/oby.20639.

[70] H. Kaga *et al.*, “Correlates of insulin clearance in apparently healthy non-obese Japanese men,” *Sci Rep*, 2017, doi: 10.1038/s41598-017-01469-x.

[71] J. Dupre, S. A. Ross, D. Watson, and J. C. Brown, “Stimulation of insulin secretion by gastric inhibitory polypeptide in man.,” *J Clin Endocrinol Metab*, vol. 37, no. 5, pp. 826–8, Nov. 1973, doi: 10.1210/jcem-37-5-826.

[72] B. Kreymann, G. Williams, M. A. Ghatei, and S. R. Bloom, “Glucagon-like peptide-1 7-36: a physiological incretin in man.,” *Lancet*, vol. 2, no. 8571, pp. 1300–4, Dec. 1987, doi: 10.1016/s0140-6736(87)91194-9.

[73] G. Pacini, K. Thomaseth, and B. Ahrén, “Dissociated effects of glucose-dependent insulinotropic polypeptide vs glucagon-like peptide–1 on β-cell secretion and insulin clearance in mice,” *Metabolism*, vol. 59, no. 7, pp. 988–992, Jul. 2010, doi: 10.1016/j.metabol.2009.10.021.

[74] B. Ahrén, K. Thomaseth, and G. Pacini, “Reduced insulin clearance contributes to the increased insulin levels after administration of glucagon-like peptide 1 in mice,” *Diabetologia*, vol. 48, no. 10, pp. 2140–2146, Oct. 2005, doi: 10.1007/s00125-005-1915-z.

[75] N. N. Rudovich, H. J. Rochlitz, and A. F. H. Pfeiffer, “Reduced hepatic insulin extraction in response to gastric inhibitory polypeptide compensates for reduced insulin secretion in normal-weight and normal glucose tolerant first-degree relatives of type 2 diabetic patients,” *Diabetes*, vol. 53, no. 9, pp. 2359–2365, Sep. 2004, doi: 10.2337/diabetes.53.9.2359.

[76] J. J. Meier, J. J. Holst, W. E. Schmidt, and M. A. Nauck, “Reduction of hepatic insulin clearance after oral glucose ingestion is not mediated by glucagon-like peptide 1 or gastric inhibitory polypeptide in humans,” *American Journal of Physiology-Endocrinology and Metabolism*, vol. 293, no. 3, pp. E849–E856, Sep. 2007, doi: 10.1152/ajpendo.00289.2007.

[77] J. J. Meier *et al.*, “The reduction in hepatic insulin clearance after oral glucose is not mediated by Gastric inhibitory polypeptide (GIP),” *Regul Pept*, vol. 113, no. 1–3, pp. 95–100, May 2003, doi: 10.1016/S0167-0115(02)00297-5.

[78] A. Tura, R. Bizzotto, Y. Yamada, Y. Seino, G. Pacini, and B. Ahrén, “Increased insulin clearance in mice with double deletion of glucagon-like peptide-1 and glucose-dependent insulinotropic polypeptide receptors,” *American Journal of Physiology-Regulatory, Integrative and Comparative Physiology*, vol. 314, no. 5, pp. R639–R646, May 2018, doi: 10.1152/ajpregu.00181.2017.

[79] D. Jung, L. Lin, H. Jiao, X. Cai, J.-X. Duan, and M. Matteucci, “Pharmacokinetics of TH-302: a hypoxically activated prodrug of bromo-isophosphoramide mustard in mice, rats, dogs and monkeys,” *Cancer*

Chemother Pharmacol, vol. 69, no. 3, pp. 643–654, Mar. 2012, doi: 10.1007/s00280-011-1741-6.

[80] G. Pacini, M. Ahrén, and B. Ahrén, "Reappraisal of the intravenous glucose tolerance index for a simple assessment of insulin sensitivity in mice," *American Journal of Physiology-Regulatory, Integrative and Comparative Physiology*, vol. 296, no. 5, pp. R1316–R1324, May 2009, doi: 10.1152/ajpregu.90575.2008.

[81] A. Katz *et al.*, "Quantitative insulin sensitivity check index: a simple, accurate method for assessing insulin sensitivity in humans," *J Clin Endocrinol Metab*, vol. 85, no. 7, pp. 2402–2410, Jul. 2000, doi: 10.1210/jcem.85.7.6661.

[82] G. Pacini, K. Thomaseth, and B. Ahrén, "Contribution to glucose tolerance of insulin-independent vs. insulin-dependent mechanisms in mice," *American Journal of Physiology-Endocrinology and Metabolism*, vol. 281, no. 4, pp. E693–E703, Oct. 2001, doi: 10.1152/ajpendo.2001.281.4.E693.

[83] S. E. Kahn *et al.*, "Quantification of the relationship between insulin sensitivity and beta-cell function in human subjects. Evidence for a hyperbolic function," *Diabetes*, vol. 42, no. 11, pp. 1663–1672, Nov. 1993, doi: 10.2337/diabetes.42.11.1663.

[84] A. Tura, A. Kautzky-Willer, and G. Pacini, "Insulinogenic indices from insulin and C-peptide: Comparison of beta-cell function from OGTT and IVGTT," *Diabetes Res Clin Pract*, vol. 72, no. 3, pp. 298–301, Jun. 2006, doi: 10.1016/j.diabres.2005.10.005.

[85] S. M. Najjar and G. Perdomo, "Hepatic insulin clearance: mechanism and physiology," *Physiology*, vol. 34, no. 3, pp. 198–215, May 2019, doi: 10.1152/physiol.00048.2018.

[86] S. K. Ramakrishnan *et al.*, "PPARα (peroxisome proliferator-activated receptor α) activation reduces hepatic CEACAM1 protein expression to regulate fatty acid oxidation during fasting-refeeding transition," *Journal of Biological Chemistry*, vol. 291, no. 15, pp. 8121–8129, Apr. 2016, doi: 10.1074/jbc.M116.714014.

[87] H. E. Ghadieh *et al.*, “Exenatide induces carcinoembryonic antigen-related cell adhesion molecule 1 expression to prevent hepatic steatosis,” *Hepatol Commun*, vol. 2, no. 1, pp. 35–47, Jan. 2018, doi: 10.1002/hep4.1117.

[88] E. Ferrannini, J. Wahren, O. K. Faber, P. Felig, C. Binder, and R. A. DeFronzo, “Splanchnic and renal metabolism of insulin in human subjects: a dose-response study,” *American Journal of Physiology-Endocrinology and Metabolism*, vol. 244, no. 6, pp. E517–E527, Jun. 1983, doi: 10.1152/ajpendo.1983.244.6.E517.

[89] A. F. Pina *et al.*, “Insulin: trigger and target of renal functions,” *Front Cell Dev Biol*, vol. 8, Jul. 2020, doi: 10.3389/fcell.2020.00519.

[90] F. Li *et al.*, “Loss of renal SNX5 results in impaired IDE activity and insulin resistance in mice,” *Diabetologia*, vol. 61, no. 3, pp. 727–737, Mar. 2018, doi: 10.1007/s00125-017-4482-1.

[91] T. Buenaventura *et al.*, “A targeted RNAi screen identifies endocytic trafficking factors that control GLP-1 receptor signaling in pancreatic β-Cells,” *Diabetes*, vol. 67, no. 3, pp. 385–399, Mar. 2018, doi: 10.2337/db17-0639.

[92] I. Caruso *et al.*, “Glucagon in type 2 diabetes: Friend or foe?,” *Diabetes Metab Res Rev*, vol. 39, no. 3, Mar. 2023, doi: 10.1002/dmrr.3609.

[93] A. Lund, J. I. Bagger, M. Christensen, F. K. Knop, and T. Vilsbøll, “Glucagon and Type 2 Diabetes: the Return of the Alpha Cell,” *Curr Diab Rep*, vol. 14, no. 12, p. 555, Dec. 2014, doi: 10.1007/s11892-014-0555-4.

[94] J. W. Hughes, A. Ustione, Z. Lavagnino, and D. W. Piston, “Regulation of islet glucagon secretion: Beyond calcium,” *Diabetes Obes Metab*, vol. 20, no. S2, pp. 127–136, Sep. 2018, doi: 10.1111/dom.13381.

[95] C. Göbl *et al.*, “Temporal Patterns of Glucagon and Its Relationships with Glucose and Insulin following Ingestion of Different Classes of Macronutrients,” *Nutrients*, vol. 14, no. 2, p. 376, Jan. 2022, doi: 10.3390/nu14020376.

[96] M. Morettini, L. Burattini, C. Göbl, G. Pacini, B. Ahrén, and A. Tura, “Mathematical Model of Glucagon Kinetics for the Assessment of Insulin-Mediated Glucagon Inhibition During an Oral Glucose Tolerance Test,” *Front Endocrinol (Lausanne)*, vol. 12, Mar. 2021, doi: 10.3389/fendo.2021.611147.

[97] S. Masroor, M. G. J. van Dongen, R. Alvarez-Jimenez, K. Burggraaf, L. A. Peletier, and M. A. Peletier, “Mathematical modeling of the glucagon challenge test,” *J Pharmacokinet Pharmacodyn*, vol. 46, no. 6, pp. 553–564, Dec. 2019, doi: 10.1007/s10928-019-09655-2.

[98] A. Shirin, F. Della Rossa, I. Klickstein, J. Russell, and F. Sorrentino, “Optimal regulation of blood glucose level in Type I diabetes using insulin and glucagon,” *PLoS One*, vol. 14, no. 3, p. e0213665, Mar. 2019, doi: 10.1371/journal.pone.0213665.

[99] D. Lv, M. D. Breton, and L. S. Farhy, “Pharmacokinetics Modeling of Exogenous Glucagon in Type 1 Diabetes Mellitus Patients,” *Diabetes Technol Ther*, vol. 15, no. 11, pp. 935–941, Nov. 2013, doi: 10.1089/dia.2013.0150.

[100] V. Mojto, Z. Rausova, J. Chrenova, and L. Dedik, “Short-term glucagon stimulation test of C-peptide effect on glucose utilization in patients with type 1 diabetes mellitus,” *Med Biol Eng Comput*, vol. 53, no. 12, pp. 1361–1369, Dec. 2015, doi: 10.1007/s11517-015-1416-2.

[101] V. Subramanian, J. I. Bagger, J. J. Holst, F. K. Knop, and T. Vilsbøll, “A glucose-insulin-glucagon coupled model of the isoglycemic intravenous glucose infusion experiment,” *Front Physiol*, vol. 13, Sep. 2022, doi: 10.3389/fphys.2022.911616.

[102] R. A. Kelly, M. J. Fitches, S. D. Webb, S. R. Pop, and S. J. Chidlow, “Modelling the effects of glucagon during glucose tolerance testing,” *Theor Biol Med Model*, vol. 16, no. 1, p. 21, Dec. 2019, doi: 10.1186/s12976-019-0115-3.

[103] M. Morettini, A. Piersanti, C. Göbl, L. Burattini, and A. Tura, “Mathematical model of glucagon kinetics during an oral glucose tolerance test based on a dual regulation mechanism,” in *Convegno Nazionale di Bioingegneria*, 2023.

[104] T. Moede *et al.*, “Glucokinase intrinsically regulates glucose sensing and glucagon secretion in pancreatic alpha cells,” *Sci Rep*, vol. 10, no. 1, p. 20145, Nov. 2020, doi: 10.1038/s41598-020-76863-z.

[105] D. P. Sonne, J. F. Rehfeld, J. J. Holst, T. Vilsbøll, and F. K. Knop, “Postprandial gallbladder emptying in patients with type 2 diabetes: potential implications for bile-induced secretion of glucagon-like peptide 1,” *Eur J Endocrinol*, vol. 171, no. 4, pp. 407–419, Oct. 2014, doi: 10.1530/EJE-14-0309.

[106] M. Omar-Hmeadi, P.-E. Lund, N. R. Gandasi, A. Tengholm, and S. Barg, “Paracrine control of α-cell glucagon exocytosis is compromised in human type-2 diabetes,” *Nat Commun*, vol. 11, no. 1, p. 1896, Apr. 2020, doi: 10.1038/s41467-020-15717-8.

[107] E. Van Schaftingen, *Energy Metabolism | Hexokinase/Glucokinase in Encyclopedia of Biological Chemistry III*, 3rd ed., vol. 1. Oxford: Elsevier, 2021.

[108] G. C. Mannino, E. Mancuso, S. Sbrignadello, M. Morettini, F. Andreozzi, and A. Tura, “Chemical Compounds and Ambient Factors Affecting Pancreatic Alpha-Cells Mass and Function: What Evidence?,” *Int J Environ Res Public Health*, vol. 19, no. 24, p. 16489, Dec. 2022, doi: 10.3390/ijerph192416489.

[109] S. Hædersdal, A. Lund, F. K. Knop, and T. Vilsbøll, “The Role of Glucagon in the Pathophysiology and Treatment of Type 2 Diabetes,” *Mayo Clin Proc*, vol. 93, no. 2, pp. 217–239, Feb. 2018, doi: 10.1016/j.mayocp.2017.12.003.

[110] E. R. Pearson, “Type 2 diabetes: a multifaceted disease,” *Diabetologia*, vol. 62, no. 7, pp. 1107–1112, Jul. 2019, doi: 10.1007/s00125-019-4909-y.

[111] American Diabetes Association, “2. Classification and Diagnosis of Diabetes: Standards of Medical Care in Diabetes-2020.,” *Diabetes Care*, vol. 43, no. Suppl 1, pp. S14–S31, 2020, doi: 10.2337/dc20-S002.

[112] I. Kavakiotis, O. Tsave, A. Salifoglou, N. Maglaveras, I. Vlahavas, and I. Chouvarda, “Machine Learning and Data Mining Methods in Diabetes Research,” *Comput Struct Biotechnol J*, vol. 15, pp. 104–116, 2017, doi: 10.1016/j.csbj.2016.12.005.

[113] T. Zheng and Y. Zhang, “A Big Data Application of Machine Learning-Based Framework to Identify Type 2 Diabetes Through Electronic Health Records,” in *Communications in Computer and Information Science*, 2017, pp. 451–458. doi: 10.1007/978-3-319-62698-7_37.

[114] S. Perveen, M. Shahbaz, A. Guergachi, and K. Keshavjee, “Performance Analysis of Data Mining Classification Techniques to Predict Diabetes,” *Procedia Comput Sci*, vol. 82, pp. 115–121, 2016, doi: 10.1016/j.procs.2016.04.016.

[115] R. Garcia-Carretero, L. Vigil-Medina, and O. Barquero-Perez, “The Use of Machine Learning Techniques to Determine the Predictive Value of Inflammatory Biomarkers in the Development of Type 2 Diabetes Mellitus.,” *Metab Syndr Relat Disord*, vol. 19, no. 4, pp. 240–248, 2021, doi: 10.1089/met.2020.0139.

[116] M. A. Sarwar, N. Kamal, W. Hamid, and M. A. Shah, “Prediction of diabetes using machine learning algorithms in healthcare,” in *ICAC 2018 - 2018 24th IEEE International Conference on Automation and Computing: Improving Productivity through Automation and Computing*, 2018.

[117] Q. Zou, K. Qu, Y. Luo, D. Yin, Y. Ju, and H. Tang, “Predicting Diabetes Mellitus With Machine Learning Techniques.,” *Front Genet*, vol. 9, p. 515, 2018, doi: 10.3389/fgene.2018.00515.

[118] N. S. El_Jerjawi and S. S. Abu-Naser, “Diabetes Prediction Using Artificial Neural Network,” *International Journal of Advanced Science and Technology*, vol. 121, pp. 54–64, 2018.

[119] M. Bernardini, M. Morettini, L. Romeo, E. Frontoni, and L. Burattini, “Early temporal prediction of Type 2 Diabetes Risk Condition from a General Practitioner Electronic Health Record: A Multiple Instance Boosting Approach.,” *Artif Intell Med*, vol. 105, p. 101847, May 2020, doi: 10.1016/j.artmed.2020.101847.

[120] K. Dalakleidi, K. Zarkogianni, A. Thanopoulou, and K. Nikita, “Comparative assessment of statistical and machine learning techniques towards estimating the risk of developing type 2 diabetes and cardiovascular complications,” *Expert Syst*, vol. 34, no. 6, p. e12214, Dec. 2017, doi: 10.1111/exsy.12214.

[121] A. Talaei-Khoei and J. M. Wilson, “Identifying people at risk of developing type 2 diabetes: A comparison of predictive analytics techniques and predictor variables,” *Int J Med Inform*, vol. 119, pp. 22–38, Nov. 2018, doi: 10.1016/j.ijmedinf.2018.08.008.

[122] R. Garcia-Carretero, L. Vigil-Medina, I. Mora-Jimenez, C. Soguero-Ruiz, O. Barquero-Perez, and J. Ramos-Lopez, “Use of a K-nearest neighbors model to predict the development of type 2 diabetes within 2 years in an obese,

hypertensive population.," *Med Biol Eng Comput*, vol. 58, no. 5, pp. 991–1002, May 2020, doi: 10.1007/s11517-020-02132-w.

[123] W. Yu, T. Liu, R. Valdez, M. Gwinn, and M. J. Khoury, "Application of support vector machine modeling for prediction of common diseases: the case of diabetes and pre-diabetes," *BMC Med Inform Decis Mak*, vol. 10, no. 1, p. 16, Dec. 2010, doi: 10.1186/1472-6947-10-16.

[124] M. Maniruzzaman *et al.*, "Comparative approaches for classification of diabetes mellitus data: Machine learning paradigm," *Comput Methods Programs Biomed*, vol. 152, pp. 23–34, Dec. 2017, doi: 10.1016/j.cmpb.2017.09.004.

[125] M. Bernardini, M. Morettini, L. Romeo, E. Frontoni, and L. Burattini, "TyG-er: An ensemble Regression Forest approach for identification of clinical factors related to insulin resistance condition using Electronic Health Records," *Comput Biol Med*, vol. 112, p. 103358, Sep. 2019, doi: 10.1016/j.compbiomed.2019.103358.

[126] Y. Huang, P. McCullagh, N. Black, and R. Harper, "Feature selection and classification model construction on type 2 diabetic patients' data," *Artif Intell Med*, vol. 41, no. 3, pp. 251–262, Nov. 2007, doi: 10.1016/j.artmed.2007.07.002.

[127] M. Lappas *et al.*, "The prediction of type 2 diabetes in women with previous gestational diabetes mellitus using lipidomics.," *Diabetologia*, vol. 58, no. 7, pp. 1436–42, Jul. 2015, doi: 10.1007/s00125-015-3587-7.

[128] S. R. Khan *et al.*, "The discovery of novel predictive biomarkers and early-stage pathophysiology for the transition from gestational diabetes to type 2 diabetes.," *Diabetologia*, vol. 62, no. 4, pp. 687–703, 2019, doi: 10.1007/s00125-018-4800-2.

[129] A. Allalou *et al.*, "A Predictive Metabolic Signature for the Transition From Gestational Diabetes Mellitus to Type 2 Diabetes.," *Diabetes*, vol. 65, no. 9, pp. 2529–39, 2016, doi: 10.2337/db15-1720.

[130] A. Klassen *et al.*, "Metabolomics: Definitions and Significance in Systems Biology.," *Adv Exp Med Biol*, vol. 965, pp. 3–17, 2017, doi: 10.1007/978-3-319-47656-8_1.

[131] F. R. Pinu, S. A. Goldansaz, and J. Jaine, “Translational Metabolomics: Current Challenges and Future Opportunities,” *Metabolites*, vol. 9, no. 6, p. 108, Jun. 2019, doi: 10.3390/metabo9060108.

[132] G. Pacini *et al.*, “Insulin sensitivity and glucose effectiveness: minimal model analysis of regular and insulin-modified FSIGT,” *American Journal of Physiology-Endocrinology and Metabolism*, 2017, doi: 10.1152/ajpendo.1998.274.4.e592.

[133] S. E. Kahn *et al.*, “Treatment with a somatostatin analog decreases pancreatic B-cell and whole body sensitivity to glucose.,” *J Clin Endocrinol Metab*, vol. 71, no. 4, pp. 994–1002, Oct. 1990, doi: 10.1210/jcem-71-4-994.

[134] C. Johnston *et al.*, “Beta-cell function and insulin sensitivity in nondiabetic HLA-identical siblings of insulin-dependent diabetics.,” *Diabetes*, vol. 36, no. 7, pp. 829–37, Jul. 1987, doi: 10.2337/diab.36.7.829.

[135] J. Demšar *et al.*, “Orange: Data Mining Toolbox in Python,” *Journal of Machine Learning Research*, vol. 14, pp. 2349–2353, 2013.

[136] M. M. Breuniq, H.-P. Kriegel, R. T. Ng, and J. Sander, “LOF: Identifying density-based local outliers,” *SIGMOD Record (ACM Special Interest Group on Management of Data)*, vol. 29, no. 2, pp. 93–104, 2000, doi: 10.1145/335191.335388.

[137] C. S. Göbl, L. Bozkurt, A. Tura, G. Pacini, A. Kautzky-Willer, and M. Mittlböck, “Application of Penalized Regression Techniques in Modelling Insulin Sensitivity by Correlated Metabolic Parameters.,” *PLoS One*, vol. 10, no. 11, p. e0141524, Nov. 2015, doi: 10.1371/journal.pone.0141524.

[138] G. Corani and A. Benavoli, “A Bayesian approach for comparing cross-validated algorithms on multiple data sets,” *Mach Learn*, vol. 100, no. 2–3, pp. 285–304, Sep. 2015, doi: 10.1007/s10994-015-5486-z.

[139] R. Pallares-Méndez, C. A. Aguilar-Salinas, I. Cruz-Bautista, and L. Del Bosque-Plata, “Metabolomics in diabetes, a review.,” *Ann Med*, vol. 48, no. 1–2, pp. 89–102, 2016, doi: 10.3109/07853890.2015.1137630.

[140] C. Lorenzo *et al.*, “Disposition index, glucose effectiveness, and conversion to type 2 diabetes: the Insulin Resistance Atherosclerosis Study (IRAS).,”

Diabetes Care, vol. 33, no. 9, pp. 2098–103, Sep. 2010, doi: 10.2337/dc10-0165.

[141] T. T. Hastie, "The Elements of Statistical Learning Second Edition," *Math. Intell.*, 2017.

[142] J. M. M. Rumbold, M. O'Kane, N. Philip, and B. K. Pierscionek, "Big Data and diabetes: the applications of Big Data for diabetes care now and in the future," *Diabetic Medicine*, vol. 37, no. 2, pp. 187–193, Feb. 2020, doi: 10.1111/dme.14044.

[143] H. F. Zhou, J. W. Zhang, Y. Q. Zhou, X. J. Guo, and Y. M. Ma, "A feature selection algorithm of decision tree based on feature weight," *Expert Syst Appl*, vol. 164, p. 113842, Feb. 2021, doi: 10.1016/J.ESWA.2020.113842.

[144] B. P. Kovatchev, "Metrics for glycaemic control — from HbA1c to continuous glucose monitoring," *Nat Rev Endocrinol*, vol. 13, no. 7, pp. 425–436, Jul. 2017, doi: 10.1038/nrendo.2017.3.

[145] M. Nguyen, J. Han, E. K. Spanakis, B. P. Kovatchev, and D. C. Klonoff, "A Review of Continuous Glucose Monitoring-Based Composite Metrics for Glycemic Control," *Diabetes Technol Ther*, vol. 22, no. 8, pp. 613–622, Aug. 2020, doi: 10.1089/dia.2019.0434.

[146] D. Rodbard, "Interpretation of continuous glucose monitoring data: glycemic variability and quality of glycemic control.," *Diabetes Technol Ther*, vol. 11 Suppl 1, no. SUPPL.1, pp. S55-67, Jun. 2009, doi: 10.1089/dia.2008.0132.

[147] R. M. Bergenstal *et al.*, "Recommendations for Standardizing Glucose Reporting and Analysis to Optimize Clinical Decision Making in Diabetes: The Ambulatory Glucose Profile (AGP)," *Diabetes Technol Ther*, vol. 15, no. 3, pp. 198–211, Mar. 2013, doi: 10.1089/dia.2013.0051.

[148] T. Danne *et al.*, "International Consensus on Use of Continuous Glucose Monitoring," *Diabetes Care*, vol. 40, no. 12, pp. 1631–1640, Dec. 2017, doi: 10.2337/dc17-1600.

[149] T. Battelino *et al.*, "Clinical Targets for Continuous Glucose Monitoring Data Interpretation: Recommendations From the International Consensus on Time in Range.," *Diabetes Care*, vol. 42, no. 8, pp. 1593–1603, Aug. 2019, doi: 10.2337/dci19-0028.

[150] D. Czerwoniuk, W. Fendler, L. Walenciak, and W. Mlynarski, “GlyCulator: a glycemic variability calculation tool for continuous glucose monitoring data.,” *J Diabetes Sci Technol*, vol. 5, no. 2, pp. 447–51, Mar. 2011, doi: 10.1177/193229681100500236.

[151] K. Pagacz, K. Stawiski, A. Szadkowska, W. Mlynarski, and W. Fendler, “GlyCulator2: an update on a web application for calculation of glycemic variability indices.,” *Acta Diabetol*, vol. 55, no. 8, pp. 877–880, Aug. 2018, doi: 10.1007/s00592-018-1140-0.

[152] J. Chrzanowski *et al.*, “GlyCulator 3.0: a web-based platform for continuous glucose monitoring analysis and center benchmarking,” *Pediatr Diabetes*, vol. 22, no. S30, pp. 33–165, Oct. 2021, doi: 10.1111/PEDI.13269.

[153] N. R. Hill, N. S. Oliver, P. Choudhary, J. C. Levy, P. Hindmarsh, and D. R. Matthews, “Normal reference range for mean tissue glucose and glycemic variability derived from continuous glucose monitoring for subjects without diabetes in different ethnic groups.,” *Diabetes Technol Ther*, vol. 13, no. 9, pp. 921–8, Sep. 2011, doi: 10.1089/dia.2010.0247.

[154] V. Moscardó, M. Giménez, N. Oliver, and N. R. Hill, “Updated Software for Automated Assessment of Glucose Variability and Quality of Glycemic Control in Diabetes.,” *Diabetes Technol Ther*, vol. 22, no. 10, pp. 701–708, Oct. 2020, doi: 10.1089/dia.2019.0416.

[155] R. A. Rawlings, H. Shi, L.-H. Yuan, W. Brehm, R. Pop-Busui, and P. W. Nelson, “Translating glucose variability metrics into the clinic via Continuous Glucose Monitoring: a Graphical User Interface for Diabetes Evaluation (CGM-GUIDE©).,” *Diabetes Technol Ther*, vol. 13, no. 12, pp. 1241–8, Dec. 2011, doi: 10.1089/dia.2011.0099.

[156] G. Marics *et al.*, “Evaluation of an open access software for calculating glucose variability parameters of a continuous glucose monitoring system applied at pediatric intensive care unit.,” *Biomed Eng Online*, vol. 14, no. 1, p. 37, Apr. 2015, doi: 10.1186/s12938-015-0035-3.

[157] A. Neinstein *et al.*, “A case study in open source innovation: developing the Tidepool Platform for interoperability in type 1 diabetes management.,” *J Am*

Med Inform Assoc, vol. 23, no. 2, pp. 324–32, Mar. 2016, doi: 10.1093/jamia/ocv104.

[158] X. D. Zhang, Z. Zhang, and D. Wang, "CGManalyzer: an R package for analyzing continuous glucose monitoring studies.," *Bioinformatics*, vol. 34, no. 9, pp. 1609–1611, May 2018, doi: 10.1093/bioinformatics/btx826.

[159] T. Vigers *et al.*, "cgmanalysis: An R package for descriptive analysis of continuous glucose monitor data.," *PLoS One*, vol. 14, no. 10, p. e0216851, Oct. 2019, doi: 10.1371/journal.pone.0216851.

[160] L. A. C. Millard, N. Patel, K. Tilling, M. Lewcock, P. A. Flach, and D. A. Lawlor, "GLU: a software package for analysing continuously measured glucose levels in epidemiology.," *Int J Epidemiol*, vol. 49, no. 3, pp. 744–757, 2020, doi: 10.1093/ije/dyaa004.

[161] A. M. De Livera, J. E. Shaw, N. Cohen, A. Reutens, and A. Salim, "An Interactive Web Application for the Statistical Analysis of Continuous Glucose Monitoring Data in Epidemiological Studies.," *J Diabetes Sci Technol*, vol. 16, no. 2, pp. 397–400, Mar. 2022, doi: 10.1177/1932296820985570.

[162] S. Broll *et al.*, "Interpreting blood GLUcose data with R package iglu.," *PLoS One*, vol. 16, no. 4, p. e0248560, Apr. 2021, doi: 10.1371/journal.pone.0248560.

[163] E. Olawsky, Y. Zhang, L. E. Eberly, E. S. Helgeson, and L. S. Chow, "A New Analysis Tool for Continuous Glucose Monitor Data.," *J Diabetes Sci Technol*, p. 19322968211028908, Jul. 2021, doi: 10.1177/19322968211028909.

[164] B. Bent, M. Henriquez, and J. Dunn, "Cgmquantify: Python and R Software Packages for Comprehensive Analysis of Interstitial Glucose and Glycemic Variability from Continuous Glucose Monitor Data," *IEEE Open J Eng Med Biol*, vol. 2, pp. 263–266, Aug. 2021, doi: 10.1109/OJEMB.2021.3105816.

[165] M. D. Costa, T. Henriques, M. N. Munshi, A. R. Segal, and A. L. Goldberger, "Dynamical glucometry: Use of multiscale entropy analysis in diabetes," *Chaos: An Interdisciplinary Journal of Nonlinear Science*, vol. 24, no. 3, p. 033139, Sep. 2014, doi: 10.1063/1.4894537.

[166] X. D. Zhang, "A pair of new statistical parameters for quality control in RNA interference high-throughput screening assays," *Genomics*, vol. 89, no. 4, pp. 552–561, Apr. 2007, doi: 10.1016/j.ygeno.2006.12.014.

[167] B. P. Kovatchev, D. J. Cox, L. A. Gonder-Frederick, and W. Clarke, “Symmetrization of the blood glucose measurement scale and its applications.,” *Diabetes Care*, vol. 20, no. 11, pp. 1655–8, Nov. 1997, doi: 10.2337/diacare.20.11.1655.

[168] F. Dubosson, J. E. Ranvier, S. Bromuri, J. P. Calbimonte, J. Ruiz, and M. Schumacher, “The open D1NAMO dataset: A multi-modal dataset for research on non-invasive type 1 diabetes management,” *Inform Med Unlocked*, vol. 13, no. September, pp. 92–100, 2018, doi: 10.1016/j.imu.2018.09.003.

[169] A. Piersanti, F. Giurato, C. Göbl, L. Burattini, A. Tura, and M. Morettini, “Software Packages and Tools for the Analysis of Continuous Glucose Monitoring Data,” *Diabetes Technol Ther*, vol. 25, no. 1, pp. 69–85, Jan. 2023, doi: 10.1089/dia.2022.0237.

[170] D. M. Nathan, J. Kuenen, R. Borg, H. Zheng, D. Schoenfeld, and R. J. Heine, “Translating the A1C Assay Into Estimated Average Glucose Values,” *Diabetes Care*, vol. 31, no. 8, pp. 1473–1478, Aug. 2008, doi: 10.2337/dc08-0545.

[171] R. W. Beck, C. G. Connor, D. M. Mullen, D. M. Wesley, and R. M. Bergenstal, “The Fallacy of Average: How Using HbA1c Alone to Assess Glycemic Control Can Be Misleading,” *Diabetes Care*, vol. 40, no. 8, pp. 994–999, Aug. 2017, doi: 10.2337/dc17-0636.

[172] B. P. Kovatchev, E. Otto, D. Cox, L. Gonder-Frederick, and W. Clarke, “Evaluation of a New Measure of Blood Glucose Variability in Diabetes,” *Diabetes Care*, vol. 29, no. 11, pp. 2433–2438, Nov. 2006, doi: 10.2337/dc06-1085.

[173] L. Leelarathna *et al.*, “Evaluating Glucose Control With a Novel Composite Continuous Glucose Monitoring Index,” *J Diabetes Sci Technol*, vol. 14, no. 2, pp. 277–283, Mar. 2020, doi: 10.1177/1932296819838525.

[174] C. M. McDonnell, S. M. Donath, S. I. Vidmar, G. A. Werther, and F. J. Cameron, “A Novel Approach to Continuous Glucose Analysis Utilizing Glycemic Variation,” *Diabetes Technol Ther*, vol. 7, no. 2, pp. 253–263, Apr. 2005, doi: 10.1089/dia.2005.7.253.

[175] C. R. Marling, J. H. Shubrook, S. J. Vernier, M. T. Wiley, and F. L. Schwartz, “Characterizing Blood Glucose Variability Using New Metrics with Continuous

Glucose Monitoring Data," *J Diabetes Sci Technol*, vol. 5, no. 4, pp. 871–878, Jul. 2011, doi: 10.1177/193229681100500408.

[176] T. Higuchi, "Approach to an irregular time series on the basis of the fractal theory," *Physica D*, vol. 31, no. 2, pp. 277–283, Jun. 1988, doi: 10.1016/0167-2789(88)90081-4.

[177] R. M. Bergenstal *et al.*, "Glucose Management Indicator (GMI): A New Term for Estimating A1C From Continuous Glucose Monitoring," *Diabetes Care*, vol. 41, no. 11, pp. 2275–2280, Nov. 2018, doi: 10.2337/dc18-1581.

[178] N. R. Hill, P. C. Hindmarsh, R. J. Stevens, I. M. Stratton, J. C. Levy, and D. R. Matthews, "A method for assessing quality of control from glucose profiles," *Diabetic Medicine*, vol. 24, no. 7, pp. 753–758, Jul. 2007, doi: 10.1111/j.1464-5491.2007.02119.x.

[179] T. A. Peyser, A. K. Balo, B. A. Buckingham, I. B. Hirsch, and A. Garcia, "Glycemic Variability Percentage: A Novel Method for Assessing Glycemic Variability from Continuous Glucose Monitor Data," *Diabetes Technol Ther*, vol. 20, no. 1, pp. 6–16, Jan. 2018, doi: 10.1089/DIA.2017.0187.

[180] I. Gaynanova, J. Urbanek, and N. M. Punjabi, "Corrections of Equations on Glycemic Variability and Quality of Glycemic Control," *Diabetes Technol Ther*, vol. 20, no. 4, pp. 317–317, Apr. 2018, doi: 10.1089/dia.2018.0057.

[181] J. M. Wojcicki, "'J'-index. A new proposition of the assessment of current glucose control in diabetic patients," *Hormone and Metabolic Research*, vol. 27, no. 1, pp. 41–42, Apr. 1995, doi: 10.1055/S-2007-979906/BIB.

[182] E. A. Ryan *et al.*, "Assessment of the severity of hypoglycemia and glycemic lability in type 1 diabetic subjects undergoing islet transplantation," *Diabetes*, vol. 53, no. 4, pp. 955–962, Apr. 2004, doi: 10.2337/DIABETES.53.4.955.

[183] J. Hermanides *et al.*, "Hypoglycemia is associated with intensive care unit mortality," *Crit Care Med*, vol. 38, no. 6, pp. 1430–1434, Jun. 2010, doi: 10.1097/CCM.0b013e3181de562c.

[184] F. J. Service, G. D. Molnar, J. W. Rosevear, E. Ackerman, L. C. Gatewood, and W. F. Taylor, "Mean Amplitude of Glycemic Excursions, a Measure of Diabetic Instability," *Diabetes*, vol. 19, no. 9, pp. 644–655, Sep. 1970, doi: 10.2337/diab.19.9.644.

[185] F. J. Service, “Glucose Variability,” *Diabetes*, vol. 62, no. 5, pp. 1398–1404, May 2013, doi: 10.2337/db12-1396.

[186] G. Fritzsche, K.-D. Kohnert, P. Heinke, L. Vogt, and E. Salzsieder, “The use of a computer program to calculate the mean amplitude of glycemic excursions.,” *Diabetes Technol Ther*, vol. 13, no. 3, pp. 319–25, Mar. 2011, doi: 10.1089/dia.2010.0108.

[187] P. A. Baghurst, “Calculating the Mean Amplitude of Glycemic Excursion from Continuous Glucose Monitoring Data: An Automated Algorithm,” *Diabetes Technol Ther*, vol. 13, no. 3, pp. 296–302, Mar. 2011, doi: 10.1089/dia.2010.0090.

[188] G. D. Molnar, W. F. Taylor, and M. M. Ho, “Day-to-day variation of continuously monitored glycaemia: A further measure of diabetic instability,” *Diabetologia*, vol. 8, no. 5, pp. 342–348, Nov. 1972, doi: 10.1007/BF01218495.

[189] J. Schlichtkrull, O. Munck, and M. Jersild, “The M-Value, an Index of Blood-sugar Control in Diabetics,” *Acta Med Scand*, vol. 177, no. 1, pp. 95–102, Apr. 2009, doi: 10.1111/j.0954-6820.1965.tb01810.x.

[190] I. B. Hirsch, A. K. Balo, K. Sayer, A. Garcia, B. A. Buckingham, and T. A. Peyser, “A Simple Composite Metric for the Assessment of Glycemic Status from Continuous Glucose Monitoring Data: Implications for Clinical Practice and the Artificial Pancreas,” *Diabetes Technol Ther*, vol. 19, no. S3, p. S-38-S-48, Jun. 2017, doi: 10.1089/dia.2017.0080.

[191] B. Kovatchev, “Glycemic Variability: Risk Factors, Assessment, and Control,” *J Diabetes Sci Technol*, vol. 13, no. 4, pp. 627–635, Jul. 2019, doi: 10.1177/1932296819826111.

[192] T. L. Hernandez and L. A. Barbour, “A Standard Approach to Continuous Glucose Monitor Data in Pregnancy for the Study of Fetal Growth and Infant Outcomes,” *Diabetes Technol Ther*, vol. 15, no. 2, pp. 172–179, Feb. 2013, doi: 10.1089/dia.2012.0223.

[193] G. E. A. P. A. Batista, E. J. Keogh, O. M. Tataw, and V. M. A. De Souza, “CID: An efficient complexity-invariant distance for time series,” *Data Min Knowl Discov*, vol. 28, no. 3, pp. 634–669, May 2014, doi: 10.1007/S10618-013-0312-3/FIGURES/30.

[194] X. D. Zhang, *Optimal High-Throughput Screening*. Cambridge: Cambridge University Press, 2011. doi: 10.1017/CBO9780511973888.

[195] I. Attaye, E. W. J. van der Vossen, D. N. Mendes Bastos, M. Nieuwdorp, and E. Levin, "Introducing the Continuous Glucose Data Analysis (CGDA) R Package: An Intuitive Package to Analyze Continuous Glucose Monitoring Data," *J Diabetes Sci Technol*, vol. 16, no. 3, pp. 783–785, May 2022, doi: 10.1177/19322968211070293.

[196] R. S. Mazze, D. Lucido, O. Langer, K. Hartmann, and D. Rodbard, "Ambulatory Glucose Profile: Representation of Verified Self-Monitored Blood Glucose Data," *Diabetes Care*, vol. 10, no. 1, pp. 111–117, Jan. 1987, doi: 10.2337/diacare.10.1.111.

[197] D. Rodbard, "The Ambulatory Glucose Profile: Opportunities for Enhancement," *Diabetes Technol Ther*, vol. 23, no. 5, pp. 332–341, May 2021, doi: 10.1089/dia.2020.0524.

[198] D. Rodbard, "Display of Glucose Distributions by Date, Time of Day, and Day of Week: New and Improved Methods," *J Diabetes Sci Technol*, vol. 3, no. 6, pp. 1388–1394, Nov. 2009, doi: 10.1177/193229680900300619.

[199] D. C. Klonoff *et al.*, "A Glycemia Risk Index (GRI) of Hypoglycemia and Hyperglycemia for Continuous Glucose Monitoring Validated by Clinician Ratings," *J Diabetes Sci Technol*, p. 193229682210852, Mar. 2022, doi: 10.1177/19322968221085273.

[200] P. A. Baghurst, D. Rodbard, and F. J. Cameron, "The Minimum Frequency of Glucose Measurements from Which Glycemic Variation Can Be Consistently Assessed," *J Diabetes Sci Technol*, vol. 4, no. 6, pp. 1382–1385, Nov. 2010, doi: 10.1177/193229681000400612.

[201] H. K. Akturk *et al.*, "Impact of Different Types of Data Loss on Optimal Continuous Glucose Monitoring Sampling Duration," *Diabetes Technol Ther*, Jun. 2022, doi: 10.1089/dia.2022.0093.

[202] P. Herrero, A. Alalitei, M. Reddy, P. Georgiou, and N. Oliver, "Robust Determination of the Optimal Continuous Glucose Monitoring Length of Intervention to Evaluate Long-Term Glycemic Control," *Diabetes Technol Ther*, vol. 23, no. 4, pp. 314–319, Apr. 2021, doi: 10.1089/dia.2020.0387.

[203] V. Moscardó, P. Herrero, M. Reddy, N. R. Hill, P. Georgiou, and N. Oliver, “Assessment of Glucose Control Metrics by Discriminant Ratio,” *Diabetes Technol Ther*, vol. 22, no. 10, pp. 719–726, Oct. 2020, doi: 10.1089/DIA.2019.0415.

[204] M. K. Sechterberger, Y. M. Luijf, and J. H. DeVries, “Poor Agreement of Computerized Calculators for Mean Amplitude of Glycemic Excursions,” *Diabetes Technol Ther*, vol. 16, no. 2, pp. 72–75, Feb. 2014, doi: 10.1089/dia.2013.0138.

[205] H. K. Akturk, T. Vigers, G. Forlenza, A. Champakanath, and L. Pyle, “Comparison of Cgmanalysis, a Free Open-Source Continuous Glucose Monitoring Data Management and Analysis Software, with Commercially Available CGM Platforms: Data Standardization for Diabetes Technology Research,” *Diabetes Technol Ther*, vol. 24, no. 1, pp. 54–60, Jan. 2022, doi: 10.1089/dia.2021.0200.

[206] H. Wolpert, W. H. Polonsky, and D. Rodbard, “Insulin Metrics: Need for Development of Consensus Standards for Reporting of Insulin Dosing Data,” *Diabetes Technol Ther*, vol. 23, no. 7, pp. 522–526, Jul. 2021, doi: 10.1089/dia.2020.0631.

[207] A. Frid, A. Tura, G. Pacini, and M. Ridderstråle, “Effect of Oral Pre-Meal Administration of Betaglucans on Glycaemic Control and Variability in Subjects with Type 1 Diabetes,” *Nutrients*, vol. 9, no. 9, p. 1004, Sep. 2017, doi: 10.3390/nu9091004.

[208] E. A. Huhn *et al.*, “Effectiveness of real-time continuous glucose monitoring to improve glycaemic control and pregnancy outcome in patients with gestational diabetes mellitus: A study protocol for a randomised controlled trial,” *BMJ Open*, 2020, doi: 10.1136/bmjopen-2020-040498.

[209] J. Werzowa *et al.*, “Comparison of glycemic control and variability in patients with type 2 and posttransplantation diabetes mellitus,” *J Diabetes Complications*, vol. 29, no. 8, pp. 1211–1216, Nov. 2015, doi: 10.1016/j.jdiacomp.2015.07.014.

[210] S. J. Salkind, R. Huizenga, S. J. Fonda, M. S. Walker, and R. A. Vigersky, “Glycemic Variability in Nondiabetic Morbidly Obese Persons,” *J Diabetes Sci*

Technol, vol. 8, no. 5, pp. 1042–1047, Sep. 2014, doi: 10.1177/1932296814537039.

[211] G. Acciaroli *et al.*, "Diabetes and Prediabetes Classification Using Glycemic Variability Indices From Continuous Glucose Monitoring Data:," *https://doi.org/10.1177/1932296817710478*, vol. 12, no. 1, pp. 105–113, Jun. 2017, doi: 10.1177/1932296817710478.

[212] L. E *et al.*, "Glycaemic variability-based classification of impaired glucose tolerance vs. type 2 diabetes using continuous glucose monitoring data," *Comput Biol Med*, vol. 96, pp. 141–146, May 2018, doi: 10.1016/J.COMPBIOMED.2018.03.007.

[213] E. Longato, G. Acciaroli, A. Facchinetti, A. Maran, and G. Sparacino, "Simple Linear Support Vector Machine Classifier Can Distinguish Impaired Glucose Tolerance Versus Type 2 Diabetes Using a Reduced Set of CGM-Based Glycemic Variability Indices," *J Diabetes Sci Technol*, vol. 14, no. 2, pp. 297–302, Mar. 2020, doi: 10.1177/1932296819838856.

[214] S. D. Solomon *et al.*, "Diabetic Retinopathy: A Position Statement by the American Diabetes Association," *Diabetes Care*, vol. 40, no. 3, pp. 412–418, Mar. 2017, doi: 10.2337/dc16-2641.

[215] Z. L. Teo *et al.*, "Global Prevalence of Diabetic Retinopathy and Projection of Burden through 2045," *Ophthalmology*, vol. 128, no. 11, pp. 1580–1591, Nov. 2021, doi: 10.1016/j.ophtha.2021.04.027.

[216] "12. Retinopathy, Neuropathy, and Foot Care: *Standards of Medical Care in Diabetes—2022*," *Diabetes Care*, vol. 45, no. Supplement_1, pp. S185–S194, Jan. 2022, doi: 10.2337/dc22-S012.

[217] T. M. Usman, Y. K. Saheed, A. Nsang, A. Ajibesin, and S. Rakshit, "A systematic literature review of machine learning based risk prediction models for diabetic retinopathy progression," *Artif Intell Med*, vol. 143, p. 102617, Sep. 2023, doi: 10.1016/j.artmed.2023.102617.

[218] M. R. Land *et al.*, "Examining the Role of Telemedicine in Diabetic Retinopathy," *J Clin Med*, vol. 12, no. 10, p. 3537, May 2023, doi: 10.3390/jcm12103537.

[219] G. Bresnick *et al.*, “Adherence to ophthalmology referral, treatment and follow-up after diabetic retinopathy screening in the primary care setting,” *BMJ Open Diabetes Res Care*, vol. 8, no. 1, p. e001154, Jun. 2020, doi: 10.1136/bmjdrc-2019-001154.

[220] T. Y. Wong and C. Sabanayagam, “The War on Diabetic Retinopathy: Where Are We Now?,” *Asia-Pacific Journal of Ophthalmology*, vol. 8, no. 6, pp. 448–456, Nov. 2019, doi: 10.1097/APO.0000000000000267.

[221] C. Gorst *et al.*, “Long-term Glycemic Variability and Risk of Adverse Outcomes: A Systematic Review and Meta-analysis,” *Diabetes Care*, vol. 38, no. 12, pp. 2354–2369, Dec. 2015, doi: 10.2337/dc15-1188.

[222] H. Hall *et al.*, “Glucotypes reveal new patterns of glucose dysregulation,” *PLoS Biol*, 2018, doi: 10.1371/journal.pbio.2005143.

[223] K. G. Brodovicz *et al.*, “Postprandial metabolic responses to mixed versus liquid meal tests in healthy men and men with type 2 diabetes,” *Diabetes Res Clin Pract*, 2011, doi: 10.1016/j.diabres.2011.09.002.

[224] Y. Wang, S. Liu, R. Chen, Z. Chen, J. Yuan, and Q. Li, “A Novel Classification Indicator of Type 1 and Type 2 Diabetes in China,” *Sci Rep*, 2017, doi: 10.1038/s41598-017-17433-8.

[225] D. Dave *et al.*, “Feature-Based Machine Learning Model for Real-Time Hypoglycemia Prediction,” *J Diabetes Sci Technol*, 2020, doi: 10.1177/1932296820922622.

[226] G. Fico *et al.*, “Exploring the Frequency Domain of Continuous Glucose Monitoring Signals to Improve Characterization of Glucose Variability and of Diabetic Profiles,” *J Diabetes Sci Technol*, 2017, doi: 10.1177/1932296816685717.

[227] Q. Cheng, P. K. Varshney, and M. K. Arora, “Logistic regression for feature selection and soft classification of remote sensing data,” *IEEE Geoscience and Remote Sensing Letters*, 2006, doi: 10.1109/LGRS.2006.877949.

[228] J. Chaki, S. Thillai Ganesh, S. K. Cidham, and S. Ananda Theertan, “Machine learning and artificial intelligence based Diabetes Mellitus detection and self-management: A systematic review,” *Journal of King Saud University - Computer and Information Sciences*. 2020. doi: 10.1016/j.jksuci.2020.06.013.

[229] W. K. Chung *et al.*, “Precision Medicine in Diabetes: A Consensus Report From the American Diabetes Association (ADA) and the European Association for the Study of Diabetes (EASD),” *Diabetes Care*, vol. 43, no. 7, p. 1617, Jul. 2020, doi: 10.2337/DCI20-0022.

[230] M. Yapanis, S. James, M. E. Craig, D. O’Neal, and E. I. Ekinci, “Complications of Diabetes and Metrics of Glycemic Management Derived From Continuous Glucose Monitoring,” *J Clin Endocrinol Metab*, vol. 107, no. 6, pp. e2221–e2236, May 2022, doi: 10.1210/clinem/dgac034.

[231] O. I. Ogunyemi *et al.*, “Detecting diabetic retinopathy through machine learning on electronic health record data from an urban, safety net healthcare system,” *JAMIA Open*, vol. 4, no. 3, Jul. 2021, doi: 10.1093/jamiaopen/ooab066.

[232] B. Bohn *et al.*, “Impact of Physical Activity on Glycemic Control and Prevalence of Cardiovascular Risk Factors in Adults With Type 1 Diabetes: A Cross-sectional Multicenter Study of 18,028 Patients,” *Diabetes Care*, vol. 38, no. 8, pp. 1536–1543, Aug. 2015, doi: 10.2337/dc15-0030.

[233] M. C. Riddell *et al.*, “Exercise management in type 1 diabetes: a consensus statement.,” *Lancet Diabetes Endocrinol*, vol. 5, no. 5, pp. 377–390, May 2017, doi: 10.1016/S2213-8587(17)30014-1.

[234] O. Moser *et al.*, “Glucose management for exercise using continuous glucose monitoring (CGM) and intermittently scanned CGM (isCGM) systems in type 1 diabetes: position statement of the European Association for the Study of Diabetes (EASD) and of the International Society for Pediatric and Adolescent Diabetes (ISPAD) endorsed by JDRF and supported by the American Diabetes Association (ADA).,” *Pediatr Diabetes*, vol. 21, no. 8, pp. 1375–1393, Dec. 2020, doi: 10.1111/pedi.13105.

[235] N. Hobbs, I. Hajizadeh, M. Rashid, K. Turksoy, M. Breton, and A. Cinar, “Improving Glucose Prediction Accuracy in Physically Active Adolescents With Type 1 Diabetes.,” *J Diabetes Sci Technol*, vol. 13, no. 4, pp. 718–727, Jul. 2019, doi: 10.1177/1932296818820550.

[236] A. Guemes *et al.*, “Predicting Quality of Overnight Glycaemic Control in Type 1 Diabetes Using Binary Classifiers,” *IEEE J Biomed Health Inform*, vol. 24, no. 5, pp. 1439–1446, May 2020, doi: 10.1109/JBHI.2019.2938305.

[237] N. S. Tyler, C. Mosquera-Lopez, G. M. Young, J. El Youssef, J. R. Castle, and P. G. Jacobs, “Quantifying the impact of physical activity on future glucose trends using machine learning,” *iScience*, vol. 25, no. 3, p. 103888, Mar. 2022, doi: 10.1016/j.isci.2022.103888.

[238] R. Reddy, N. Resalat, L. M. Wilson, J. R. Castle, J. El Youssef, and P. G. Jacobs, “Prediction of Hypoglycemia During Aerobic Exercise in Adults With Type 1 Diabetes.,” *J Diabetes Sci Technol*, vol. 13, no. 5, pp. 919–927, Sep. 2019, doi: 10.1177/1932296818823792.

[239] E. Tsalikian *et al.*, “Impact of exercise on overnight glycemic control in children with type 1 diabetes mellitus.,” *J Pediatr*, vol. 147, no. 4, pp. 528–34, Oct. 2005, doi: 10.1016/j.jpeds.2005.04.065.

[240] M. H. Jensen, C. Dethlefsen, P. Vestergaard, and O. Hejlesen, “Prediction of Nocturnal Hypoglycemia From Continuous Glucose Monitoring Data in People With Type 1 Diabetes: A Proof-of-Concept Study,” *J Diabetes Sci Technol*, vol. 14, no. 2, pp. 250–256, Mar. 2020, doi: 10.1177/1932296819868727.

[241] O. Mujahid, I. Contreras, and J. Vehi, “Machine Learning Techniques for Hypoglycemia Prediction: Trends and Challenges,” *Sensors*, vol. 21, no. 2, p. 546, Jan. 2021, doi: 10.3390/s21020546.

[242] M. Coolen *et al.*, “The impact of hypoglycemia on quality of life and related outcomes in children and adolescents with type 1 diabetes: A systematic review,” *PLoS One*, vol. 16, no. 12, p. e0260896, Dec. 2021, doi: 10.1371/JOURNAL.PONE.0260896.

[243] A. Hayashi *et al.*, “Hemodialysis-Related Glycemic Disarray Proven by Continuous Glucose Monitoring; Glycemic Markers and Hypoglycemia,” *Diabetes Care*, vol. 44, no. 7, pp. 1647–1656, Jul. 2021, doi: 10.2337/dc21-0269.

[244] S. Puhr, J. B. Welsh, C. E. Bauza, and T. C. Walker, “Patients with Type 2 Diabetes and Residual Insulin Secretory Capacity Realize Glycemic Benefits from Real-Time Continuous Glucose Monitoring.,” *J Diabetes Sci Technol*, vol. 15, no. 4, pp. 965–967, Jul. 2021, doi: 10.1177/19322968211007880.

[245] R. A. Gubitosi-Klug *et al.*, "Residual β cell function in long-term type 1 diabetes associates with reduced incidence of hypoglycemia," *Journal of Clinical Investigation*, vol. 131, no. 3, Feb. 2021, doi: 10.1172/JCI143011.

[246] J. S. Skyler, "Importance of residual insulin secretion in type 1 diabetes.," *Lancet Diabetes Endocrinol*, vol. 11, no. 7, pp. 443–444, Jul. 2023, doi: 10.1016/S2213-8587(23)00149-3.

[247] L. Desborough, K. Jaffe, J. Hanna, J. Ulloa, and K. Kaiserman, "Transforming Evidence Generation for Drug Label Changes: A Case Study.," *Ann Biomed Eng*, vol. 51, no. 1, pp. 137–149, Jan. 2023, doi: 10.1007/s10439-022-03062-4.

[248] E. Potocka, R. A. Baughman, and H. Derendorf, "Population pharmacokinetic model of human insulin following different routes of administration," *J Clin Pharmacol*, vol. 51, no. 7, pp. 1015–1024, Jul. 2011, doi: 10.1177/0091270010378520.

[249] H. Liu, T. Li, H. Yu, J. Li, H. Tan, and Y. Yu, "How to Achieve Sufficient Endogenous Insulin Suppression in Euglycemic Clamps Assessing the Pharmacokinetics and Pharmacodynamics of Long-Acting Insulin Preparations Employing Healthy Volunteers," *Front Pharmacol*, vol. 13, Jul. 2022, doi: 10.3389/FPHAR.2022.899798.

[250] T. Zhou, M. Boettger, J. L. Knopp, M. Lange, A. Heep, and J. G. Chase, "Model-based subcutaneous insulin for glycemic control of pre-term infants in the neonatal intensive care unit," *Comput Biol Med*, vol. 160, p. 106808, Jun. 2023, doi: 10.1016/j.compbiomed.2023.106808.

[251] R. Visentin *et al.*, "Improving Efficacy of Inhaled Technosphere Insulin (Afrezza) by Postmeal Dosing: In-silico Clinical Trial with the University of Virginia/Padova Type 1 Diabetes Simulator," *Diabetes Technol Ther*, vol. 18, no. 9, pp. 574–585, Sep. 2016, doi: 10.1089/dia.2016.0128.

[252] D. R. Owens, "Clinical-Pharmacological Studies," in *Human Insulin*, Dordrecht: Springer Netherlands, 1986, pp. 46–236. doi: 10.1007/978-94-009-4161-8_4.

[253] M. T. Marino, J. P. Cassidy, R. A. Baughman, A. H. Boss, and P. C. Richardson, "A new C-Peptide correction model used to assess bioavailability of regular

human insulin," *Biopharm Drug Dispos*, vol. 31, no. 7, pp. 428–435, Oct. 2010, doi: 10.1002/BDD.723.

[254] R. P. Eaton, R. C. Allen, D. S. Schade, K. M. Erickson, and J. Standefer, "Prehepatic insulin production in man: kinetic analysis using peripheral connecting peptide behavior," *J Clin Endocrinol Metab*, vol. 51, no. 3, pp. 520–528, 1980, doi: 10.1210/JCEM-51-3-520.

[255] D. D'Argenio, A. Schumitzky, and X. Wang, *ADAPT 5 User's Guide: Pharmacokinetic/Pharmacodynamic Systems Analysis Software*. . Los Angeles, CA, 2009.

[256] R. Hovorka, P. A. Soons, and M. A. Young, "ISEC: a program to calculate insulin secretion.," *Comput Methods Programs Biomed*, vol. 50, no. 3, pp. 253–64, Aug. 1996, doi: 10.1016/0169-2607(96)01755-5.

[257] J. E. Liljenquist, D. L. Horwitz, A. S. Jennings, J. L. Chiasson, U. Keller, and A. H. Rubenstein, "Inhibition of Insulin Secretion by Exogenous Insulin in Normal Man as Demonstrated by C-peptide Assay," *Diabetes*, vol. 27, no. 5, pp. 563–570, May 1978, doi: 10.2337/DIAB.27.5.563.

[258] G. M. Argoud, D. S. Schade, and R. P. Eaton, "Insulin Suppresses Its Own Secretion In Vivo," *Diabetes*, vol. 36, no. 8, pp. 959–962, Aug. 1987, doi: 10.2337/DIAB.36.8.959.

[259] M. Hecking *et al.*, "Glucose metabolism after renal transplantation," *Diabetes Care*, vol. 36, no. 9, pp. 2763–2771, Sep. 2013, doi: 10.2337/DC12-2441.

[260] C. K. Kramer, H. Choi, B. Zinman, and R. Retnakaran, "Determinants of reversibility of β-cell dysfunction in response to short-term intensive insulin therapy in patients with early type 2 diabetes.," *Am J Physiol Endocrinol Metab*, vol. 305, no. 11, pp. E1398-407, Dec. 2013, doi: 10.1152/ajpendo.00447.2013.

[261] A. L. J. Carr, C. Evans-Molina, and R. A. Oram, "Precision medicine in type 1 diabetes.," *Diabetologia*, vol. 65, no. 11, pp. 1854–1866, Nov. 2022, doi: 10.1007/s00125-022-05778-3.

[262] A. G. Jones *et al.*, "Assessment of endogenous insulin secretion in insulin treated diabetes predicts postprandial glucose and treatment response to prandial insulin," *BMC Endocr Disord*, vol. 12, no. 1, pp. 1–7, Jun. 2012, doi: 10.1186/1472-6823-12-6.

[263] F. W. Gibb, J. A. McKnight, C. Clarke, and M. W. J. Strachan, “Preserved C-peptide secretion is associated with fewer low-glucose events and lower glucose variability on flash glucose monitoring in adults with type 1 diabetes.,” *Diabetologia*, vol. 63, no. 5, pp. 906–914, May 2020, doi: 10.1007/s00125-020-05099-3.

[264] A. Jeyam *et al.*, “Clinical Impact of Residual C-Peptide Secretion in Type 1 Diabetes on Glycemia and Microvascular Complications,” *Diabetes Care*, vol. 44, no. 2, pp. 390–398, Feb. 2021, doi: 10.2337/dc20-0567.

[265] J. M. Lachin, P. McGee, and J. P. Palmer, “Impact of C-Peptide Preservation on Metabolic and Clinical Outcomes in the Diabetes Control and Complications Trial,” *Diabetes*, vol. 63, no. 2, pp. 739–748, Feb. 2014, doi: 10.2337/db13-0881.

[266] A. Miya *et al.*, “Log-linear relationship between endogenous insulin secretion and glycemic variability in patients with type 2 diabetes on continuous glucose monitoring.,” *Sci Rep*, vol. 11, no. 1, p. 9057, Apr. 2021, doi: 10.1038/s41598-021-88749-9.

[267] H. K. Akturk *et al.*, “Improved Postprandial Glucose with Inhaled Technosphere Insulin Compared with Insulin Aspart in Patients with Type 1 Diabetes on Multiple Daily Injections: The STAT Study,” *Diabetes Technol Ther*, vol. 20, no. 10, pp. 639–647, Oct. 2018, doi: 10.1089/dia.2018.0200.

[268] P. Arpaia, U. Cesaro, M. Frosolone, N. Moccaldi, and M. Taglialatela, “A micro-bioimpedance meter for monitoring insulin bioavailability in personalized diabetes therapy.,” *Sci Rep*, vol. 10, no. 1, p. 13656, Aug. 2020, doi: 10.1038/s41598-020-70376-5.

[269] P. Arpaia, D. Cuneo, F. Mancino, and N. Moccaldi, “A Bioimpedance-based Transducer for Insulin Bioavailability Assessment after Subcutaneous Administration,” in *2022 IEEE International Instrumentation and Measurement Technology Conference (I2MTC)*, IEEE, May 2022, pp. 1–5. doi: 10.1109/I2MTC48687.2022.9806567.

[270] A. Tura *et al.*, “Estimation of prehepatic insulin secretion: Comparison between standardized C-peptide and insulin kinetic models,” *Metabolism*, vol. 61, no. 3, pp. 434–443, Mar. 2012, doi: 10.1016/j.metabol.2011.08.001.

[271] E. Maddaloni *et al.*, “C-peptide determination in the diagnosis of type of diabetes and its management: A clinical perspective,” *Diabetes Obes Metab*, vol. 24, no. 10, pp. 1912–1926, Oct. 2022, doi: 10.1111/dom.14785.

[272] R. C. Boston, D. Pei, and P. J. Moate, “A numerical deconvolution method to estimate C-peptide secretion in humans after an intravenous glucose tolerance test,” *Metabolism*, vol. 58, no. 7, pp. 891–900, Jul. 2009, doi: 10.1016/J.METABOL.2009.03.003.

[273] H.-C. E. Koh, C. Cao, and B. Mittendorfer, “Insulin Clearance in Obesity and Type 2 Diabetes,” *Int J Mol Sci*, vol. 23, no. 2, p. 596, Jan. 2022, doi: 10.3390/ijms23020596.

[274] E. Ferrannini and C. Cobelli, “The kinetics of insulin in man. I. General aspects.,” *Diabetes Metab Rev*, vol. 3, no. 2, pp. 335–363, Apr. 1987, doi: 10.1002/DMR.5610030201.

[275] C. Cobelli and G. Pacini, “Insulin secretion and hepatic extraction in humans by minimal modeling of C-peptide and insulin kinetics,” *Diabetes*, vol. 37, no. 2, pp. 223–231, 1988, doi: 10.2337/DIAB.37.2.223.

[276] H. Liu *et al.*, “Effects of Unsuppressed Endogenous Insulin on Pharmacokinetics and/or Pharmacodynamics of Study Insulin in the Healthy: A Retrospective Study,” *Clin Pharmacol Drug Dev*, vol. 11, no. 8, pp. 930–937, Aug. 2022, doi: 10.1002/CPDD.1093.

[277] D. Rüppel *et al.*, “A Population Dose-Response Model for Inhaled Technosphere Insulin Administered to Healthy Subjects,” *CPT Pharmacometrics Syst Pharmacol*, vol. 6, no. 6, pp. 365–372, Jun. 2017, doi: 10.1002/psp4.12189.

[278] S. Steiner, A. Pfützner, B. R. Wilson, O. Harzer, L. Heinemann, and K. Rave, “Technosphere™/insulin - Proof of concept study with a new insulin formulation for pulmonary delivery,” *Experimental and Clinical Endocrinology and Diabetes*, vol. 110, no. 1, pp. 17–21, 2002, doi: 10.1055/S-2002-19989/ID/16/BIB.

[279] P. G. Jacobs *et al.*, “Artificial intelligence and machine learning for improving glycemic control in diabetes: best practices, pitfalls and opportunities,” *IEEE Rev Biomed Eng*, pp. 1–19, 2023, doi: 10.1109/RBME.2023.3331297.

[280] M. I. McCarthy, “Painting a new picture of personalised medicine for diabetes,” *Diabetologia*, vol. 60, no. 5, pp. 793–799, May 2017, doi: 10.1007/s00125-017-4210-x.

[281] M. Morettini *et al.*, “Hepatic and Extrahepatic Insulin Clearance in Mice with Double Deletion of Glucagon-Like Peptide-1 and Glucose-Dependent Insulinotropic Polypeptide Receptors,” *Biomedicines*, vol. 9, no. 8, p. 973, Aug. 2021, doi: 10.3390/biomedicines9080973.

[282] A. Piersanti *et al.*, “Model-Based Assessment of Hepatic and Extrahepatic Insulin Clearance from Short Insulin-Modified IVGTT in Women with a History of Gestational Diabetes,” in *2021 43rd Annual International Conference of the IEEE Engineering in Medicine & Biology Society (EMBC)*, IEEE, Nov. 2021, pp. 4311–4314. doi: 10.1109/EMBC46164.2021.9630405.

[283] L. Ilari *et al.*, “Unraveling the Factors Determining Development of Type 2 Diabetes in Women With a History of Gestational Diabetes Mellitus Through Machine-Learning Techniques.,” *Front Physiol*, vol. 13, p. 789219, Feb. 2022, doi: 10.3389/fphys.2022.789219.

[284] A. Piersanti, F. Giurato, L. Burattini, A. Tura, and M. Morettini, “Comparison of Software Packages for the Analysis of Continuous Glucose Monitoring Data,” in *2021 IEEE International Symposium on Medical Measurements and Applications (MeMeA)*, IEEE, Jun. 2021, pp. 1–6. doi: 10.1109/MeMeA52024.2021.9478698.

[285] A. Piersanti, B. Salvatori, C. Göbl, L. Burattini, A. Tura, and M. Morettini, “A Machine-Learning Framework based on Continuous Glucose Monitoring to Prevent the Occurrence of Exercise-Induced Hypoglycemia in Children with Type 1 Diabetes,” in *2023 IEEE 36th International Symposium on Computer-Based Medical Systems (CBMS)*, IEEE, Jun. 2023, pp. 281–286. doi: 10.1109/CBMS58004.2023.00231.

[286] A. Piersanti, E. Creato, C. Göbl, A. Tura, L. Burattini, and M. Morettini, “Identifying Differences in Postprandial Glycemic Responses of Normal and Type 2 Diabetic/Prediabetic Subjects using Continuous Glucose Monitoring,”

[287] A. Piersanti *et al.*, “Diabetic Retinopathy Detection: a Machine-Learning Approach based on Continuous Glucose Monitoring Metrics,” in *11th IEEE*

International Conference on E-Health and Bioengineering - EHB 2023, Bucharest, Romania, Nov. 2023.

[288] A. Piersanti, B. Salvatori, C. Göbl, L. Burattini, A. Tura, and M. Morettini, "HIKE: A COMPOSITE METRIC FOR HYPOGLYCEMIA RISK IN EXERCISE UNDER CONTROLLED CONDITIONS," in *The Official Journal of ATTD Advanced Technologies & Treatments for Diabetes Conference*, Florence , Mar. 2024.

[289] A. Piersanti *et al.*, "HEMODIALYSIS-INDUCED HYPOGLYCEMIA: A MACHINE-LEARNING APPROACH BASED ON CONTINUOUSGLUCOSE MONITORING METRICS TO UNDERSTAND THE RISK FOR UPCOMING EVENTS," in *The Official Journal of ATTD Advanced Technologies & Treatments for Diabetes Conference*, Florence, Mar. 2024.

[290] A. Piersanti, G. Pacini, A. Tura, D. Z. D'Argenio, and M. Morettini, "An in-silico modeling approach to separate exogenous and endogenous plasma insulin appearance, with application to inhaled insulin," 2024.